KAZUAKI TOKUHASHI ▪ LIANG CHEN
KENJI TAKIZAWA ▪ AKIFUMI TAKAHASHI
TADAFUMI UCHIMARU ▪ MASAAKI SUGIE
SHIGEO KONDO ▪ AKIRA SEKIYA

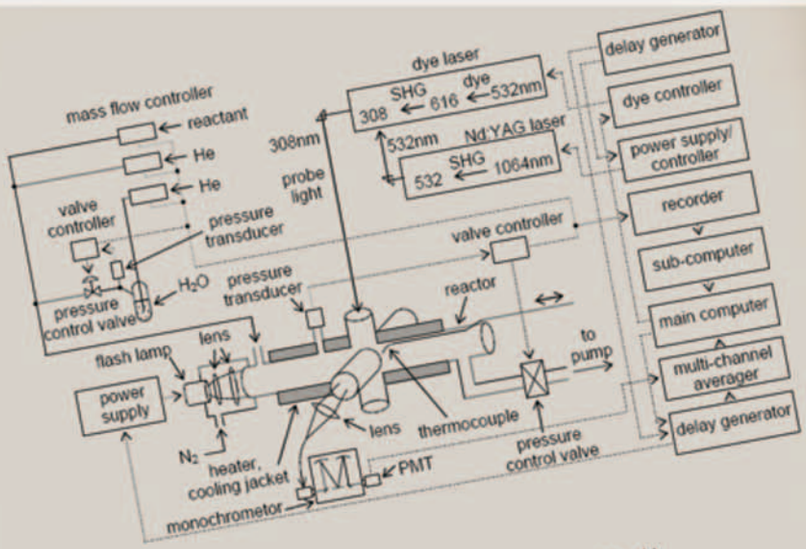

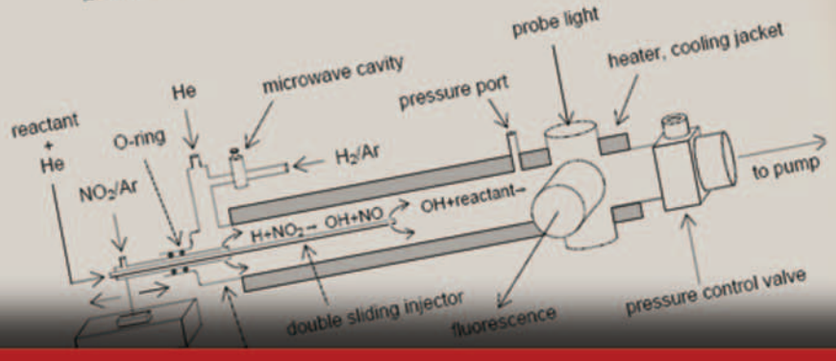

LIFETIMES OF FLUORINATED COMPOUNDS

Novinka

LIFETIMES OF FLUORINATED COMPOUNDS

LIFETIMES OF FLUORINATED COMPOUNDS

KAZUAKI TOKUHASHI, LIANG CHEN,
KENJI TAKIZAWA, AKIFUMI TAKAHASHI,
TADAFUMI UCHIMARU, MASAAKI SUGIE,
SHIGEO KONDO AND AKIRA SEKIYA

Nova Science Publishers, Inc.
New York

LIBRARY OF CONGRESS CATALOGING-IN-PUBLICATION DATA

Lifetimes of fluorinated compounds / Kazuaki Tokuhashi ... [et al.].
p. cm.
ISBN 978-1-60876-251-4 (E-Book)
1. Fluorine compounds--Research. I. Tokuhashi, Kazuaki.
QD181.F1L54 2008
546'.731--dc22

2007049240

Published by Nova Science Publishers, Inc. ✣ New York

CONTENTS

PREFACE

Rate constants for reactions of 11 hydrochlorofluorocarbons and 12 hydrofluorocarbons were measured by means of the absolute rate method over the temperature range 250–430 K. OH radicals were generated by flash photolysis, laser photolysis, or a discharge flow methods; and the concentration of OH radicals was monitored by means of the laser-induced fluorescence technique. The fluorinated compounds were purified by gas chromatography; impurities remaining in the samples after purification were found to have no sizable effect on the measured rate constants. The Arrhenius rate expressions were determined from the kinetic data obtained in this study as well as from available literature data. A method for estimating rates of reactions with OH radicals using an artificial neural network method was developed. An algorithm for a back-propagation method for determining optimized weights was developed for cases in which the reactivities of individual reaction sites of a molecule are not known. The ability of the neural network method to predict rate constants was evaluated by using the leave-one-out method. Rate constants for 94 compounds, including hydrocarbons, hydrofluorocarbons, hydrochlorofluorocarbons, hydrochlorocarbons, and brominated compounds, were calculated within a factor of 2.

Keywords: environmental evaluation, CFC alternatives, hydrofluorocarbon, hydrochlorofluorocarbon, kinetic measurement, absolute rate method, neural network.

Chapter 1

INTRODUCTION

Fluorinated compounds have been used as refrigerants, foaming agents, and cleaning solvents and for many other applications, because they have excellent properties. Because fully halogenated chlorofluorocarbons (CFCs) contribute to the depletion of the stratospheric ozone layer and to global warming, a number of replacement compounds, such as hydrofluorocarbons (HFCs) and hydrochlorofluorocarbons (HCFCs), have been investigated and used for industrial applications. Partially fluorinated ethers (HFEs) have also been developed as new alternatives. Because HCFCs contain Cl atoms, they still contribute to the depletion of the stratospheric ozone layer as well as to global warming, and these compounds are scheduled to be phased out in the near future. In contrast, because HFCs and HFEs do not contain Cl atoms, they do not contribute to ozone depletion, but they may contribute to global warming. HCFCs, HFCs, and HFEs contain at least one hydrogen atom, and they are expected to be oxidized by OH radicals in the troposphere. In fact, the main loss process of HCFCs, HFCs, and HFEs is reaction with OH radicals. Thus, the atmospheric lifetimes of these compounds are determined primarily by the rate at which they react with OH radicals [1]. Therefore, studies of their reactivity with OH radicals are crucial for evaluation of the global impact of fluorinated compounds.

There have been a number of studies of rate constants for reactions of OH radicals with HCFCs and HFCs. On the basis of experimental results, rate constants for some of these fluorinated compounds have been evaluated and recommended [2, 3]. However, there are by no means enough kinetic data for HCFCs and HFCs, because there are many isomeric HCFCs and HFCs. Furthermore, in some cases, measured rate constants are not accurate. Therefore,

to assess the environmental effects of these substances, the rate constants of their reactions with OH radicals must be accurately measured. Accumulation of accurate rate data may also contribute to development of estimation methods by theoretical and empirical approach.

In this paper, we report kinetic data for the reactions of OH radicals with 11 HCFCs and 12 HFCs: HCFC-22 (CHF_2Cl), HCFC-123 ($CHCl_2CF_3$), HCFC-123a ($CHFClCF_2Cl$), CFC-124 ($CHFClCF_3$), HCFC-132b (CH_2ClCF_2Cl), HCFC-133a (CH_2ClCF_3), HCFC-141 ($CH_2ClCHFCl$), HCFC-141b (CH_3CFCl_2), HCFC-142b (CH_3CF_2Cl), HCFC-243db ($CF_3CHClCH_2Cl$), HCFC-253fb ($CF_3CH_2CH_2Cl$), HFC-32 (CH_2F_2), HFC-125 (CHF_2CF_3), HFC-134a (CH_2FCF_3), HFC-143 (CH_2FCHF_2), HFC-152a (CH_3CHF_2), HFC-236ea ($CF_3CHFCHF_2$), HFC-245ca ($CH_2FCF_2CHF_2$), HFC-245eb (CF_3CHFCH_2F), HFC-245fa ($CHF_2CH_2CF_3$), HFC-254fb ($CF_3CH_2CH_2F$), FC-272ca ($CH_3CF_2CH_3$), and HFC-43-10mee ($CF_3CHFCHFCF_2CF_3$). The kinetic data were measured by means of the absolute rate technique over the temperature range 250–430 K. Values measured with this technique are more accurate than values measured with the relative rate technique. However, reactive impurities contained in the samples can seriously affect the accuracy of the measured rate constants because the reactivities of HCFCs and HFCs are relatively low. Sample purity and its influence on measured kinetic data must be examined very carefully, and kinetic measurements must be carried out on samples with sufficient purity. Therefore, in this study, we carefully investigated the effects of reactive impurities on the measured rate constant by purifying samples by gas chromatography and comparing data obtained before and after purification.

There have been many efforts to predict the reactivity with OH radicals by theoretical and empirical methods. Atkinson and a co-worker developed an empirical estimation method based on evaluating structure–activity relationships (SAR) [4, 5, 6]; and DeMore [7] has proposed a similar method. We have also studied a similar method, which focuses on evaluating the synergistic effects of various substituents on rate constants for reactions with OH radicals [8]. Urata et al. [9] have studied a method for estimating bond dissociation enthalpies (BDEs) of the C–H bonds of HFCs and HFEs using the neural network technique; rates of reaction with OH radicals were then calculated from the estimated BDEs [10].

The neural network method has been used successfully in many fields. However, it has not been used to estimate rate constants directly. In this study, we investigated a method for estimating the rates of reactions with OH radicals using the neural network method. We developed an algorithm for using back propagation to determine optimized weights in cases in which the reactivities of individual reaction sites of a molecule are not known. We evaluated the predictive

ability of the neural network method using the leave-one-out method. We discuss trends for the reactivities of various types of structural sites on the basis of the results obtained by means of the neural network method.

Chapter 2

EXPERIMENTAL APPARATUS AND METHODS

2.1. KINETIC MEASUREMENTS

Methods for measuring the reaction rates of gaseous compounds with OH radicals can be roughly classified into two types: the absolute rate method and the relative rate method.

In the case of the absolute rate method, the reaction is carried out under first-order conditions; that is, the initial concentration of the target compound, such as a fluorinated compound, is high relative to the concentration of OH radicals, and the rate constant is determined from the change in the OH radical concentration as the reaction proceeds. The absolute value of the rate constant can be obtained from the OH radical concentration in arbitrary units. Therefore, an accurate absolute rate constant can be determined directly because the measured rate constant is not affected by the error that would be introduced by calibration of the OH radical concentration. However, if the sample of the target compound contains reactive impurities such as unsaturated compounds, the concentration of the OH radicals is reduced by reactions both with the target compound and with the impurities. As a result, the measured rate constant is an overestimation of the actual rate constant. Therefore, when the absolute rate method is used, samples must be highly pure.

In the case of the relative rate method, the target compound and a reference compound with a known reaction rate are allowed to react simultaneously with OH radicals. The ratio of the rate constant for the target compound, k_{target}, to the rate constant for the reference compound, $k_{\text{reference}}$, can be obtained from the changes in the concentrations of the two compounds. Thus, in principle, the results are not affected by the presence of reactive impurities in the target or reference compound. With this method, the absolute value of k_{target} is obtained

from $k_{target}/k_{reference}$ and the absolute value of $k_{reference}$. Because $k_{target}/k_{reference}$ and $k_{reference}$ each contain individual errors, the absolute value of k_{target} includes the error accumulated from these two values, and the precision of the k_{target} value is lower than for the absolute rate method. Moreover, because $k_{target}/k_{reference}$ is obtained from changes in the concentrations of the target and reference compounds, the results can be affected by reactions between chemical compounds initially present in the reactor (for example, H_2O and O_3, which are used as a source of OH radicals [11]) or produced during measurement, heterogeneous reactions on the walls of the reactor, or photolysis of the target or reference compound. Therefore, these reactions must be considered carefully.

2.2. APPARATUS AND PROCEDURE FOR THE ABSOLUTE RATE METHOD

OH radicals were generated by flash photolysis (FP), laser photolysis (LP), or a discharge flow (DF) method, and the OH radical concentration was monitored by means of a laser-induced fluorescence (LIF) technique.

A schematic diagram of the FP-LIF apparatus is shown in Figure 1. A Pyrex reactor (25 mm i.d., ~40 cm long) was used for the FP experiments.

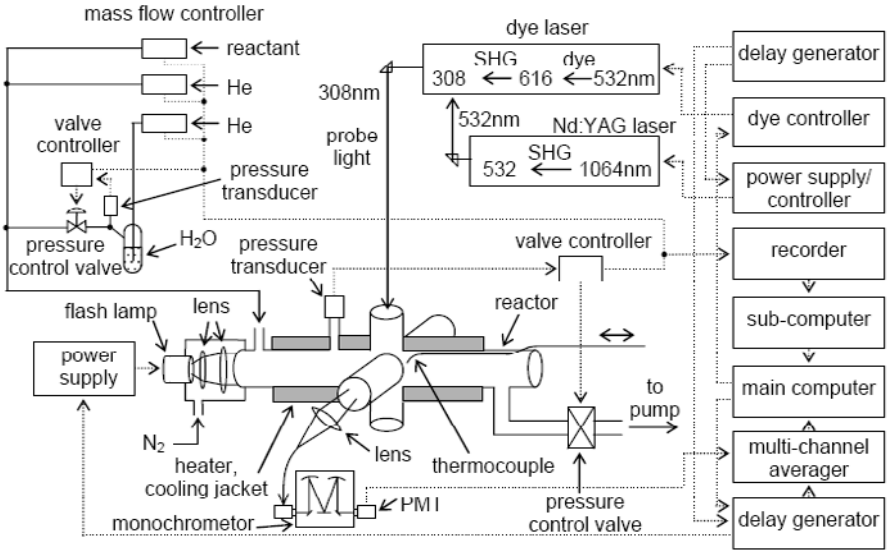

Figure 1. Schematic diagram of flash photolysis-laser induced fluorescence apparatus.

H_2O (100–200 mtorr) was directly photolyzed with pulsed light from a Xe flash lamp (EG&G, FX-193U; 600–1300 V and 2 μF; 0.36–1.69 J $pulse^{-1}$, typically 0.64–1 J $pulse^{-1}$; pulse width, 10–20 μs; $\lambda \geq 180$ nm, quartz cut-off). The photolyzing light was weakly focused by two quartz lenses, and the reaction cell was irradiated along the axial line through the quartz window. Ar was the carrier gas in most experiments. The region between the flash lamp and the reaction cell was purged with dry N_2 to minimize the absorption of UV light by O_2.

The flow rates of gas and vapor were measured and controlled by means of calibrated mass flow controllers. For gaseous materials, the mass flow controllers were calibrated with a gas meter or a soap-film flow meter. For fluorinated compounds with boiling points higher than about 273 K, the mass flow controller was calibrated by measuring the time–pressure relationship in a vessel with a known volume using a capacitance manometer (MKS Baratron). During the calibration, the sample vapor was supplied to the evacuated vessel through the mass flow controller. The total gas pressure of the reactor was monitored with a capacitance manometer and was kept constant with an electrically controlled exhaust throttle valve located downstream of the reactor. Water vapor was supplied by bubbling a portion of the carrier gas through a vessel filled with water at room temperature. The total pressure of carrier gas containing water vapor was measured with a capacitance manometer and was kept constant by means of a control valve. The amount of water vapor supplied to the reaction cell was estimated from the flow rate of the carrier gas, the water temperature measured by a CA thermocouple (type K), and the total pressure of carrier gas containing water vapor, on the assumption that the gas was saturated with water vapor.

The concentration of OH radicals was measured by the LIF method. The excitation light was generated with a frequency-doubled tunable dye laser, and the wavelength was tuned at about 308 nm. The dye laser was pumped by pulsed light from a frequency-doubled Nd:YAG laser (LAS INTEGRA). The repetition rate of the laser was set at 10 Hz. Fluorescence signals due to OH radicals were monitored at a right angle with respect to both the excitation light and the photolysis light; the signals were focused by two quartz lenses and detected with a photomultiplier tube. The scattered light from the excitation light (and the photolysis light source) was reduced by a monochromator (Jarrell-Ash, MonoSpec 25, 2360 G/mm, 25 cm focal length). The output signal of the photomultiplier tube was amplified by a preamplifier, accumulated (usually 400 shots) with a multichannel scaler/averager (Stanford, SR430), and stored in a main computer for further data processing. Trigger pulses for the Nd:YAG laser (flash lamp and a Q-switch) were generated by a delay generator (Stanford,

DG535). Trigger pulses for the multichannel scaler/averager and the photolysis light source (flash lamp or excimer laser) were generated by another delay generator. The main computer was used to control the latter delay generator (for the LP and FP methods) or the pulse controller (to determine the position of the sliding injector for the DF method; discussed later); the mass flow controllers and pressure controllers through a D-A converter; and the sub computer (see later).

The apparatus and gas-handling system used in the LP method (LP-H_2O method) were almost the same as those used for the FP method (Figure 1), except for the photolysis light source and the gases used. In the case of the LP-H_2O method, OH radicals were produced by the following reaction:

$$O(^1D) + H_2O \rightarrow 2OH, \tag{2.2.1}$$

where $O(^1D)$ atoms were generated by photodissociation of N_2O with an ArF excimer laser (Japan Storage Battery, EXL-210) in the presence of a He bath. The power density of the excimer laser at the exit window of the reaction cell was 2–5 mJ cm^{-2} $pulse^{-1}$. To ensure rapid conversion of $O(^1D)$ atoms to OH radicals, the ratio of H_2O to N_2O was kept larger than about 20:1. The N_2O concentration was about 5.0×10^{13}–5.0×10^{14} molecule cm^{-3}. The reaction cell was irradiated with photolyzing light along the axial line of the cell through a quartz window.

In some cases, direct photolysis of H_2O_2 with a KrF excimer laser was also studied (LP-H_2O_2 method). In the case of the LP-H_2O_2 method, helium was the bath gas. To prevent accumulation of photofragments or reaction products or both, all experiments were carried out under slow-flow conditions. The repetition rate was 10 Hz for both the FP lamp and the excimer laser.

A schematic diagram of the discharge flow reactor is shown in Figure 2. The Pyrex flow tube (20 mm i.d., ~900 mm long) was equipped with a movable double sliding injector [12] made of stainless steel. Helium was the primary carrier gas. OH radicals were produced by the following reaction:

$$H + NO_2 \rightarrow OH + NO, \tag{2.2.2}$$

where hydrogen atoms were generated by a microwave discharge in Ar gas containing a trace amount of hydrogen molecule. NO_2 diluted with Ar was supplied in excess to the flow tube through the top of the outer tube (o.d. 6 mm) of the sliding injector. The target compound was added to the gas stream through the top of the inner tube (o.d. 3 mm) of the sliding injector. The top of the inner tube was located 500 mm downstream from the top of the outer tube. Both the flow tube and the sliding injector were coated with Teflon to minimize wall loss

of OH radicals. To rapidly establish a stable profile of the target compound concentration, helium gas was always slowly supplied to the inner tube of the sliding injector together with the target compound. The position of the sliding injector was controlled by a pulse stage connected with a pulse controller. In the case of the DF method, a small correction factor (usually 1–3%) was applied to each pseudo-first-order rate constant to account for the axial diffusion effects [13]. Monitoring of the OH radical concentration and gas handling for the DF method were the same as for the FP method shown in Figure 1.

The temperature of the reactor was maintained either by an electric heater or by circulating water or a refrigerant (Fluorinert or ethanol–water mixture) in the outer jacket of the reaction cell from a thermostated bath. The temperature was measured with a CA thermocouple at a spot 1–2 cm downstream from the probe laser beam (LP and FP methods) or at the top of the inner tube of the sliding injector (DF method). During the experiments, the temperature across the reaction volume was maintained within ±2 K over the temperature range examined. The measurements were carried out over the temperature range 250–430 K. The gas flow rates, the total pressure, and the reaction temperature were monitored by the sub computer through a digital recorder and were stored in the main computer via an RS-232C circuit. To ensure that the experimental data were free from unexpected errors, the experiments were repeated at intervals from several days to several months under a variety of flow conditions.

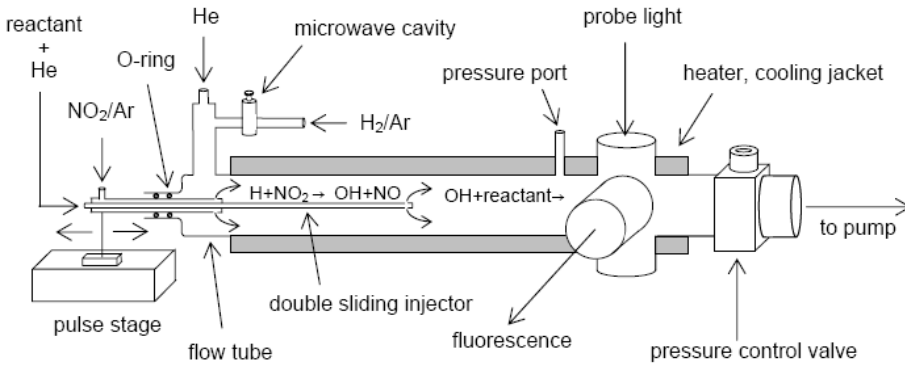

Figure 2. Schematic diagram of discharge flow reactor.

In the case of the DF method, the initial concentration of OH radicals, which is a function of the hydrogen flow rate, was $2 \times 10^{10} - 1.0 \times 10^{11}$ molecule cm^{-3}. For the LP and FP methods, the initial concentration of OH radicals, which was

estimated from comparison with fluorescence intensities obtained by the DF method, was always kept less than 10^{11} molecule cm^{-3}.

2.3. PURIFICATION AND ANALYSIS OF FLUORINATED COMPOUNDS

As stated in section 2.1, the effect of reactive impurities contained in the target compound is a serious problem with the absolute rate method. Therefore, we purified the samples by means of gas chromatography.

Figure 3 shows a schematic diagram of the sample purification apparatus. An evacuated sampling tube (10–25 cm^3 inner volume) was charged with the sample gas or vapor through an electromagnetic valve (V_3) and then introduced into a stainless steel column (7.4–9.6 mm i.d., 4–8 m long) by means of a six-way switching cock (V_1). For many of the samples, a column packed with Silicone DC 702 (Shimadzu) was used. Nitrogen was used as the carrier gas. The middle fraction of the main peak was collected through a four-way switching cock (V_2) into a trap cooled with liquid nitrogen at the timing shown in a example of chromatograph of Figure 3. The switching cock (V_1) and the electromagnetic valves (V_3 and V_4) were operated by a valve controller according to the predetermined interval, and the switching cock (V_2) was operated at timing that depended on the retention time of the main peak. During a purification, the sampling tube was evacuated with a pump through a electromagnetic valve (V_4), and new sample was introduced into the tube for the next cycle through a valve (V_3). This procedure was automatically repeated hundreds of times to collect sufficient amounts of the purified sample. For purification of liquid samples, the sample was supplied to the column by an autoinjector (Shimadzu, AOC-20 i) instead of the sampling tube and V_1. The purification rate was approximately a few cubic centimeters (purified liquid base) per day at most. The actual purification rate depended on such factors as the purity of the original sample, the required purity level of the purified sample, the retention times of the impurity peaks relative to the retention time of the main peak, the sample vapor pressure, and so on. The yield of the purified sample was approximately one-quarter of the original sample. If the residue that effused during the time before and after collection of the purified sample and the residue in the dead volume of the sample supply line were collected with additional traps (T_2 and T_3), the total recovery was approximately 80% or more. Because the impurity level of the material collected in trap T_2 was only slightly higher than that of the original sample, the material

collected in traps T_2 and T_3 could be used in the purification cycle again. To obtain an amount of sample that was sufficient for measuring the temperature dependence of the reaction rate by means of several techniques, the purification process had to be carried out continuously for at least a month.

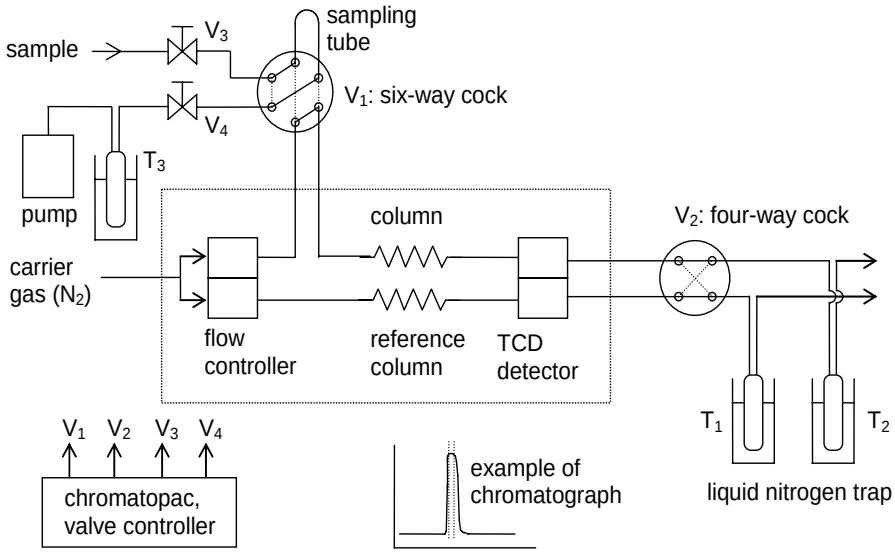

Figure 3. Schematic diagram of sample purification apparatus.

The purities of the purified samples and the original samples were determined by using a gas chromatograph with an FID detector, and the integrated intensity of the main peak relative to the total area was taken as the sample purity. Usually, the samples were analyzed with a stainless steel column packed with Silicone DC 702 (3 mm i.d., 5–15 m long) and with G-205 (1.2 mm i.d., 40 m long, 5 μm film thickness, Chemicals Inspection & Testing Institute, Japan). In addition to these two columns, a different column packing, such as Porapak QS (Waters) or Silicone SE-54 (GL Science) was used, and columns such as G-950 and so on were also used in the analyses. The lowest of the values obtained with the various columns was taken as the sample purity.

Chapter 3

RESULTS OF KINETIC MEASUREMENTS

3.1. DATA ANALYSIS FOR THE ABSOLUTE RATE METHOD

As mentioned in section 2.1, in the case of the absolute rate method, the reaction is carried out under first-order conditions, and the rate constant is obtained from the decrease in the OH radical concentration during the reaction. The following reactions occur in this system:

$$OH + RH \rightarrow \text{Product(s)} \tag{3.1.1}$$

$$OH \rightarrow \text{Loss} \tag{3.1.2}$$

where RH refers to the target compound, such as a fluorinated compound. Equation 3.1.2 represents the loss of OH radicals to reactions other than reaction with the target compound. Loss processes include diffusion, heterogeneous wall reactions, and reactions with trace impurities in the carrier gas. If the initial concentration of OH radicals is less than about 10^{11} molecule cm^{-3}, the effect of reaction of OH radicals with reaction products can be ignored. Because the concentration of the target compound is on the order of 10^{14}–10^{16} molecule cm^{-3}, the reaction conditions are clearly pseudo-first-order, and the changes in the concentration of the target compound during the reaction can be ignored. From Equations 3.1.1 and 3.1.2, the change in OH radical concentration can be expressed as follows:

$$\ln \frac{[\mathrm{OH}]_t}{[\mathrm{OH}]_0} = -(k_1[\mathrm{RH}]_0 + k_2)t = -k't \tag{3.1.3}$$

where k_1 and k_2 are the rate constants for the reactions shown in Equations 3.1.1 and 3.1.2, respectively; $[OH]_0$ and $[RH]_0$ are the initial concentrations of OH radicals and the target compound, respectively; and $[OH]_t$ is the OH radical concentration at reaction time t. Here, k' can be expressed as follows:

$$k' = k_1[RH]_0 + k_2 \tag{3.1.4}$$

The pseudo-first-order rate constant k' can be obtained from the slope of the plot of the logarithm of OH radical concentration in arbitrary units as function of reaction time t. The value of k' is measured for various values of $[RH]_0$; and using Equation 3.1.4, the absolute value of k_1 can be obtained from the slope of the plot of k' as a function of $[RH]_0$.

As is apparent from Equation 3.1.3, calibration of the OH radical concentration is not necessary, because the absolute rate constant can be calculated from the ratio of the OH radical concentration at reaction time t, $[OH]_t$, to the initial OH radical concentration, $[OH]_0$, which removes the error that would be introduced by calibration of the OH radical concentration. Therefore, an accurate rate constant can be obtained directly. However, if the target compound contains reactive impurities such as unsaturated compounds, the reaction of OH radicals with the impurities reduces the OH radical concentration. As a result, the measured rate constant is an overestimation of the actual rate constant. Therefore, high-purity samples must be used to avoid the influence of reactive impurities.

Figure 4 shows a typical example of a pseudo-first-order OH radical decay plot obtained with the FP method for various CH_2FCHF_2 (HFC-143) concentrations. Values of k' can be derived from the slopes of the straight lines by a least-squares fit to each decay plot. In Figure 5, the observed values of k' are plotted against HFC-143 concentration. The plotted points are distributed along a straight line, and the bimolecular rate constant for the reaction of OH radicals with HFC-143 can be derived from the slope by the linear least-squares fit to the observed data.

In the case of the FP and LP methods, the small intercept observed when there is no target compound (k_d) is mainly caused by diffusion of OH radicals from the viewing zone, and partially caused by reaction of OH radicals with impurities contained in the gas mixture. In contrast, in the case of the DF method, the intercept for zero reactant (k_w) is attributable to the wall loss of OH radicals and also to a gas-phase reaction, such as $OH + NO_2 + M \rightarrow HNO_3 + M$. Thus, the origins of k_d and k_w depend on the experimental conditions.

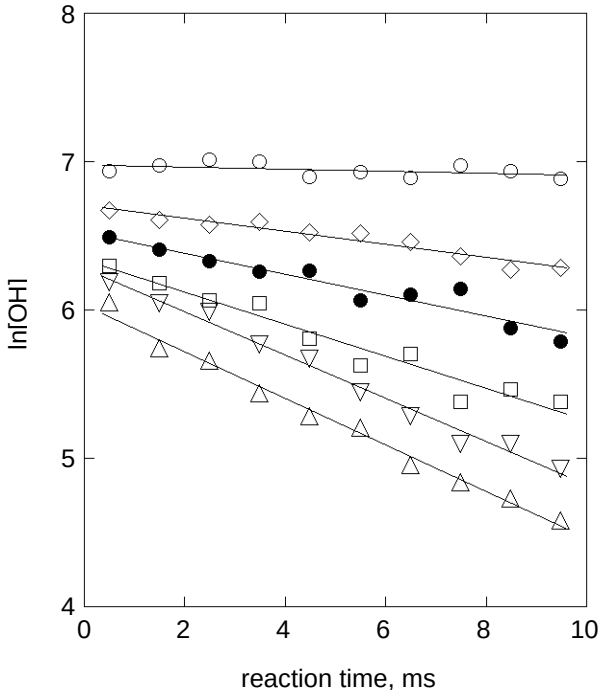

Figure 4. Pseudo-first-order decay of OH for various HFC-143 concentrations. FP-LIF method, p=20torr, T=298K. [HFC-143], 1015 molecule cm-3; (○), 0; (◊), 1.91; (●), 3.83; (□), 5.72; (▽), 7.60; (Δ), 9.48.

To ensure that there were no unexpected errors, the experiments were repeated at intervals ranging from several days to a few months under a variety of experimental conditions; the following parameters were varied: linear flow velocity of the gas mixture, total pressure, H_2O concentration (FP method), H_2O and N_2O concentrations (LP-H_2O method), H_2O_2 concentration (LP-H_2O_2 method), energy of flash lamp or excimer laser (FP or LP methods), and NO_2 and H_2 concentrations (DF method). For each reaction temperature and method, the experiments were typically repeated six times, and the results are summarized in plots like the one shown in Figure 6. In this figure, the observed data for ($k' - k_d$) are plotted against HFC-143 concentration for various temperatures. The background value (k_d) is subtracted from each set of k' values, and the resulting values are plotted as a function of HFC-143 concentration. All the plots give linear relationships with relatively small scatters.

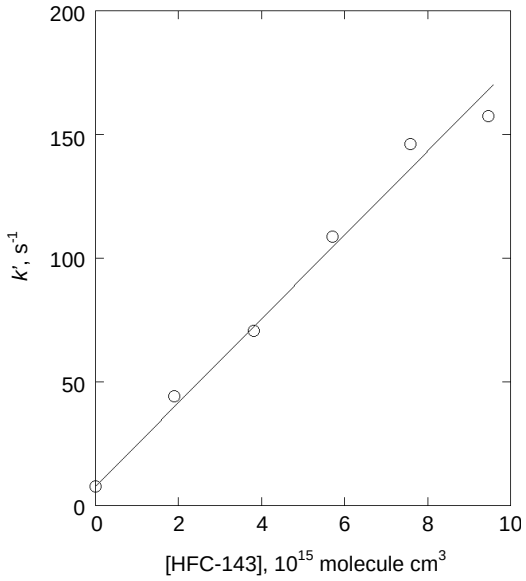

Figure 5. Plot of the observed pseudo-first-order rate constant k_{obs} against HFC-143 concentration. FP-LIF method, p=20torr, T=298K.

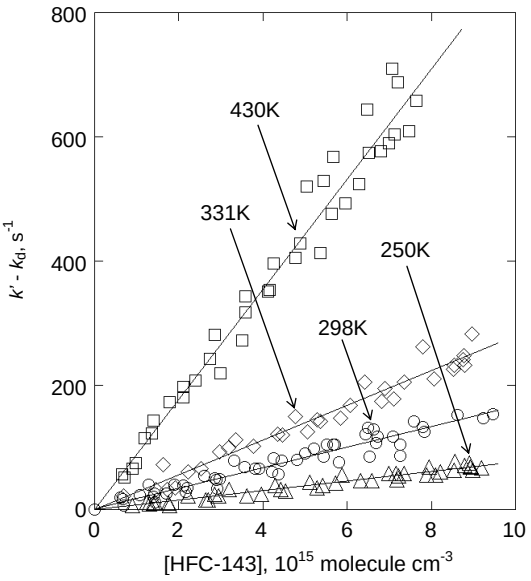

Figure 6. Plot of the pseudo-first-order rate constants corrected for wall loss, k_{obs}-k_d, against HFC-143 concentration. FP-LIF method. (Δ), 250K; (○), 298K; (◊), 331K; (□), 430K.

Thus, we concluded that the rate constants derived from the least-squares fits to the plot were not affected by any experimental factors, such as the total pressure, the residence time of the gas mixture, or the H_2O concentration.

3.2. EFFECTS OF IMPURITIES

Figure 7 shows the GC traces for HCFC-142b before and after purification. Both traces were recorded at the same sensitivity, and the actual height of the main peak is around 1000 times as high as the height shown in the figure. In the original sample, there were two large impurity peaks before the main peak and a few additional small peaks before and after the main peak. The impurities were not identified. After purification, the intensities of the two main impurity peaks were drastically reduced, and the smaller peaks disappeared. The purities were estimated to be 99.9 and 99.9987%, respectively, for the original and purified samples. Thus, the impurity level of the sample was reduced by about two orders of magnitude by a single purification process.

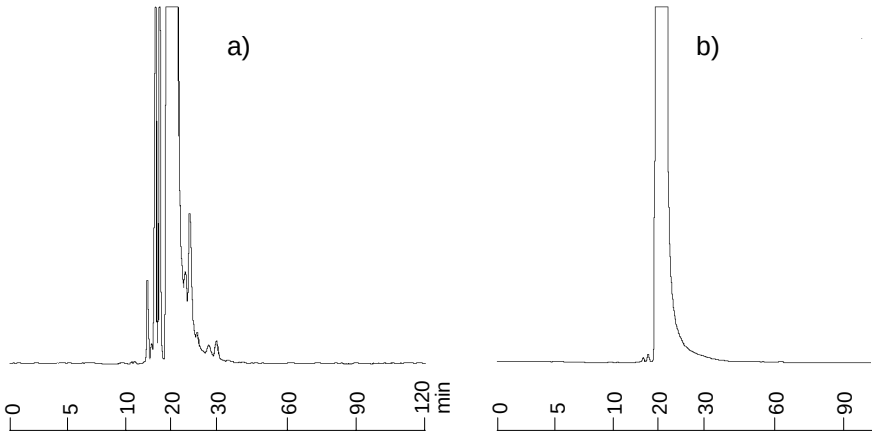

Figure 7. Analytical results of HCFC-142b. a) original sample (99.9%), b) purified sample (99.9987%). Analytical conditions; Silicone DC 702 3mmφ×15m, N2 carrier (30cm3 min-1), column temp. 313K, sample volume 1cm3, FID detector.

To examine the adequacy of this purification method for kinetic measurements, we prepared samples with different purity levels by the GC method and subjected them to kinetic measurements. The rate constants at 298 K

measured by means of the FP, LP-H_2O, and DF methods are plotted in Figure 8 as a function of the logarithm of the impurity concentration. The error limits are at the 95% confidence level derived from the linear least-squares fit. The systematic errors are not contained here. We estimated the systematic errors in our experiments to be less than ±10%. The solid line in this figure represents the result of the linear least-squares fit to the measured rate constants versus impurity concentration. The rate constant for the original sample (99.9% pure) at 298 K was found to be about 1.2×10^{-14} cm^3 $molecule^{-1}$ s^{-1} on average, which is about 3.5 times as large as the value recommended by the Jet Propulsion Laboratory (JPL) [2]. As can be seen in the figure, the apparent rate constant decreases as the impurity level decreases and almost reaches a constant value when the impurity level falls below about 0.004% (purity > 99.996%). By extrapolating to an impurity level of zero, we obtained a rate constant of $(3.52 \pm 0.32) \times 10^{-15}$ cm^3 $molecule^{-1}$ s^{-1}. From the values of the measured rate constant, we estimated the influence of the impurities to be 11.4% for the sample with 99.996% purity on the assumption that the rate constant for the impurities was as large as 1×10^{-11} cm^3 $molecule^{-1}$ s^{-1} (the worst case conceivable).

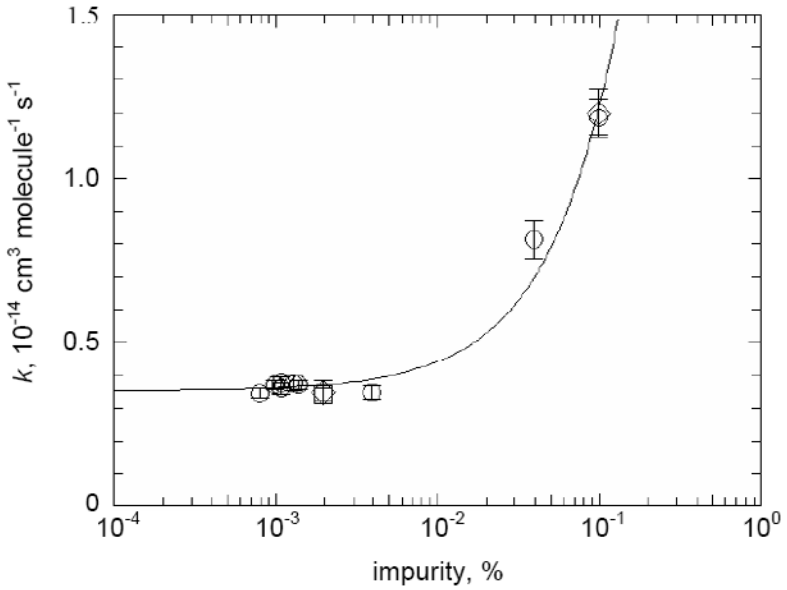

Figure 8. Measured rate constant of OH with HCFC-142b for various impurity level. (◇), FP; (□), LP-H_2O; (○), DF. T=298K. The error bars represent 95% confidence level from linear least squares analysis.

If the sum total of impurities removed from the original sample was responsible for the decrease in the observed rate constant, the corresponding rate constant for reaction of the impurities with OH radicals would be 8.5×10^{-12} cm^3 $molecule^{-1}$ s^{-1}. The estimated rate constant for the impurities contained in the original sample indicates that their influence on the measured rate constants can be no larger than 8.8% for a sample of 99.996% purity. Therefore, we concluded that the effects of any remaining impurities in the purified HCFC-142b sample can be neglected and that the GC purification method is adequate for kinetic measurements.

3.3. Rate Constants for Reactions of OH Radicals with Fluorinated Compounds

As will be described later, in some cases, the effects of impurities in the original samples on the measurement of rate constants at room temperature were negligible. At lower temperatures, however, because reactive impurities can strongly affect the rate constant measurement if their activation energies are low, purified samples were used for measurements of the temperature dependence of the rate constants. The purities of the original and purified samples used in the measurements are listed in Table 1 together with the measured rate constants obtained by various methods at 298 K.

Experiments were usually repeated at least six times (40–60 measurements of OH radical decay) at a given temperature for each experimental method. In all cases, the OH radical decay showed exponential behavior, and the linearity and scatter of the plotted points for individual experiments were much the same as those shown in Figure 4. In addition, the linearity and scatter of the plotted points for the pseudo-first-order rate constants versus the concentration of the target compound for individual experiments were much the same as those shown in Figures 5 and 6.

Experimental conditions and measured rate constants for reactions of 11 HCFCs and 12 HFCs with OH radicals over the temperature range 250–430 K obtained by means of the FP, LP-H_2O, LP-H_2O_2, and DF methods combined with LIF are listed in even-numbered tables numbered from 2 to 46. In these tables, the concentration ranges for the HCFC or HFC (sixth column) represent the minimum and maximum concentrations during repeated experiments. The error limits are at the 95% confidence level derived from the linear least-squares fit to the plot of ($k' - k_d$) (FP and LP methods) or ($k' - k_w$) (DF method) versus reactant concentration.

Table 1. Observed values of the rate constants for the reactions of OH radicals with fluorinated compounds at 298K

fluorinated compound	technique	original sample		purified sample	
		k, 10^{-15} cm^3 $molecule^{-1}$ s^{-1}	purity, %	k, 10^{-15} cm^3 $molecule^{-1}$ s^{-1}	purity, %
HCFC-22	FP	4.75±0.24	99.994	4.44±0.22	99.997
	LP-H_2O	4.79±0.25			
	DF	5.15±0.15		4.89±0.17	
HCFC-123	FP		99.94	35.6±1.2	99.98
	DF	35.4±0.8		36.0±0.8	
HCFC-123a	FP	17.3±0.5	98.5	11.7±0.3	99.98
	LP-H_2O	17.5±0.9		11.4±0.6	
HCFC-124	FP	11.7±0.9	98.9	9.41±0.43	99.999
	LP-H_2O			9.25±0.40	
	LP-H_2O_2	10.7±0.4		9.74±0.39	
HCFC-132b	LP-H_2O		99.4	17.3±1.7	99.982
	DF	25.6±3.7		18.3±0.6	
HCFC-133a	FP	35.4±1.8	99.8		99.993
	LP-H_2O			14.2±0.7	
	DF	41.2±2.0		15.3±0.5	
HCFC-141	FP	71.3±2.4	99.8	71.9±3.2	99.98
	LP-H_2O	70.0±4.1		76.2±3.2	
	DF	80.2±2.2		80.8±3.4	
HCFC-141b	LP-H_2O_2		98.9	6.40±0.22	99.99
	DF	16.3±0.7		6.84±0.26	
HCFC-142b	FP	12.0±0.7	99.9	3.47±0.34	99.998
	LP-H_2O			3.40±0.19	
	DF	11.9±0.6		3.62±0.06	99.996
HCFC-243db	FP	46.4±2.3	99.72	45.4±1.9	99.996
	LP-H_2O	44.7±2.5		48.0±1.8	
	DF	47.7±3.3		50.1±4.1	
HCFC-253fb	FP	64.4±2.7	99.83	62.3±2.5	99.993
	LP-H_2O	65.4±2.5		68.5±3.0	
	DF	68.2±2.1		64.7±1.5	
HFC-32	FP	10.1±0.5	99.95	10.4±0.5	99.99
	LP-H_2O	10.7±0.2		10.8±0.4	
	DF	9.30±0.27		9.70±0.46	
HFC-125	FP	1.86±0.12	99.87	1.94±0.13	99.99
	LP-H_2O	2.24±0.07		2.04±0.05	
	DF	2.19±0.13		2.08±0.11	

Table 1. (Continued)

fluorinated compound	technique	original sample		purified sample	
		k, 10^{-15} cm^3 $molecule^{-1}$ s^{-1}	purity, %	k, 10^{-15} cm^3 $molecule^{-1}$ s^{-1}	purity, %
HFC-134a	FP	4.28±0.30	99.8	4.17±0.39	99.965
	DF	4.68±0.14		4.63±0.09	
HFC-143	FP		99.96	16.4±0.9	99.992
	LP-H_2O			18.4±0.9	
	DF	19.4±1.5		17.1±0.4	
HFC-152a	FP		99.998	36.1±2.4	99.999
	LP-H_2O			36.5±1.1	
	DF	37.1±0.9		37.2±1.0	
HFC-236ea	FP	7.95±0.27	98.5	4.56±0.23	99.997
	LP-H_2O	8.30±0.61		4.63±0.28	
HFC-245ca	FP	8.18±0.33	99.1	7.50±0.37	99.98
	LP-H_2O	9.20±0.52		8.24±0.34	
HFC-245eb	FP	32.4±1.4	94.3	14.5±0.6	99.98
	LP-H_2O	32.1±1.3		15.3±0.6	
HFC-245fa	FP	6.39±0.26	99.82	5.79±0.20	99.9998
	LP-H_2O	6.49±0.25		5.87±0.24	
HFC-254fb	FP	42.1±1.2	99.0	42.3±1.1	99.995
	LP-H_2O	44.4±1.6		43.9±1.5	
HFC-272ca	FP	48.8±1.6	97.8	21.4±0.6	99.94
	LP-H_2O	48.3±2.1		21.3±1.0	
HFC-43-10mee	FP	2.55±0.10	99.52	2.48±0.14	99.98
	LP-H_2O	2.58±0.18		2.56±0.13	

The quoted errors represent 95% confidence level from the linear least squares analysis.

Figures 9–31 show Arrhenius plots of the rate constants for reactions of the HCFCs and HFCs with OH radicals. The Arrhenius rate parameters and the room temperature rate constants obtained in the present study are summarized in odd-numbered tables from 3 to 47. Results reported by other groups are also shown in these figures and tables. In the tables, the error limits for the published results are those quoted by the respective authors, and our error values are at the 95% confidence level derived from the unit-weighted nonlinear least-squares fit to the data shown in Figures 9–31. In our results, systematic errors were not considered; the systematic errors in our experiments were estimated to be less than ±10%. The recommended rate expressions and the room temperature rate constants based on the present work and on values reported by other groups, if available, are also listed in odd-numbered tables from 3 to 47. In deriving the recommendations, we considered the rate constants in the temperature range 250–500 K.

CHF_2Cl (HCFC-22)

The rate constants for reaction of the purified sample of CHF_2Cl (HCFC-22) with OH radicals are on average about 4.7% smaller than those of the original sample (Table 2).

Table 2. Experimental conditions and results for measurements of OH radicals with HCFC-22

temperature, K	technique	k, 10^{-15}, cm^3 $molecule^{-1}$ s^{-1}	$\bar{t}$, s or U, m s^{-1} [a]	pressure, torr	[HCFC-22], 10^{15} molecule cm^{-3}	no. of expts.
250	FP	1.56±0.09	0.31 - 0.42	20 - 40	1.28 - 9.10	6
	LP-H_2O	1.64±0.15	0.33 - 0.56	40 - 80	1.64 - 27.4	7
273	LP-H_2O	2.78±0.24	0.36 - 0.52	40 - 80	1.90 - 15.6	6
	DF	2.88±0.15	4.8 - 6.1	6	1.71 - 11.3	5
298	FP	4.44±0.22	0.27 - 0.40	20 - 60	1.02 - 9.44	6
	DF	4.89±0.17	4.2 - 8.5	6	1.27 - 9.10	9
331	DF	7.78±0.35	5.9 - 7.5	6	0.77 - 9.14	7
375	DF	13.4±0.4	7.1 - 9.2	6	0.68 - 6.92	9
403	DF	18.5±0.9	6.5 - 10.1	6	0.43 - 7.14	7
430	FP	22.9±0.9	0.25 - 0.35	20 - 40	0.85 - 9.44	6
	LP-H_2O	23.6±0.6	0.25 - 0.36	20 - 60	0.94 - 9.44	6
	DF	25.6±0.8	6.9 - 14.4	4 - 6	0.44 - 5.32	6

[a] $\bar{t}$, residence time for FP and LP methods; U, linear flow velocity for DF method.
The quoted errors represent 95% confidence level from linear least squares analysis.
The purity of the sample used in the measurement was 99.997%.

Even if the rate constant of the impurities remaining in the purified sample is as large as 1×10^{-11} cm^3 $molecule^{-1}$ s^{-1}, their influence on the measured rate constants can be no larger than 6.4% of the observed value. Therefore, we concluded that the effect of any impurities remaining in the purified samples was negligible.

The results of our measurements of the rate constants for HCFC-22 are listed in Table 2. Figure 9 shows the Arrhenius plots. Table 3 summarizes the room temperature rate constants and Arrhenius parameters obtained in this study as well as values reported by other groups.

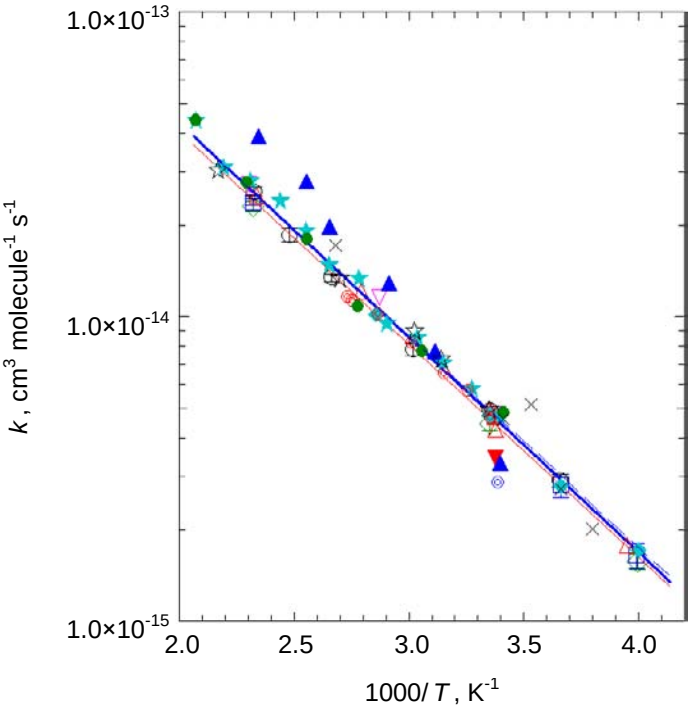

Figure 9. Arrhenius plots of the reaction rate coefficients for OH with HCFC-22. The error bars represent 95% confidence level from linear least squares analysis. (◇), FP; (□), LP-H_2O; (○), DF; red solid line, nonlinear fit to the present work. (☆), Orkin and Khamaganov [18]; (▼), Howard and Evenson [17]; (▽), Atkinson et al. [19]; (◎), Cavalli et al. [15]; (◆), Watson et al. [20]; (■), Paraskevopoulos et al. [25]; (Δ), Chang and Kaufman [21]; (●), Jeong and Kaufman [22]; (▲), Clyne and Holt [16]; (×), Handwerk and Zellner [23]; (◎), Hsu and DeMore [14]; (★), Fang et al. [24]; blue dashed line, JPL 06-2 [2]; blue thick line, recommendation of this work.

The results of Hsu and DeMore [14] and Cavalli et al. [15] obtained by means of the relative rate method were recalculated on the basis of the value recommended by JPL [2] for reference reaction of OH radicals with CH_4. The frequency factor and temperature dependence reported by Clyne and Holt [16] are considerably larger than ours.

Table 3. Summary of the rate constants for the reaction of OH radicals with HCFC-22

A [a], 10^{-12} cm^3 $molecule^{-1}$ s^{-1}	E/R [a], K	k_{298} [a], 10^{-15} cm^3 $molecule^{-1}$ s^{-1}	T range, K	technique [b]	reference
0.81 +0.15, -0.12	1516±53	4.9±0.45	298-460	DF-EPR	Orkin and Khamaganov [18]
		3.4 ±0.7 [f]	296	DF-LMR	Howard and Evenson [17]
1.21	1635±151	4.75±0.48 [g]	297-434	FP-RF	Atkinson et al. [19]
		2.84 [c, e]	295	RR	Cavalli et al. [15]
0.925±0.10	1575±71	4.8±0.3	250-350	FP-RF	Watson et al. [20]
		4.58±0.58 [g]	297	FP-RA	Paraskevopoulos et al. [25]
1.20±0.16	1657±39	4.3	253-427	DF-RF	Chang and Kaufman [21]
1.28±0.33	1671±96	4.75±0.63	293-482	DF-RF	Jeong and Kaufman [22]
9.55 +1.67, -1.42	2300±200	4.1±0.9	294-426	DF-RF	Clyne and Holt [16]
2.1 ±0.6	1780±150	5.3	263-373	FP-RA	Handwerk and Zellner [H2]
0.588 [c]	1433 [c]	4.80 [c, d]	298-366	RR	Hsu and DeMore [14]
$(3.10\pm0.2)\times10^{-6}\ T^{1.94\pm0.01}$	1112±26	4.69 [d]	294-807	LP-LIF	Fang et al. [24]
1.00±0.13	1610±40	4.57±0.12 [d]	250-430	FP-LIF LP-LIF DF-LIF	this work
1.05	1600	4.8			JPL 06-2 [2]
1.10±0.13	1620±40	4.77±0.12			this work

[a] The error limits are those quoted by the authors. Our values are 95% confidence level and do not include systematic errors.

[b] FP, flash photolysis; LP; laser photolysis; DF, discharge flow; LIF, laser induced fluorescence; EPR, electron paramagnetic resonance; LMR, laser magnetic resonance; RF, resonance fluorescence; RA, resonance absorption; RR, relative rate method.

[c] Recalculated based on the recommendation [2] of reference reaction.

[d] Derived from the Arrhenius rate parameters.

[e] at 295K.

[f] at 296K.

[g] at 297K.

The room temperature rate constants reported by Howard and Evenson [17] and Cavalli et al. [15] are about 26 and 38% smaller than ours.The results of other groups agree reasonably well with the present results. The recommended rate expression listed in Table 3 was derived from the present results; those of Orkin and Khamaganov [18], Atkinson et al. [19], Watson et al. [20], Chang and Kaufman [21], Jeong and Kaufman [22], Handwerk and Zellner [23], Hsu and DeMore [14], and Fang et al. [24] (below 481 K); and the room temperature rate constant of Paraskevopoulos et al. [25]. The present recommended rate expression agrees with that of JPL within 5% over the temperature range 250–500 K.

$CHCl_2CF_3$ (HCFC-123)

The concentration of impurities in the purified sample of $CHCl_2CF_3$ (HCFC-123) is approximately 1/3 that in the original sample, and the measured rate constants of the original and purified samples are essentially identical (Table 1). From the purity and the measured rate constants, the influence of impurities was estimated to be 0.6%, on the assumption that the rate constant for the reaction of the impurities with OH radicals is as large as 1×10^{-11} cm^3 $molecule^{-1}$ s^{-1} (the worst case conceivable).

The rate constants for the reaction of HCFC-123 with OH radicals and the experimental conditions are summarized in Table 4. The Arrhenius plots and rate parameters measured in this work and reported by other groups are shown in Figure 10 and Table 5. The results obtained by Hsu and DeMore [14] using the relative rate method were recalculated on the basis of the value recommended by JPL [2] for HFC-152a as a reference compound ($k = 2.33 \times 10^{-12}\exp(-1260/T)$ at temperatures above room temperature). The results reported by Clyne and Holt [16], Nielsen [26], and Brown et al. [27] are higher than ours over the entire temperature range. The room temperature rate constant of Howard and Evenson [28] is about 20% smaller than ours. Watson et al. [29] studied this reaction using a 99.8% pure sample and corrected for the effects of alkene impurities. As is apparent in Figure 10, the results of Watson et al. are very close to ours. At higher temperature, the results of Yamada et al. [30] are slightly higher than ours.

Table 4. Experimental conditions and results for measurements of OH radicals with HCFC-123

temperature, K	technique	k, 10^{-14}, cm^3 $molecule^{-1}$ s^{-1}	$\bar{t}$, s or U, m s^{-1} [a]	pressure, torr	[HCFC-123], 10^{15} molecule cm^{-3}	no. of expts.
250	FP	1.84±0.07	0.08 - 0.36	5 - 30	0.95 - 9.66	7
	LP-H_2O	1.84±0.08	0.24 - 0.42	20 - 60	0.34 - 4.68	8
273	DF	2.64±0.15	5.8 - 10.6	4 - 5	0.58 - 4.41	6
298	FP	3.56±0.12	0.29 - 0.41	20 - 40	0.83 - 9.45	6
	DF	3.60±0.08	9.0 - 12.5	3 - 4	0.51 - 3.78	12
331	DF	4.91±0.18	9.4 - 15.1	3 - 4	0.43 - 3.28	6
375	LP-H_2O	7.07±0.34	0.28 - 0.35	20 - 40	0.91 - 9.40	6
	DF	6.80±0.17	8.3 - 14.0	4 - 5	0.27 - 2.79	6
403	DF	8.20±0.20	8.4 - 14.8	4 - 6	0.22 - 2.38	5
430	FP	9.52±0.38	0.25 - 0.35	20 - 40	0.67 - 9.17	7
	LP-H_2O	10.6±0.4	0.21 - 0.37	20 - 40	0.34 - 9.74	6
	DF	10.1±0.4	11.9 - 21.2	3 - 4	0.26 - 1.85	6

[a] $\bar{t}$, residence time for FP and LP methods; U, linear flow velocity for DF method.

The quoted errors represent 95% confidence level from linear least squares analysis.

The purity of the sample used in the measurement was 99.98%.

Table 5. Summary of the rate constants for the reaction of OH radicals with HCFC-123

A [a], 10^{-12} cm^3 $molecule^{-1}$ s^{-1}	E/R [a], K	k_{298} [a], 10^{-15} cm^3 $molecule^{-1}$ s^{-1}	T range, K	technique [b]	reference
1.12 +0.05, -0.05	1000±100	4.2±0.2	293-429	DF-RF	Clyne and Holt [16]
0.652 [c)]	895 [c)]	3.24 [c, d)]	298-359	RR	Hsu and DeMore [14]
1.4 ±0.4	1102 +157, -106	3.6±0.4	245-375	FP-RF	Watson et al. [29]
1.1±0.2	1040±140	3.36 [d)]	270-400	FP-RF	Liu et al. [32]
0.65 +0.11, -0.10	840± 40	3.69±0.37	213-322	FP-LIF DF-LMR	Gierczak et al. [31]
		2.84±0.43 [e)]	296	DF-LMR	Howard and Evenson [28]
$(2.20\pm0.25)\times10^{-7}\cdot T^{2.26\pm0.10}$	266±51	4.03 [d)]	296-866	LP-LIF	Yamada et al. [30]
1.1	940±200	4.69 [d)]	295-385	PR-KS	Nielsen [26]
1.18	900±150	5.9±0.6	303-426	DF-RF	Brown et al. [27]
1.02±0.10	1000±30	3.53±0.08 [d)]	250-430	FP-LIF LP-LIF DF-LIF	this work
0.63	850	3.6			JPL 06-2 [2]
1.08±0.24	1020±70	3.55±0.14			this work

[a] The error limits are those quoted by the authors. Our values are 95% confidence level and do not include systematic errors.

[b] FP, flash photolysis; LP, laser photolysis; DF, discharge flow; PR, pulse radiolysis; LIF, laser induced fluorescence; KS, kinetic spectroscopy; LMR, laser magnetic resonance; RF, resonance fluorescence; RR, relative method.

[c] Recalculated based on the recommendation [2] of reference reaction.

[d] Derived from the Arrhenius rate parameters.

[e] at 296K.

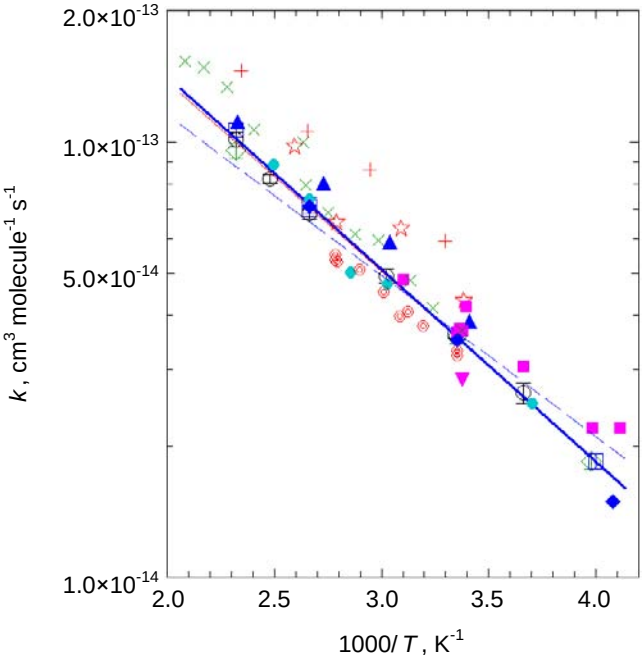

Figure 10. Arrhenius plots of the reaction rate coefficients for OH with HCFC-123. The error bars represent 95% confidence level from linear least squares analysis. (◇), FP; (□), LP-H_2O; (○), DF; red solid line, nonlinear fit to the present work. (▲), Clyne and Holt [16]; (◎), Hsu and DeMore [14]; (◆), Watson et al. [29]; (●), Liu et al. [32]; (■), Gierczak et al. [31]; (▼), Howard and Evenson [28]; (×), Yamada et al. [30]; (☆), Nielsen [26]; (+), Brown et al. [27]; blue dashed line, JPL 06-2 [2]; blue thick line, recommendation of this work.

In contrast, at lower temperature, the results of Gierczak et al. [31] are slightly higher than ours. However, these two results agree with ours in the middle temperature range (about room temperature to 400 K). The recommended rate expression was derived from the present results; the results of Liu et al. [32], Gierczak et al. [31] (above 251 K), and Yamada et al. [30] (below 479.6 K); and the relative rate study of Hsu and DeMore [14]. The present recommended room temperature rate constant is very close to the JPL value (within 3%), and the temperature dependence observed in this study is about 20% larger than that of JPL. The difference between our temperature dependence and that of JPL seems to be due to the difference in the temperature ranges considered.

$CHFClCF_2Cl$ (HCFC-123a)

The concentration of impurities in the purified sample of $CHFClCF_2Cl$ (HCFC-123a) is approximately 1/75 that in the original sample, and the measured room temperature rate constants of the purified sample are on average about 34% smaller than those of the original sample (Table 1). If the sum total of impurities removed from the original sample is responsible for the decreases in the observed rate constants, the rate constant for reaction of the impurities with OH radicals is 4×10^{-13} cm^3 $molecule^{-1}$ s^{-1}. If the rate constant for reaction of impurities remaining in the purified sample is as large as 1×10^{-11} cm^3 $molecule^{-1}$ s^{-1}, the influence of the impurities on the measured rate constant can be estimated to be about 17%. If the rate constant for the impurities remaining in the purified sample is as large as 4×10^{-13} cm^3 $molecule^{-1}$ s^{-1}, the influence of the impurities on the measured rate constant can be no larger than 0.7% of the observed values for the purified sample. Thus, the effect of any impurities remaining in the purified sample seems to be negligible.

Table 6. Experimental conditions and results for measurements of OH radicals with HCFC-123a

Temperature, K	technique	k, 10^{-15}, cm^3 $molecule^{-1}$ s^{-1}	$\bar{t}$, s [a]	pressure, torr	[HCFC-123a], 10^{15} molecule cm^{-3}	no. of expts.
250	FP	4.98±0.16	0.26 - 0.47	20 - 80	0.68 - 9.63	7
	LP-H_2O	4.67±0.35	0.27 - 0.43	40 - 100	0.75 - 9.80	7
273	FP	7.78±0.32	0.28 - 0.44	20 - 80	0.81 - 9.41	7
298	FP	11.7±0.3	0.16 - 0.47	20 - 40	0.69 - 9.25	8
	LP-H_2O	11.4±0.6	0.37 - 0.54	20 - 60	0.98 - 9.39	6
331	FP	18.2±0.6	0.31 - 0.46	40 - 60	1.04 - 11.6	7
375	FP	28.9±1.6	0.23 - 0.45	20 - 60	0.76 - 9.39	7
430	FP	48.1±1.9	0.32 - 0.45	20 - 80	0.84 - 10.0	8
	LP-H_2O	46.9±2.3	0.22 - 0.48	20 - 60	0.83 - 9.62	7

[a] $\bar{t}$, residence time for FP and LP methods. The quoted errors represent 95% confidence level from linear least squares analysis. The purity of the sample used in the measurement was 99.98%.

The results and experimental conditions for the reaction of OH radicals with HFC-123a are summarized in Table 6. The Arrhenius plots are shown in Figure 11, and the Arrhenius rate parameters are summarized in Table 7.

Table 7. Summary of the rate constants for the reaction of OH radicals with HCFC-123a

A [a], 10^{-12} cm^3 $molecule^{-1}$ s^{-1}	E/R [a], K	k_{298} [a], 10^{-14} cm^3 $molecule^{-1}$ s^{-1}	T range, K	technique [b]	reference
0.92 +0.25, -0.20	1281±85	1.23±0.10	298-460	DF-EPR	Orkin and Khamaganov [18]
1.10±0.11	1360±30	1.16±0.02 [c]	250-430	FP-LIF LP-LIF	this work
0.86	1250	1.3			JPL 06-2 [2]
1.00±0.16	1320±50	1.19±0.04			this work

[a] The error limits are those quoted by the authors. Our values are 95% confidence level and do not include systematic errors.

[b] FP, flash photolysis; LP, laser photolysis; DF, discharge flow; LIF, laser induced fluorescence; EPR, electron paramagnetic resonance.

[c] Derived from the Arrhenius rate parameters.

The only available published data are those of Orkin and Khamaganov [18], which are also shown in Figure 11 and Table 7. The results of Orkin and Khamaganov are about 10% higher than ours over the entire temperature range, but the two sets of results agree with each other within experimental errors. The recommended rate expression was derived from this work and that of Orkin and Khamaganov [18]. The rate constant at 250 K derived from the present recommended rate expression is about 13% smaller than the JPL value, and the difference between the two values becomes small with increasing temperature.

$CHFClCF_3$ (HCFC-124)

The measured rate constants of the purified sample are on average around 15% smaller than those of the original sample (Table 1). From the values of sample purity and the measured rate constants listed in Table 1, the influence of impurities was estimated to be less than 1%, on the assumption that the rate constant for reaction of the impurities with OH radicals is as large as 1×10^{-11}

cm^3 $molecule^{-1}$ s^{-1} (the worst case conceivable). Therefore, we concluded that the effect of any impurities remaining in the purified samples was negligible.

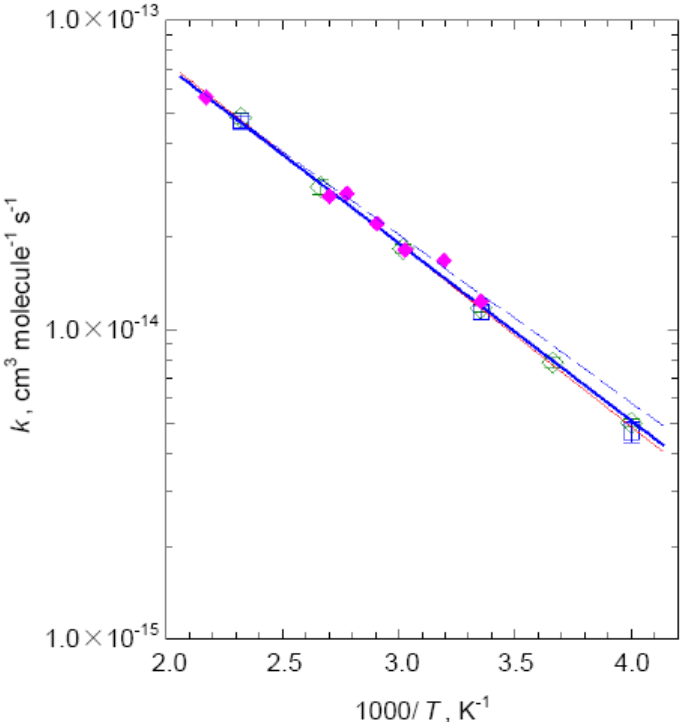

Figure 11. Arrhenius plots of the reaction rate coefficients for OH with HCFC-123a. The error bars represent 95% confidence level from linear least squares analysis. (◇), FP; (□), LP-H_2O; red solid line, nonlinear fit to the present work. (◆), Orkin and Khamaganov [18]; blue dashed line, JPL 06-2 [2]; blue thick line, recommendation of this work.

Our results for reaction of HCFC-124 with OH radicals are summarized in Table 8. The Arrhenius plots and rate parameters together with results published by other groups are shown in Figure 12 and Table 9. The results of the relative rate study by Hsu and DeMore [14] were recalculated on the basis of the JPL recommendations [2] for reference reactions of OH radicals with CH_4 and with HFC-134. The results of this work and those of other groups agree with one another within about 20%, although the room temperature rate constant of Howard and Evenson [28] is about 30% higher than ours. The recommended rate expression was derived from the present results and those of Gierczak et al. [31] (above 258 K), Yamada et al. [30] (below 481 K), Watson et al. [29], and Hsu and

DeMore [14]. The present recommended rate expression agrees with that of JPL within 5% over the temperature range 250–500 K.

Table 8. Experimental conditions and results for measurements of OH radicals with HCFC-124

temperature, K	technique	k, 10^{-15}, cm^3 $molecule^{-1}$ s^{-1}	$\bar{t}$, s [a]	pressure, torr	[HCFC-124], 10^{15} molecule cm^{-3}	no. of expts.
250	FP	3.87±0.17	0.28 - 0.49	20 - 60	0.89 - 9.32	7
	LP-H_2O	3.63±0.18	0.27 - 0.53	20 - 80	1.00 - 9.25	7
273	FP	6.16±0.28	0.35 - 0.45	20 - 60	0.88 - 9.24	6
298	FP	9.41±0.43	0.26 - 0.41	20 - 60	0.80 - 9.28	8
	LP-H_2O	9.25±0.40	0.27 - 0.45	20 - 60	0.80 - 9.42	8
	LP-H_2O_2	9.74±0.39	0.33 - 0.47	40 - 80	0.99 - 9.61	7
331	FP	14.2±0.6	0.32 - 0.46	20 - 60	0.98 - 9.40	6
375	FP	23.1±1.0	0.32 - 0.46	20 - 60	0.99 - 9.29	6
	LP-H_2O	24.0±0.9	0.27 - 0.40	20 - 60	1.14 - 9.31	7
430	FP	40.4±1.0	0.30 - 0.47	20 - 60	0.93 - 9.33	7
	LP-H_2O_2	38.2±1.6	0.32 - 0.42	20 - 60	0.95 - 9.16	7

[a] $\bar{t}$, residence time for FP and LP methods.
The quoted errors represent 95% confidence level from linear least squares analysis.
The purity of the sample used in the measurement was 99.999%.

Table 9. Summary of the rate constants for the reaction of OH radicals with HCFC-124

A [a], 10^{-12} cm^3 $molecule^{-1}$ s^{-1}	E/R [a], K	k_{298} [a], 10^{-15} cm^3 $molecule^{-1}$ s^{-1}	T range, K	technique [b]	reference
0.445 +0.110, -0.088	1150±60	9.44±0.75	210-349	FP-LIF DF-LMR	Gierczak et al. [31]
		12.4±1.9 [e]	296	DF-LMR	Howard and Evenson [28]
$(7.72\pm0.60)\times10^{-8}$ $T^{2.35\pm0.06}$	458±30	10.8 [d]	297-867	LP-LIF	Yamada et al. [30]
0.797 [c]	1384 [c]	7.66 [c, d]	298-366	RR	Hsu and DeMore [14]

Table 9. (Continued)

A [a], 10^{-12} cm^3 molecule^{-1} s^{-1}	E/R [a], K	k_{298} [a], 10^{-15} cm^3 molecule^{-1} s^{-1}	T range, K	technique [b]	reference
0.613±0.04	1244±90	9.43 [d]	250-375	FP-RF	Watson et al. [29]
0.970±0.128	1390±40	9.28±0.23 [d]	250-430	FP-LIF LP-LIF	this work
0.71	1300	9.0			JPL 06-2 [2]
0.813±0.214	1350±90	8.90±0.39			this work

[a] The error limits are those quoted by the authors. Our values are 95% confidence level and do not include systematic errors.

[b] FP, flash photolysis; LP, laser photolysis; DF, discharge flow; LIF, laser induced fluorescence LMR, laser magnetic resonance; RF, resonance fluorescence; RR, relative method.

[c] Recalculated based on the recommendation [2] of reference reaction.

[d] Derived from the Arrhenius rate parameters.

[e] at 296K.

CH_2ClCF_2Cl (HCFC-132b)

The measured rate constants of the purified sample of CH_2ClCF_2Cl (HCFC-132b) were on average about 30% smaller than those of the original sample, and the concentration of impurities in the purified sample was approximately 1/33 that in the original sample (Table 1). Even if the rate constant for reaction of the impurities remaining in the purified sample is as large as 1×10^{-11} cm^3 molecule^{-1} s^{-1}, their influence on the measured rate constants can be no larger than 10% of the observed value. If the sum total of impurities removed from the original sample is responsible for the decreases in the observed rate constants, the rate constant for the impurities is 1.3×10^{-12} cm^3 molecule^{-1} s^{-1}. The estimated rate constant for the impurities in the original sample indicates that their influence on the measured rate constants can be no larger than 1.3% for the purified sample.

Therefore, we concluded that the effect of any impurities remaining in the purified samples was negligible. The results of our measurements of the rate constants for the reaction of OH radicals with HCFC-132b are listed in Table 10. Figure 13 shows the Arrhenius plots. Table 11 summarizes the room temperature rate constants and the Arrhenius parameters obtained in this study as well as values reported by other groups [29, 33, 34]. Watson et al. [29] measured rate constants for HCFC-132b in the temperature range 250–350 K and corrected their values for the presence of alkene impurities in their sample. Fang et al. [34]

studied this reaction over the temperature range 295–788 K. Our result at 298 K derived from the Arrhenius parameters is (1.61 ± 0.07) × 10^{-14} cm^3 $molecule^{-1}$ s^{-1}.

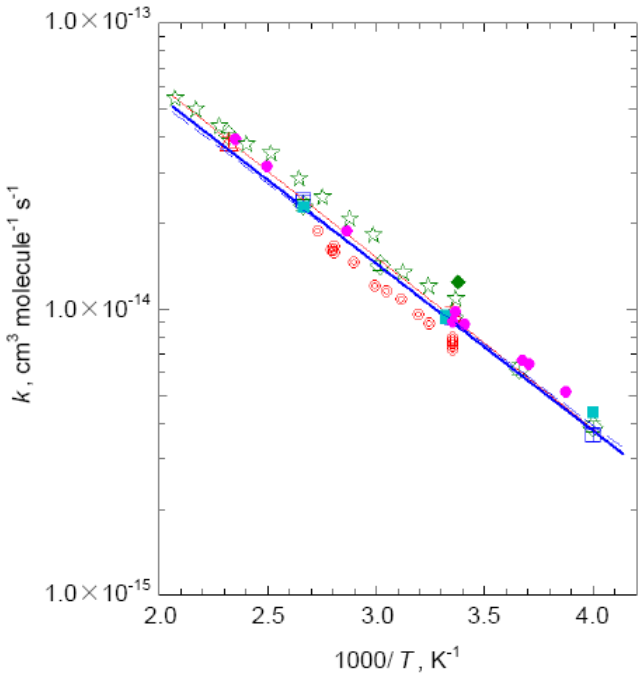

Figure 12. Arrhenius plots of the reaction rate coefficients for OH with HCFC-124. The error bars represent 95% confidence level from linear least squares analysis. (◇), FP; (□), LP-H_2O; (△), LP-H_2O_2; red solid line, nonlinear fit to the present work. (●), Gierczak et al. [31]; (◆), Howard and Evenson [28]; (☆), Yamada et al. [30]; (◎), Hsu and DeMore [14]; (■), Watson et al. [29]; blue dashed line, JPL 06-2 [2]; blue thick line, recommendation of this work.

This value is in excellent agreement with the values of Watson et al. [29] and Fang et al. [34]. The rate constant at 298 K reported by Jeong et al. [33] derived from their Arrhenius rate parameters is about 80% larger than ours. The recommended rate expression was derived from the present results and those of Watson et al. [29] and Fang et al. [34] (below 486 K). As is apparent in Figure 13, the recommended room temperature rate constant is very close to the JPL value [2], although the frequency factor and temperature dependence are 33 and 8% smaller than those of JPL.

Table 10. Experimental conditions and results for measurements of OH radicals with HCFC-132b

Temperature, K	technique	k, 10^{-15}, cm^3 $molecule^{-1}$ s^{-1}	$\bar{t}$, s or U, m s^{-1} [a]	pressure, torr	[HCFC-132b], 10^{15} molecule cm^{-3}	no. of expts.
250	FP	6.11±0.27	0.28 - 0.48	20 - 40	0.80 - 9.49	5
	LP-H_2O	6.52±0.60	0.34 - 0.56	40 - 80	0.57 - 9.02	7
273	LP-H_2O	10.2±0.9	0.38 - 0.52	40 - 80	0.49 - 7.13	6
298	LP-H_2O	17.3±1.7	0.25 - 0.38	20 - 60	0.43 - 5.42	6
	DF	18.3±0.6	5.8 - 7.3	5 - 6	0.61 - 4.80	10
331	FP	24.0±1.7	0.30 - 0.39	20 - 40	0.79 - 5.64	5
	DF	26.5±1.0	5.3 - 7.3	6	0.12 - 2.68	6
375	LP-H_2O	40.2±1.9	0.33 - 0.35	20 - 40	0.50 - 5.77	6
	DF	42.5±1.7	6.9 - 9.3	5 - 6	0.37 - 2.75	6
403	DF	56.2±2.6	5.6 - 10.7	5 - 6	0.19 - 2.28	5
430	FP	70.0±3.0	0.25 - 0.38	20 - 40	0.68 - 5.63	6
	LP-H_2O	77.1±3.7	0.26 - 0.34	20 - 40	0.80 - 5.33	6
	DF	72.9±3.1	8.4 - 12.5	5 - 6	0.28 - 1.83	6

[a] $\bar{t}$, residence time for FP and LP methods; U, linear flow velocity for DF method.
The quoted errors represent 95% confidence level from linear least squares analysis.
The purity of the sample used in the measurement was 99.982%.

Table 11. Summary of the rate constants for the reaction of OH radicals with HCFC-132b

A [a], 10^{-12} cm^3 $molecule^{-1}$ s^{-1}	E/R [a], K	k_{298} [a], 10^{-14} cm^3 $molecule^{-1}$ s^{-1}	T range, K	technique [b]	reference
$(8.53\pm4.06)\times10^{-7}$ $T^{2.28\pm0.18}$	937±296	1.61 [c]	295-788	LP-LIF	Fang et al. [34]
2.02±0.24	1263±35	2.92 [c]	249-473	DF-RF	Jeong et al. [33]
3 +6, -1	1578 +400, -230	1.9±0.2	250-350	FP-RF	Watson et al. [29]
2.03±0.42	1440±70	1.61±0.07 [c]	250-430	FP-LIF LP-LIF DF-LIF	this work

Table 11. (Continued)

A [a], 10^{-12} cm^3 molecule^{-1} s^{-1}	E/R [a], K	k_{298} [a], 10^{-14} cm^3 molecule^{-1} s^{-1}	T range, K	technique [b]	reference
3.6	1600	1.7			JPL 06-2 [2]
2.44±0.63	1480±90	1.74±0.10			this work

[a] The error limits are those quoted by the authors. Our values are 95% confidence level and do not include systematic errors.

[b] FP, flash photolysis; LP, laser photolysis; DF, discharge flow; LIF, laser induced fluorescence, RF, resonance fluorescence.

[c] Derived from the Arrhenius rate parameters.

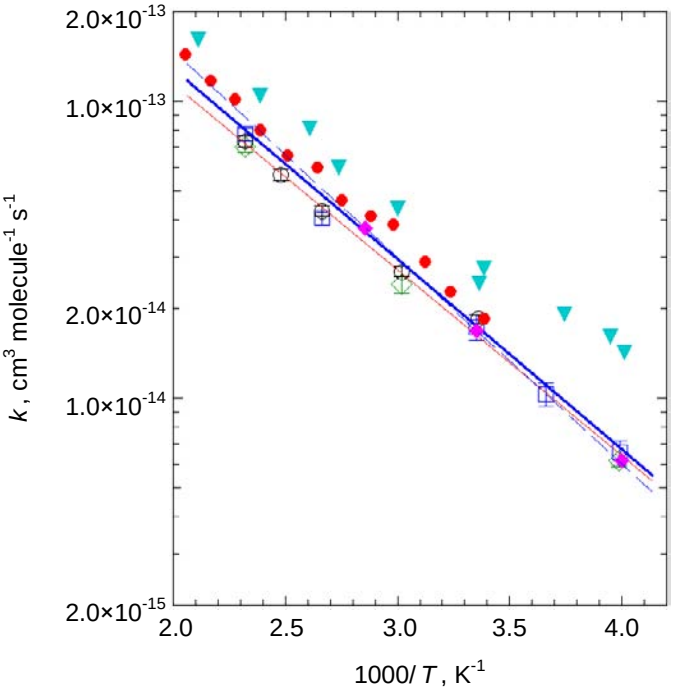

Figure 13. Arrhenius plots of the reaction rate coefficients for OH with HCFC-132b. The error bars represent 95% confidence level from linear least squares analysis. (◇), FP; (□), LP-H_2O; (○), DF; red solid line, nonlinear fit to the present work. (●), Fang et al. [34]; (▼), Jeong et al. [33]; (◆), Watson et al. [29]; blue dashed line, JPL 06-2 [2]; blue thick line, recommendation of this work.

CH_2ClCF_3 (HCFC-133a)

The concentration of impurities in the purified sample of CH_2ClCF_3 (HCFC-133a) is approximately 1/29 that in the original sample, and the measured rate constants of the purified sample are on average about 40 % those of the original sample (Table 1). From the values of sample purity and the measured rate constants, the influence of impurities was estimated to be less than 5% for the worst case conceivable.

The rate constants for reaction of HCFC-133a with OH radicals and the experimental conditions for individual measurements over the temperature range 250–430 K are summarized in Table 12. Figure 14 and Table 13 show the present results and the values reported by other groups. The results reported by Fang et al. [34] and Handwerk and Zellner [23] are higher than ours over the entire temperature range, but the results agree with each other within 30%. The room temperature rate constant of Howard and Evenson [28] is about 30% smaller than ours. The frequency factor and temperature dependence reported by Clyne and Holt [16] are very different from those reported by other groups. The recommended rate expression was derived from the present results; those of Fang et al. [34] (below 484 K) and Handwerk and Zellner [23]; and the room temperature rate constant of Howard and Evenson [28].

Table 12. Experimental conditions and results for measurements of OH radicals with HCFC-133a

temperature, K	technique	k, 10^{-15}, cm^3 $molecule^{-1}$ s^{-1}	$\bar{t}$, s or U, m s^{-1} [a]	pressure, torr	[HCFC-133a], 10^{15} molecule cm^{-3}	no. of expts.
250	LP-H_2O	6.69±0.73	0.30 - 0.56	40 - 80	0.55 - 9.29	8
273	LP-H_2O	9.87±0.83	0.38 - 0.52	60 - 80	1.19 - 7.68	6
298	LP-H_2O	14.2±0.7	0.25 - 0.36	20 - 60	0.44 - 9.23	6
	DF	15.3±0.5	5.9 - 7.8	5 - 6	0.59 - 5.86	12
331	DF	21.6±0.9	7.8 - 9.6	5	0.33 - 3.71	6
375	LP-H_2O	35.8±1.4	0.27 - 0.41	20 - 60	0.99 - 7.21	7
430	FP	56.5±2.7	0.24 - 0.30	20 - 40	0.66 - 5.66	7
	LP-H_2O	58.5±2.2	0.26 - 0.36	20 - 60	0.96 - 7.32	7

[a] $\bar{t}$, residence time for FP and LP methods; U, linear flow velocity for DF method.
The quoted errors represent 95% confidence level from linear least squares analysis.
The purity of the sample used in the measurement was 99.993%.

Table 13. Summary of the rate constants for the reaction of OH radicals with HCFC-133a

A [a], 10^{-12} cm^3 molecule^{-1} s^{-1}	E/R [a], K	k_{298} [a], 10^{-14} cm^3 molecule^{-1} s^{-1}	T range, K	technique [b]	reference
$(3.06\pm4.02)\times10^{-6}$ $T^{1.91\pm0.03}$	644±313	1.87 [c]	295-866	LP-LIF	Fang et al [34]
38.9 +46.2, -21.1	2300±300	1.5±0.2	294-427	DF-RF	Clyne and Holt [16]
1.1±0.3	1260±60	1.6	263-373	FP-RA	Handwerk and Zellner [23]
		1.05±0.23 [d]	296	DF-LMR	Howard and Evenson [28]
1.13±0.22	1290±60	1.49±0.06 [c]	250-430	FP-LIF LP-LIF DF-LIF	this work
0.56	1100	1.4			JPL 06-2 [2]
1.05±0.41	1240±130	1.67±0.12			this work

[a] The error limits are those quoted by the authors. Our values are 95% confidence level and do not include systematic errors.

[b] FP, flash photolysis; LP, laser photolysis; DF, discharge flow; LIF, laser induced fluorescence; LMR, laser magnetic resonance; RF, resonance fluorescence; RA, resonance absorption.

[c] Derived from the Arrhenius rate parameters. [d] at 296K.

The room temperature rate constant and the temperature dependence of both recommended values agree with each other within about 20%, although our frequency factor is about 2 times the JPL value.

$CH_2ClCHFCl$ (HCFC-141)

The concentration of impurities in the purified sample of $CH_2ClCHFCl$ (HCFC-141) is approximately 1/10 that in the original sample, and the measured rate constants of the original and purified samples are identical (Table 1).

From the purity and the measured rate constants of the purified sample, the influence of impurities was estimated to be 2.6%, on the assumption that the rate constant for the reaction of impurities with OH radicals is as large as 1×10^{-11} cm^3 molecule^{-1} s^{-1} (the worst case conceivable). Therefore, we concluded that the effect of any impurities remaining in the purified samples was negligible.

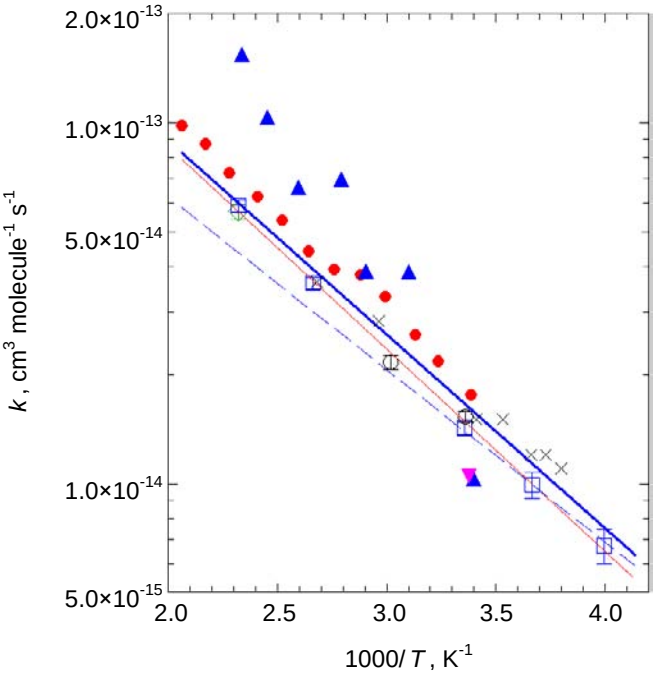

Figure 14. Arrhenius plots of the reaction rate coefficients for OH with HCFC-133a. The error bars represent 95% confidence level from linear least squares analysis. (◇), FP; (□), LP-H_2O; (○), DF; red solid line, nonlinear fit to the present work. (●), Fang et al. [34]; (▲), Clyne and Holt [16]; (×), Handwerk and Zellner [23]; (▼), Howard and Evenson [28]; blue dashed line, JPL 06-2 [2]; blue thick line, recommendation of this work.

Table 14. Experimental conditions and results for measurements of OH radicals with HCFC-141

temperature, K	technique	k, 10^{-14}, cm^3 $molecule^{-1}$ s^{-1}	$\bar{t}$, s or U, m s^{-1} [a]	pressure, torr	[HCFC-141], 10^{15} molecule cm^{-3}	no. of expts.
250	FP	3.79±0.13	0.31 - 0.46	20 - 30	0.79 - 4.64	6
	LP-H_2O	3.74±0.24	0.31 - 0.42	20 - 60	0.46 - 7.42	7
273	LP-H_2O	5.35±0.34	0.31 - 0.38	40 - 60	0.94 - 7.83	6
298	FP	7.19±0.32	0.24 - 0.38	20 - 40	0.47 - 5.84	7
	LP-H_2O	7.62±0.32	0.26 - 0.35	20 - 60	0.46 - 5.85	5
	DF	8.08±0.34	7.8 - 12.1	3 - 5	0.17 - 1.39	10

Table 14. (Continued)

temperature, K	technique	k, 10^{-14}, cm^3 $molecule^{-1}$ s^{-1}	$\bar{t}$, s or U, m s^{-1} [a]	pressure, torr	[HCFC-141], 10^{15} molecule cm^{-3}	no. of expts.
331	FP	9.93±0.45	0.24 - 0.35	10 - 40	0.42 - 4.76	6
	DF	11.3±0.4	7.2 - 9.8	5	0.20 - 1.31	6
375	DF	15.3±0.5	8.9 - 12.4	5	0.11 - 1.21	6
403	DF	19.5±0.5	9.0 - 13.4	4 - 5	0.12 - 0.91	6
430	FP	23.1±0.8	0.25 - 0.35	20 - 40	0.59 - 4.74	6
	LP-H_2O	22.3±0.8	0.19 - 0.34	20 - 40	0.54 - 3.64	7
	DF	22.4±0.7	10.1 - 14.4	4 - 5	0.12 - 0.87	6

[a] $\bar{t}$, residence time for FP and LP methods; U, linear flow velocity for DF method.
The quoted errors represent 95% confidence level from linear least squares analysis.
The purity of the sample used in the measurement was 99.98%.

The results of our measurements and the experimental conditions are listed in Table 14. The results are plotted in Figure 15 and summarized in Table 15. No data are available for the reaction of OH radicals with HCFC-141. Therefore, the recommended rate expression is that derived from the present results.

Table 15. Summary of the rate constant for the reaction of OH radicals with HCFC-141

A [a], 10^{-12} cm^3 $molecule^{-1}$ s^{-1}	E/R [a], K	k_{298} [a], 10^{-14} cm^3 $molecule^{-1}$ s^{-1}	T range, K	technique [b]	reference
2.71±0.37	1070±40	7.50±0.21 [c]	250-430	FP-LIF LP-LIF DF-LIF	this work

[a] The error limits are 95% confidence level and do not include systematic errors.
[b] FP, flash photolysis; LP, laser photolysis; DF, discharge flow; LIF, laser induced fluorescence.
[c] Derived from the Arrhenius rate parameters.

CH_3CFCl_2 (HCFC-141b)

The concentration of impurities in the purified sample of CH_3CFCl_2 (HCFC-141b) is approximately 1/110 that in the original sample, and the measured rate constants of the purified sample are about 60% smaller than those of the original sample.

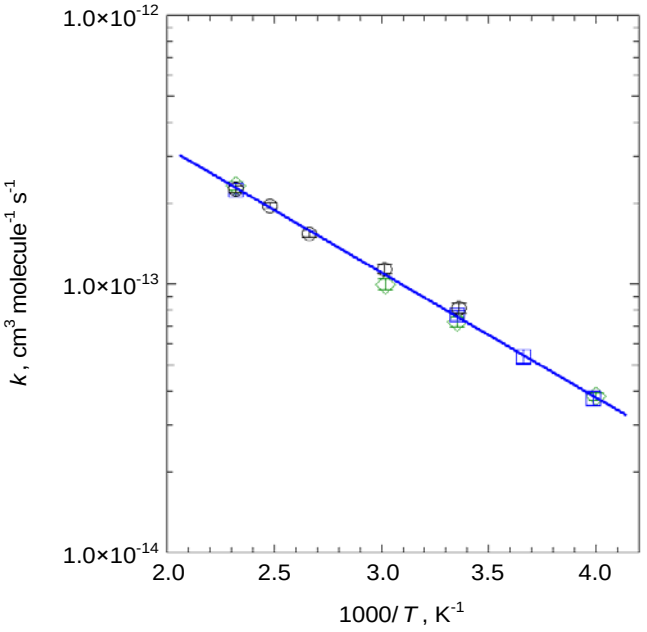

Figure 15. Arrhenius plots of the reaction rate coefficients for OH with HCFC-141. The error bars represent 95% confidence level from linear least squares analysis. (◇), FP; (□), LP-H_2O; (○), DF; blue thick line, nonlinear fit to the present work.

If the sum total of impurities removed from the original sample is responsible for the decreases in the observed rate constants, the rate constant for reaction of the impurities with OH radicals is 8.9×10^{-13} cm^3 $molecule^{-1}$ s^{-1}. If the rate constant for reaction of impurities remaining in the purified sample is as large as 1×10^{-11} cm^3 $molecule^{-1}$ s^{-1}, their influence on the measured rate constant can be estimated to be about 15%. If the rate constant for the impurities is as large as 8.9×10^{-13} cm^3 $molecule^{-1}$ s^{-1}, their influence on the measured rate constants can be no larger than 1.3% of the observed values for the purified sample. Thus, the effect of any impurities remaining in the purified sample seems to be negligible.

Talukdar et al. [35] reported that the measured rate constants for HCFC-141b with OH radicals obtained by flash photolysis of H_2O depend on the photolysis energy and that the OH radical decay plots show nonexponential behavior. To avoid this problem, they generated OH radicals by photolysis of HONO with 355-nm light (third harmonic of an Nd:YAG laser). We observed the same behavior in the present study using direct photodissociation of H_2O (FP method, $\lambda \geq 180$ nm) and photolysis of N_2O using an ArF excimer laser (LP-H_2O method, $\lambda = 193$ nm). Thus, the reactions of OH radicals with HCFC-141b were carried out using photodissociation of H_2O_2 with a KrF excimer laser (LP-H_2O_2 method, $\lambda = 248$ nm), as well as the discharge flow method.

Table 16. Experimental conditions and results for measurements of OH radicals with HCFC-141b

temperature, K	technique	k, 10^{-15}, cm^3 $molecule^{-1}$ s^{-1}	$\bar{t}$, s or U, m s^{-1} [a]	pressure, torr	[HCFC-141b], 10^{15} molecule cm^{-3}	no. of expts.
250	LP-H_2O_2	2.20±0.13	0.28 - 0.47	40 - 100	0.96 - 9.38	6
273	LP-H_2O_2	3.59±0.17	0.29 - 0.40	40 - 100	0.58 - 9.11	7
298	LP-H_2O_2	6.40±0.22	0.29 - 0.41	20 - 80	0.60 - 9.34	7
	DF	6.84±0.26	5.0 - 6.1	5 - 6	0.68 - 7.38	10
331	LP-H_2O_2	10.6±0.3	0.36 - 0.43	40 - 60	1.01 - 9.31	6
	DF	10.7±0.4	5.9 - 7.3	6	0.53 - 5.80	6
375	DF	17.7±0.7	7.5 - 10.1	5 - 6	0.62 - 4.84	7
403	DF	25.2±0.7	6.2 - 10.9	5 - 6	0.38 - 4.85	6
430	LP-H_2O_2	34.2±0.9	0.31 - 0.42	20 - 60	1.04 - 9.29	7
	DF	33.7±1.2	8.6 - 12.2	5 - 6	0.51 - 3.71	6

[a] $\bar{t}$, residence time for LP method; U, linear flow velocity for DF method. The quoted errors represent 95% confidence level from linear least squares analysis. The purity of the sample used in the measurement was 99.99%.

The rate constants for reactions with OH radicals and the experimental conditions used for HCFC-141b are summarized in Table 16. Figure 16 and Table 17 show the present results and the values reported by other groups. The results reported by Huder and DeMore [36] using the relative rate method were recalculated on the basis of the values recommended by JPL [2] for reference compounds CH_4 and CH_3CCl_3. In Figure 16 and Table 17, the results of Huder and DeMore [36] are the unit-weighted averaged values obtained with these two

reference compounds. The room temperature rate constant reported by Brown et al. [27] is about 2 times as large as ours. The results of Liu et al. [32] are considerably higher than those of others at lower temperature (especially below 270 K), whereas at temperatures above 330 K their results agree with those of others.

Table 17. Summary of the rate constants for the reaction of OH radicals with HCFC-141b

A [a], 10^{-12} cm^3 molecule^{-1} s^{-1}	E/R [a], K	k_{298} [a], 10^{-15} cm^3 molecule^{-1} s^{-1}	T range, K	technique[b]	reference
		4.6±0.8 [e]	293	LP-LA	Mors et al. [39]
0.58	1100±250	13.6±2.7	238-426	DF-RF	Brown et al. [27]
1.42±0.60	1623±293	6.12 [d]	250-297	FP-RF	Zhang et al. [37]
1.25 [c]	1590 [c]	6.01 [c, d]	293-358	RR	Huder and DeMore [36]
2.4±0.6	1790±100	5.7±1.5	298-479	DF-EPR	Lanca et al. [38]
3.6±1.1	1140±210	7.85 [d]	243-400	FP-RF	Liu et al. [32]
1.47±0.32	1640±100	5.92±0.54	253-393	DF-LMR LP-LIF	Talukdar et al. [35]
1.42±0.30	1620±70	6.25±0.27 [d]	250-430	LP-LIF DF-LIF	this work
1.25	1600	5.8			JPL 06-2 [2]
1.30±0.25	1610±60	5.93±0.18			this work

[a]The error limits are those quoted by the authors. Our values are 95% confidence level and do not include systematic errors.

[b]FP, flash photolysis; LP, laser photolysis; DF, discharge flow; LIF, laser induced fluorescence; LMR, laser magnetic resonance; EPR, electron paramagnetic resonance; RF, resonance fluorescence; LA, laser absorption; RR, relative method.

[c]Recalculated based on the recommendation [2] of reference reaction. The value is an average of the results obtained from two reference compounds (CH4 and CH3CCl3).

[d]Derived from the Arrhenius rate parameters.

[e]at 293K.

The recommended rate expression was derived from the present results; those of Zhang et al. [37], Lanca et al. [38], Liu et al. [32] (above 330 K), and Talukdar et al. [35]; and the room temperature rate constants of Mors et al. [39] and Huder and DeMore [36] obtained using the relative rate method. The present recommended rate expression agrees with that of JPL within 3% over the temperature range 250–500 K.

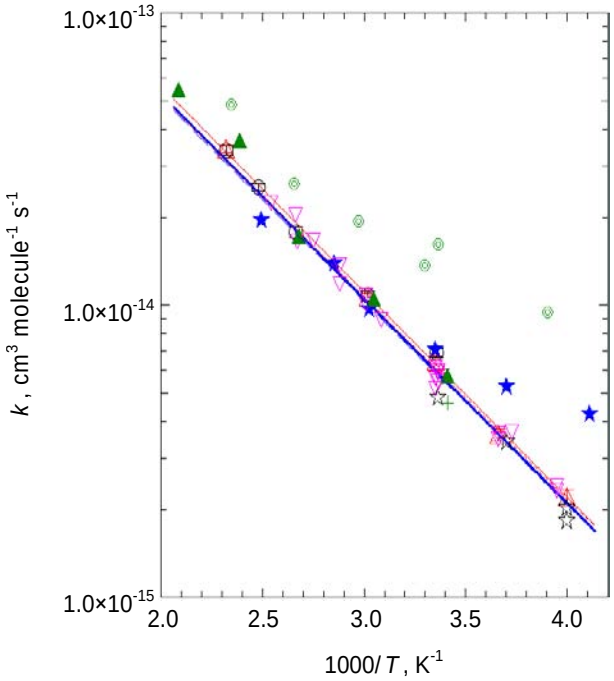

Figure 16. Arrhenius plots of the reaction rate coefficients for OH with HCFC-141b. The error bars represent 95% confidence level from linear least squares analysis. (△), LP-H_2O_2; (○), DF; red solid line, nonlinear fit to the present work. (✚), Mors et al. [39]; (◎), Brown et al. [27]; (☆), Zhang et al. [37]; (▲), Lanca et al. [38]; (★), Liu et al. [32]; (▽), Talukdar et al. [35]; red dotted line, Huder and DeMore [36]; blue dashed line, JPL 06-2 [2]; blue thick line, recommendation of this work.

CH_3CF_2Cl (HCFC-142b)

As discussed in section 3.2, the measured rate constants for the purified sample of CH_3CF_2Cl (HCFC-142b) were 1/3 (or less) those of the original sample. However, when the purified sample was used for the kinetic measurements, the rate constants were not affected by the reactive impurities.

Table 18 summarizes our experimental conditions and results. The Arrhenius plots and rate parameters are shown in Figure 17 and Table 19, along with literature data. At 298 K, the rate constant reported by Clyne and Holt [16] is about 2 times as large as ours. The frequency factor and temperature dependence reported by Brown et al. [27] are considerably smaller than ours.

Table 18. Experimental conditions and results for measurements of OH radicals with HCFC-142b

Temperature, K	technique	k, 10^{-15}, cm^3 $molecule^{-1}$ s^{-1}	$\bar{t}$, s or U, m s^{-1} [a]	pressure, torr	[HCFC-142b], 10^{15} molecule cm^{-3}	no. of expts.
250	FP	1.01±0.06	0.35 - 0.85	20 - 60	0.98 - 9.42	9
	LP-H_2O	1.00±0.08	0.42 - 0.57	60 - 80	2.15 - 18.5	6
273	LP-H_2O	1.73±0.07	0.38 - 0.52	60 - 80	1.58 - 19.0	8
298	FP	3.47±0.34	0.26 - 0.38	20 - 60	0.80 - 9.24	9
	LP-H_2O	3.40±0.19	0.31 - 0.47	40 - 80	0.81 - 14.0	8
	DF	3.62±0.06	4.4 - 8.1	4 - 6	0.98 - 8.55	35
331	DF	6.26±0.29	5.0 - 6.7	6	0.94 - 7.34	6
375	DF	11.3±0.5	4.9 - 9.2	6	0.75 - 7.14	6
403	DF	15.2±0.5	5.0 - 8.5	6	0.67 - 7.00	7
430	FP	20.1±1.1	0.33 - 0.37	20 - 40	0.84 - 9.27	6
	LP-H_2O	20.2±0.7	0.29 - 0.39	40 - 60	1.07 - 9.61	6
	DF	21.1±1.0	6.6 - 13.3	5 - 6	0.57 - 4.28	6

[a] $\bar{t}$, residence time for FP and LP methods; U, linear flow velocity for DF method.
The quoted errors represent 95% confidence level from linear least squares analysis.
The purity of the sample used in the measurement was higher than 99.996%.

The recommended rate expression was derived from the present results; the results of Handwerk and Zellner [23], Watson et al. [20], Fang et al. [40] (below 484 K), Liu et al. [32], and Gierczak et al. [31] (above 243 K); the room temperature rate constants of Paraskevopoulos et al. [25], Mors et al. [39], and Howard and Evenson [28]; and the 270 K rate constant of Zhang et al. [37].

The rate constant derived from the present recommended rate expression is about 7% smaller than the JPL value at 250 K and about 12% larger than the JPL value at 500 K, because the temperature dependence of the present recommendation is about 5% larger than that of JPL.

Table 19. Summary of the rate constants for the reaction of OH radicals with HCFC-142b

A [a], 10^{-12} cm^3 molecule^{-1} s^{-1}	E/R [a], K	k_{298} [a], 10^{-15} cm^3 molecule^{-1} s^{-1}	T range, K	technique [b]	reference
0.26	1230±250	3.7±1.4	231-423	DF-RF	Brown et al. [27]
		4.63±1.73 [d]	297	FP-RF	Paraskevopoulos et al. [25]
1.8±0.5	1790±150	3.4	293-373	FP-RA	Handwerk and Zellner [23]
3.31 +4.27, -1.87	1800±300	6.7±1.3	293-417	DF-RF	Clyne and Holt [16]
1.15±0.15	1748±30	3.22±0.3	273-375	FP-RF	Watson et al. [20]
		2.6±0.4 [f]	293	LP-LA	Mors et al. [39]
		2.83±0.42 [e]	296	DF-LMR	Howard and Evenson [28]
$(1.20\pm0.32)\times10^{-5}$ $T^{1.89\pm0.05}$	1541±128	3.23 [c]	295-808	LP-LIF	Fang et al. [40]
0.98±0.28	1660±200	3.73 [c]	270-400	FP-RF	Liu et al. [32]
		2.45±0.31 [g]	270	FP-RF	Zhang et al. [37]
1.14 +0.35, -0.26	1750±75	2.95±0.25	223-374	FP-LIF DF-LMR	Gierczak et al. [31]
1.36±0.24	1800±60	3.28±0.13 [c]	250-430	FP-LIF LP-LIF DF-LIF	this work
1.3	1770	3.4			JPL 06-2 [2]
1.78±0.45	1870±80	3.42±0.17			this work

[a] The error limits are those quoted by the authors. Our values are 95% confidence level and do not include systematic errors.

[b] FP, flash photolysis; LP, laser photolysis; DF, discharge flow; LIF, laser induced fluorescence; LMR, laser magnetic resonance; RF, resonance fluorescence; RA, resonance absorption; LA, laser absorption.

[c] Derived from the Arrhenius rate parameters.

[d] at 297K.

[e] at 296K.

[f] at 293K.

[g] at 270K.

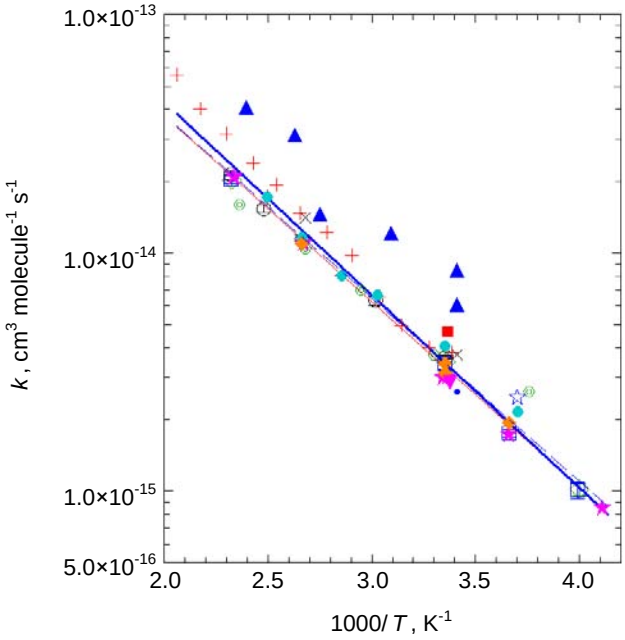

Figure 17. Arrhenius plots of the reaction rate coefficients for OH with HCFC-142b. The error bars represent 95% confidence level from linear least squares analysis. (◇), FP; (□), LP-H_2O; (○), DF; red solid line, nonlinear fit to the present work. (◎), Brown et al. [27]; (■), Paraskevopoulos et al. [25]; (×), Handwerk and Zellner [23]; (▲), Clyne and Holt [16]; (◆), Watson et al. [20]; (•), Mors et al. [39]; (▼), Howard and Evenson [28]; (+), Fang et al. [40]; (●), Liu et al. [32]; (☆), Zhang et al. [37]; (★), Gierczak et al. [31]; blue dashed line, JPL 06-2 [2]; blue thick line, recommendation of this work.

$CF_3CHClCH_2Cl$ (HCFC-243db)

The concentration of impurities in the purified sample of $CF_3CHClCH_2Cl$ (HCFC-243db) is approximately 1/70 that in the original sample, and the measured rate constants of the original and purified samples are identical (Table 1). From the purity and the measured rate constants, the influence of the impurities on the rate constants of the purified sample was estimated to be 0.8%, on the assumption that the rate constant for reaction of the impurities with OH radicals is as large as 1×10^{-11} cm^3 $molecule^{-1}$ s^{-1} (the worst case conceivable). Therefore, we concluded that the effect of any impurities remaining in the purified samples was negligible.

The measurement results and experimental conditions are listed in Table 20. The results are plotted in Figure 18 and summarized in Table 21. No data are available for the reaction of OH radicals with HCFC-243db. Therefore, the recommended rate expression is that derived from the present results.

Table 20. Experimental conditions and results for measurements of OH radicals with HCFC-243db

Temperature,K	technique	k, 10^{-14} cm^3 $molecule^{-1}$ s^{-1}	$\bar{t}$, s or U, m s^{-1} [a]	pressure, torr	[HCFC-243db], 10^{15} molecule cm^{-3}	no. of expts.
250	FP	2.63±0.09	0.35 - 0.45	20 - 40	0.66 - 7.58	6
	LP-H_2O	2.71±0.12	0.36 - 0.47	20 - 60	0.87 - 7.50	6
273	FP	3.65±0.13	0.32 - 0.41	20 - 40	0.62 - 5.77	6
298	FP	4.54±0.19	0.28 - 0.41	20 - 40	0.44 - 5.37	6
	LP-H_2O	4.80±0.18	0.25 - 0.33	20 - 40	0.78 - 7.19	7
	DF	5.01±0.41	5.0 - 8.5	5 - 6	0.12 - 0.94	8
331	FP	6.85±0.27	0.28 - 0.39	20 - 40	0.50 - 5.72	6
375	FP	10.6±0.4	0.30 - 0.38	20 - 40	0.44 - 4.71	6
430	FP	16.6±0.4	0.25 - 0.40	20 - 40	0.38 - 4.70	7
	LP-H_2O	14.3±0.7	0.31 - 0.40	20 - 60	0.74 - 4.66	6

[a] $\bar{t}$, residence time for FP and LP methods; U, linear flow velocity for DF method.
The quoted errors represent 95% confidence level from linear least squares analysis.
The purity of the sample used in the measurement was 99.996%.

Table 21. Summary of the rate constant for the reaction of OH radicals with HCFC-243db

A [a], 10^{-12} Cm^3 $molecule^{-1}$ s^{-1}	E/R [a], K	k_{298} [a], 10^{-14} cm^3 $molecule^{-1}$ s^{-1}	T range, K	technique [b]	reference
1.70±0.47	1050±80	5.01±0.25 [c]	250-430	FP-LIF LP-LIF DF-LIF	this work

[a] The error limits are 95% confidence level and do not include systematic errors.
[b] FP, flash photolysis; LP, laser photolysis; DF, discharge flow; LIF, laser induced fluorescence.
[c] Derived from the Arrhenius rate parameters.

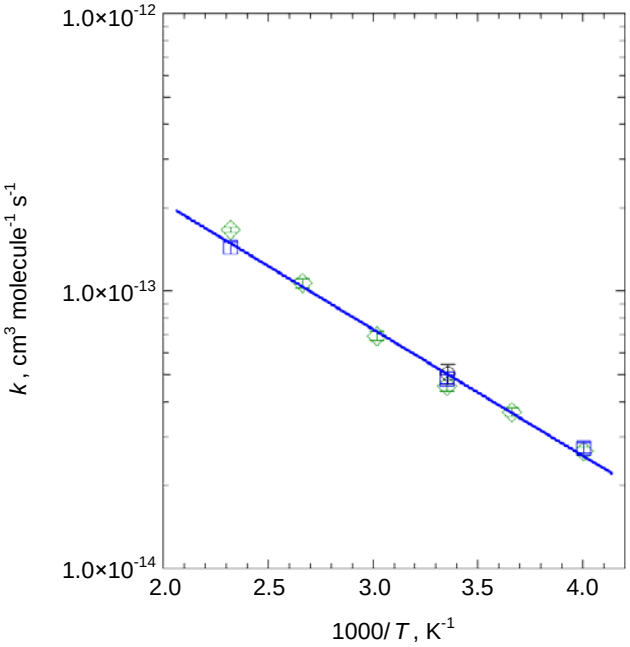

Figure 18. Arrhenius plots of the reaction rate coefficients for OH with HCFC-243db. The error bars represent 95% confidence level from linear least squares analysis. (◇), FP; (□), LP-H_2O; (○), DF; blue thick line, nonlinear fit to the present work.

$CF_3CH_2CH_2Cl$ (HCFC-253fb)

The concentration of impurities in the purified sample of $CF_3CH_2CH_2Cl$ (HCFC-253fb) is approximately 1/24 that in the original sample, and the measured rate constants of the original and purified samples are identical. From the purity and the measured rate constants, the influence of impurities was estimated to be 1.1% for the worst case conceivable. Therefore, we concluded that the effect of any impurities remaining in the purified samples was negligible.

The measurement results and experimental conditions are listed in Table 22. The results are plotted in Figure 19 and summarized in Table 23. No data for the reaction of OH radicals with HCFC-253fb are available. Therefore, the recommended rate expression is that derived from the present results.

Table 22. Experimental conditions and results for measurements of OH radicals with HCFC-253fb

temperature, K	technique	k, 10^{-14} cm^3 $molecule^{-1}$ s^{-1}	$\bar{t}$, s or U, m s^{-1} [a]	pressure, torr	[HCFC-253fb], 10^{15} molecule cm^{-3}	no. of expts.
250	FP	3.08±0.13	0.32 - 0.41	20 - 40	0.39 - 4.69	6
	LP-H_2O	3.51±0.21	0.29 - 0.42	20 - 60	0.41 - 4.65	6
273	LP-H_2O	4.93±0.25	0.31 - 0.38	40 - 60	0.54 - 9.63	6
298	FP	6.23±0.25	0.24 - 0.38	20 - 40	0.33 - 5.68	6
	LP-H_2O	6.85±0.30	0.23 - 0.35	20 - 60	0.88 - 8.90	5
	DF	6.47±0.15	8.5 - 12.7	4 - 5	0.47 - 2.75	7
331	FP	8.72±0.36	0.25 - 0.39	20 - 40	0.74 - 4.94	5
	DF	9.31±0.32	7.1 - 9.7	5	0.25 - 2.21	6
375	LP-H_2O	14.1±0.4	0.28 - 0.35	20 - 40	0.41 - 4.80	6
	DF	14.4±0.5	10.7 - 14.0	4 - 5	0.17 - 1.54	6
403	DF	19.5±0.7	8.0 - 14.2	5	0.10 - 0.72	6
430	FP	22.6±0.7	0.24 - 0.34	20 - 40	0.36 - 4.61	6
	LP-H_2O	23.2±0.7	0.24 - 0.34	20 - 40	0.37 - 4.80	6
	DF	22.9±0.8	7.8 - 13.1	4 - 6	0.11 - 0.75	5

[a] $\bar{t}$, residence time for FP and LP methods; U, linear flow velocity for DF method.
The quoted errors represent 95% confidence level from linear least squares analysis.
The purity of the sample used in the measurement was 99.993%.

Table 23. Summary of the rate constant for the reaction of OH radicals with HCFC-253fb

A [a], 10^{-12} cm^3 $molecule^{-1}$ s^{-1}	E/R [a], K	k_{298} [a], 10^{-14} cm^3 $molecule^{-1}$ s^{-1}	T range, K	technique [b]	reference
3.27±0.69	1160±70	6.63±0.29 [c]	250-430	FP-LIF LP-LIF DF-LIF	this work

[a] The error limits are 95% confidence level and do not include systematic errors.
[b] FP, flash photolysis; LP, laser photolysis; DF, discharge flow; LIF, laser induced fluorescence.
[c] Derived from the Arrhenius rate parameters.

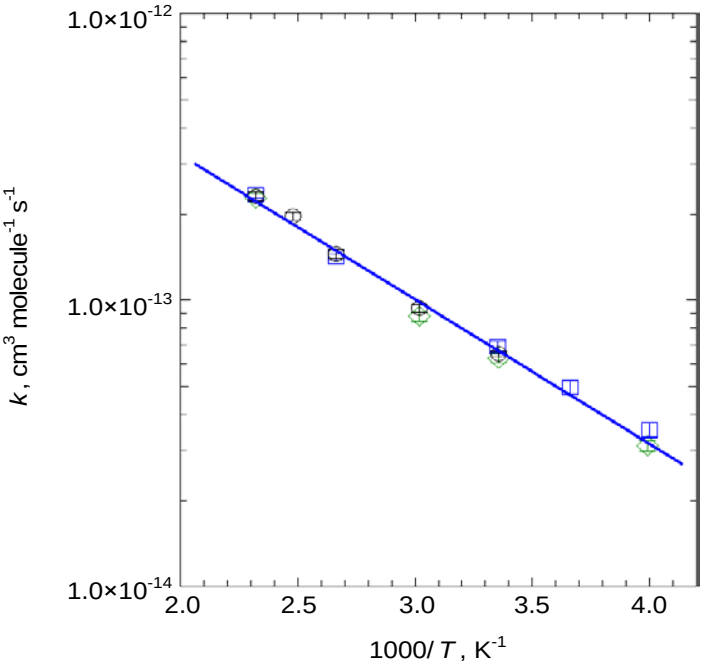

Figure 19. Arrhenius plots of the reaction rate coefficients for OH with HCFC-253fb. The error bars represent 95% confidence level from linear least squares analysis. (◇), FP; (□), LP-H_2O; (○), DF; blue thick line, nonlinear fit to the present work.

CH_2F_2 (HFC-32)

The concentration of impurities in the purified sample of CH_2F_2 (HFC-32) is 1/5 that in the original sample, and the measured rate constants of the original and purified samples are identical. From the purity and the measured rate constants, the influence of impurities was estimated to be 9.7% for the worst case conceivable. Therefore, we concluded that the effect of any impurities remaining in the purified samples was negligible.

Table 24 summarizes our experimental conditions and the results for reaction of OH radicals with HFC-32. Figure 20 and Table 25 show the present results and the values reported by other groups. The results Hsu and DeMore [14] obtained by the relative rate method were recalculated on the basis of the value recommended by JPL [2] for HFC-152a as a reference compound ($k = 2.33 \times 10^{-12}\exp(-1260/T)$ for temperatures above room temperature). The frequency factor and temperature dependence reported by Clyne and Holt [16] are considerably larger than those of

others. The room temperature rate constants reported by Howard and Evenson [17] and Bera and Hanrahan [41] are about 26 and 16%, respectively, smaller than our result. In the middle temperature range, the results of Jeong and Kaufman [22] are close to ours, whereas their values are larger than ours at higher temperature. The recommended rate expression was derived from the present results; those of Talukdar et al. [35] (above 245 K) and Jeong and Kaufman [22] (below 432 K); the relative rate study by Hsu and DeMore [14]; and the room temperature rate constants of Szilagyi et al. [42] and Nip et al. [43]. The rate constant derived from the present recommended rate expression is about 8% smaller than the JPL value at 250 K and about 10% larger than the JPL value at 500 K, because the temperature dependence of the present recommendation is about 6% larger than that of JPL.

Table 24. Experimental conditions and results for measurements of OH radicals with HFC-32

temperature, K	technique	k, 10^{-14}, cm^3 $molecule^{-1}$ s^{-1}	$\bar{t}$, s or U, m s^{-1} [a]	pressure, torr	[HFC-32], 10^{15} molecule cm^{-3}	no. of expts.
250	FP	3.78±0.20	0.30 - 0.46	20 - 40	1.54 - 9.45	6
	LP-H_2O	3.90±0.21	0.24 - 0.42	20 - 60	1.30 - 9.24	6
273	FP	6.39±0.30	0.26 - 0.38	20 - 40	1.31 - 9.48	6
298	FP	10.4±0.5	0.24 - 0.33	20 - 40	0.99 - 10.0	6
	LP-H_2O	10.8±0.4	0.23 - 0.31	20 - 40	1.30 - 9.33	6
	DF	9.70±0.46	5.7 - 7.7	5 - 6	0.39 - 4.71	6
331	FP	17.9±0.8	0.21 - 0.32	20 - 40	0.90 - 9.37	6
375	FP	31.5±0.8	0.25 - 0.33	20 - 40	1.10 - 9.86	6
430	FP	55.8±2.3	0.25 - 0.38	20 - 40	1.01 - 9.66	6
	LP-H_2O	57.6±1.4	0.26 - 0.38	20 - 80	0.99 - 9.63	7

[a] $\bar{t}$, residence time for FP and LP methods; U, linear flow velocity for DF method.
The quoted errors represent 95% confidence level from linear least squares analysis.
The purity of the sample used in the measurement was 99.99%.

Table 25. Summary of the rate constants for the reaction of OH radicals with HFC-32

A [a], 10^{-12} cm^3 $molecule^{-1}$ s^{-1}	E/R [a], K	k_{298} [a], 10^{-14} cm^3 $molecule^{-1}$ s^{-1}	T range, K	technique [b]	reference
1.57±0.21	1470±100	1.13±0.10	220-380	FP-LIF	Talukdar et al. [35]
4.40±0.37	1771±30	1.12±0.15	250-492	DF-RF	Jeong and Kaufman [22]
7.41 +7.38, -3.70	2100±200	0.72±0.10	293-429	DF-RF	Clyne and Holt [16]
		0.88±0.14 [g]	r. t.	PR-RA	Bera and Hanrahan [41]
		1.00±0.03	298	DF-RF	Szilagyi et al. [42]
1.86 [c]	1537 [c]	1.07 [c, d]	297-383	RR	Hsu and DeMore [14]
		1.17±0.14 [e]	297	FP-RA	Nip et al. [43]
		0.78±0.12 [f]	296	DF-LMR	Howard and Evenson [17]
2.35±0.38	1610±50	1.05±0.03 [d]	250-430	FP-LIF LP-LIF DF-LIF	this work
1.7	1500	1.1			JPL 06-2 [2]
2.28±0.43	1590±60	1.09±0.03			this work

[a] The error limits are those quoted by the authors. Our values are 95% confidence level and do not include systematic errors.

[b] FP, flash photolysis; LP; laser photolysis; DF, discharge flow; PR, pulse radiolysis; LIF, laser induced fluorescence; LMR, laser magnetic resonance; RF, resonance fluorescence; RA, resonance absorption; RR, relative method.

[c] Recalculated based on the recommendation [2] of reference reaction.

[d] Derived from the Arrhenius rate parameters.

[e] at 297K

[f] at 296K.

[g] at room temperature (r. t.).

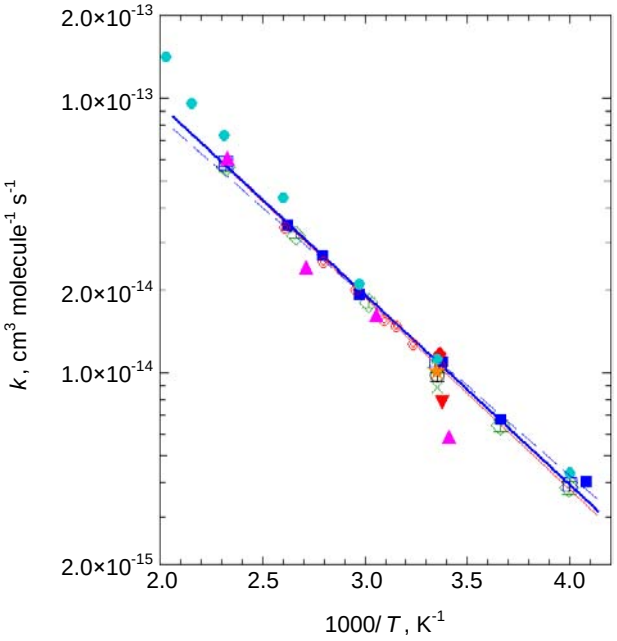

Figure 20. Arrhenius plots of the reaction rate coefficients for OH with HFC-32. The error bars represent 95% confidence level from linear least squares analysis. (◇), FP; (□), LP-H_2O; (○), DF; red solid line, nonlinear fit to the present work. (■), Talukdar et al. [35]; (●), Jeong and Kaufman [22]; (▲), Clyne and Holt [16]; (×), Bera and Hanrahan [41]; (★), Szilagyi et al. [42]; (◎), Hsu and DeMore [14]; (◆), Nip et al. [43]; (▼), Howard and Evenson [17]; blue dashed line, JPL 06-2 [2]; blue thick line, recommendation of this work.

CHF_2CF_3 (HFC-125)

The concentration of impurities in the purified sample of CHF_2CF_3 (HFC-125) is approximately 1/13 that in the original sample, and the measured rate constants of the original and purified samples are identical (Table 1). Thus, the effect of any impurities remaining in the purified sample seems to be negligible.
The rate constants for reaction of HFC-125 with OH radicals and the experimental conditions used for individual measurements in the present study are summarized in Table 26. The Arrhenius plots obtained in this work as well as values reported by other groups are plotted in Figure 21 and summarized in Table 27. The results of DeMore [44] obtained by the relative rate technique were recalculated on the basis of the value recommended by JPL [2] for reference reactions of OH radicals

with HFC-134 and HFC-134a. In Figure 21 and Table 27, the results of DeMore [44] are the unit-weighted averaged values obtained with these two reference compounds. The room temperature rate constants of Clyne and Holt [16] and Brown et al. [27] are about 2.5 and 1.45 times, respectively, as large as ours. The present results agree with those of Talukdar et al. [35] and DeMore [44]. The room temperature rate constant of Martin and Paraskevopoulos [45] is about 25% larger than ours, but the two values agree with each other within the estimated uncertainties. The recommended rate expression was derived from the present work and the results of Talukdar et al. [35], DeMore [44], and Martin and Paraskevopoulos [45]. Our recommended rate expression agrees with that of JPL within 1% over the temperature range 250–500 K.

Table 26. Experimental conditions and results for measurements of OH radicals with HFC-125

Temperature, K	technique	k, 10^{-15}, cm^3 $molecule^{-1}$ s^{-1}	$\bar{t}$, s or U, m s^{-1} [a]	pressure, torr	[HFC-125], 10^{15} molecule cm^{-3}	no. of expts.
250	FP	0.668±0.048	0.35 - 0.77	20 - 40	1.13 - 9.13	10
	LP-H_2O	0.715±0.061	0.35 - 0.57	40 - 80	1.19 - 9.45	9
273	FP	1.18±0.07	0.31 - 0.44	20 - 60	0.94 - 9.33	6
298	FP	1.94±0.13	0.29 - 0.41	20 - 60	1.04 - 9.14	6
	LP-H_2O	2.04±0.05	0.32 - 0.46	40 - 80	0.96 - 9.54	6
	DF	2.08±0.11	3.7 - 4.5	8	0.40 - 4.78	6
331	FP	3.05±0.18	0.31 - 0.38	40 - 60	1.13 - 9.46	6
375	FP	6.36±0.30	0.29 - 0.35	20 - 60	0.71 - 9.20	6
430	FP	12.0±0.5	0.25 - 0.38	20 - 40	0.81 - 9.25	6
	LP-H_2O	11.6±0.5	0.31 - 0.39	40 - 80	0.75 - 9.42	6

[a] $\bar{t}$, residence time for FP and LP methods; U, linear flow velocity for DF method.
The quoted errors represent 95% confidence level from linear least squares analysis.
The purity of the sample used in the measurement was 99.99%.

Table 27. Summary of the rate constants for the reaction of OH radicals with HFC-125

A [a], 10^{-12} cm^3 $molecule^{-1}$ s^{-1}	E/R [a], K	k_{298} [a], 10^{-15} cm^3 $molecule^{-1}$ s^{-1}	T range, K	technique [b]	reference
0.28	1350±100	2.9±1.0	257-423	DF-RF	Brown et al. [27]
0.17 +0.10, -0.06	1100±100	5.0±1.0	294-441	DF-RF	Clyne and Holt [16]
0.541±0.083	1700±100	1.90±0.27	220-364	DF-LMR FP-LIF	Talukdar et al. [35]
		2.49±0.28	298	FP-RA	Martin and Paraskevopoulos [45]
0.636 [c]	1694 [c]	2.12 [c, d]	298-358	RR	DeMore [44]
0.569±0.150	1690±80	1.99±0.10 [d]	250-430	FP-LIF LP-LIF DF-LIF	this work
0.60	1700	2.0			JPL 06-2 [2]
0.616±0.182	1710±90	2.00±0.09			this work

[a] The error limits are those quoted by the authors. Our values are 95% confidence level and do not include systematic errors.

[b] FP, flash photolysis; LP, laser photolysis; DF, discharge flow; LIF, laser induced fluorescence; RF, resonance fluorescence; RA, resonance absorption; RR, relative method.

[c] Recalculated based on the recommendation [2] of reference reaction. The value is an average of the results obtained from two reference compounds (HFC-134 and HFC-134a).

[d] Derived from the Arrhenius rate parameters.

Table 28. Experimental conditions and results for measurements of OH radicals with HFC-134a

temperature, K	technique	k, 10^{-15}, cm^3 $molecule^{-1}$ s^{-1}	$\bar{t}$, s or U, m s^{-1} [a]	pressure, torr	[HFC-134a], 10^{15} molecule cm^{-3}	no. of expts.
250	FP	1.35±0.14	0.08 - 0.44	5 - 40	1.47 - 19.1	9
	LP-H_2O	1.55±0.07	0.41 - 0.57	60 - 80	2.23 - 18.9	6
273	LP-H_2O	2.41±0.10	0.37 - 0.52	40 - 80	1.93 - 18.7	7
298	FP	4.17±0.39	0.23 - 0.33	20 - 40	0.76 - 9.16	6
	DF	4.63±0.09	4.3 - 5.3	6	1.40 - 8.78	9
331	DF	7.23±0.28	4.4 - 6.2	6	0.91 - 8.69	6
375	DF	12.8±0.4	5.1 - 8.5	6	0.97 - 7.35	6
375	DF	19.3±0.6	5.1 - 9.1	6	0.91 - 7.23	6
430	FP	25.9±0.9	0.30 - 0.37	20 - 40	0.97 - 9.44	6
	LP-H_2O	24.9±1.0	0.29 - 0.37	40 - 60	1.11 - 9.22	6
	DF	25.2±0.8	5.9 - 9.7	5 - 6	0.59 - 5.71	9

[a] $\bar{t}$, residence time for FP and LP methods; U, linear flow velocity for DF method.
The quoted errors represent 95% confidence level from linear least squares analysis.
The purity of the sample used in the measurement was 99.965%.

Table 29. Summary of the rate constants for the reaction of OH radicals with HFC-134a

A [a], 10^{-12} cm^3 $molecule^{-1}$ s^{-1}	E/R [a], K	k_{298} [a], 10^{-15} cm^3 $molecule^{-1}$ s^{-1}	T range, K	technique [b]	reference
0.58	1350±100	6.9±1.5	231-423	DF-RF	Brown et al. [27]
1.10±0.11	1424±35	9.25 [d]	249-473	DF-RF	Jeong et al. [33]
0.99±0.10	1640±150	3.9±0.6	255-424	DF-RF	Leu and Lee [46]
3.24 +2.26, -1.33	1800±200	6.9±0.9	294-429	DF-RF	Clyne and Holt [16]
		2.38±0.22 [f]	270	FP-RF	Zhang et al. [37]
3.7±1.5	1990±280	4.66 [d]	270-400	FP-RF	Liu et al. [32]
		4.6±0.5 [e]	295	LP-LA	Bednarek et al. [47]
		5.15±0.58	298	FP-RA	Martin and Paraskevopoulos [45]
1.03 +0.18, -0.15	1588±52	5.0±0.44	298-460	DF-EPR	Orkin and Khamaganov [18]
1.26 [c]	1721 [c]	3.90 [c, d]	298-358	RR	DeMore [44]
0.57 +0.14, -0.11	1430±60	4.34±0.35	223-324	FP-LIF DF-LMR	Gierczak et al. [31]
1.36±0.29	1720±70	4.23±0.20 [d]	250-430	FP-LIF LP-LIF DF-LIF	this work
1.05	1630	4.4			JPL 06-2 [2]
1.36±0.28	1710±70	4.39±0.18			this work

[a] The error limits are those quoted by the authors. Our values are 95% confidence level and do not include systematic errors. [b] FP, flash photolysis; LP, laser photolysis; DF, discharge flow; LIF, laser induced fluorescence; EPR, electron paramagnetic resonance; LMR, laser magnetic resonance; RF, resonance fluorescence; RA, resonance absorption; LA, laser absorption; RR, relative method. [c] Recalculated based on the recommendation [2] of reference reaction. The value is an average of the results obtained from four reference compounds (CH_3CCl_3, CH_4, HFC-125 and HFC-134). [d] Derived from the Arrhenius rate parameters. [e] at 295K. [f] at 270K.

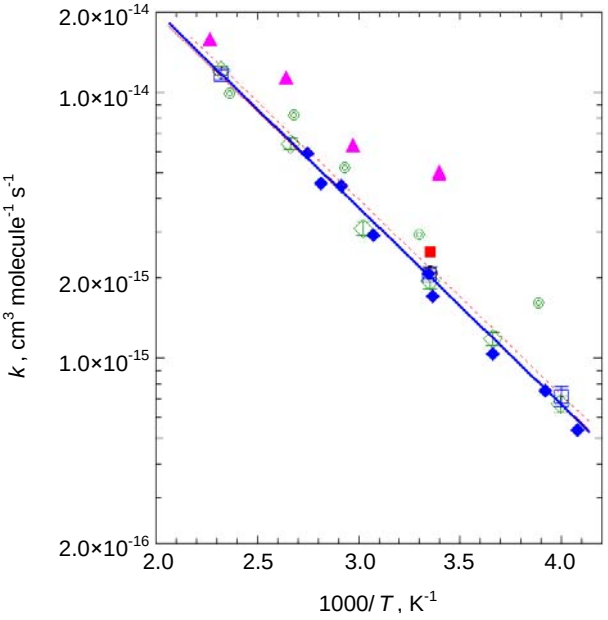

Figure 21. Arrhenius plots of the reaction rate coefficients for OH with HFC-125. The error bars represent 95% confidence level from linear least squares analysis. (◇), FP; (□), LP-H_2O; (○), DF; red solid line, nonlinear fit to the present work. (◎), Brown et al. [27]; (▲), Clyne and Holt [16]; (◆), Talukdar et al. [35]; (■),Martin and Paraskevopoulos [45]; red dotted line, DeMore [44]; blue dashed line, JPL 06-2 [2]; blue thick line, recommendation of this work.

CH_2FCF_3 (HFC-134a)

The concentration of impurities in the purified sample of CH_2FCF_3 (HFC-134a) is approximately 1/6 that in the original sample, and the measured rate constants of the purified sample are on average about 2% smaller than those of the original sample (Table 1). From the purity and the measured rate constants, the influence of the impurities in the purified sample was estimated to be 80%, on the assumption that the rate constant for reaction of the impurities with OH radicals is as large as 1×10^{-11} cm^3 $molecule^{-1}$ s^{-1} (the worst case conceivable). If the sum total of the impurities removed from the original sample is responsible for the decreases in the observed rate constants, the rate constant for the impurities is 4.4×10^{-14} cm^3 $molecule^{-1}$ s^{-1}. From the estimated rate constant for the impurities contained in the original sample, their influence on the measured rate constants of

the purified sample can be no larger than 0.4%. Therefore, we concluded that the effect of any impurities remaining in the purified samples was negligible.

Table 28 summarizes our experimental conditions and the results for reaction of HFC-134a with OH radicals. The Arrhenius plots and rate parameters are shown in Figure 22 and Table 29, together with literature data. The results of the relative rate study reported by DeMore [44] were recalculated on the basis of the value recommended by JPL [2] for four reference compounds: CH_4, CH_3CCl_3, HFC-125, and HFC-134. In Figure 22 and Table 29, the results of DeMore [44] are the unit-weighted averaged values obtained with these four reference compounds. The frequency factor and temperature dependence reported by Brown et al. [27] are considerably smaller than ours.

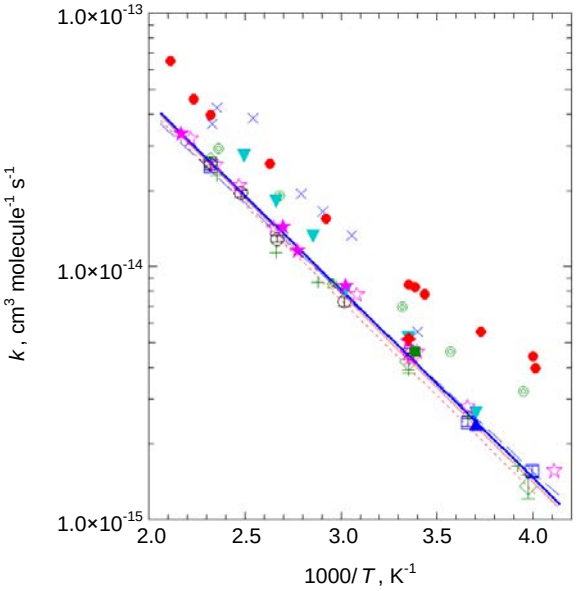

Figure 22. Arrhenius plots of the reaction rate coefficients for OH with HFC-134a. The error bars represent 95% confidence level from linear least squares analysis. (◇), FP; (□), LP-H_2O; (○), DF; red solid line, nonlinear fit to the present work. (◎), Brown et al. [27]; (●), Jeong et al. [33]; (+), Leu and Lee [46]; (×), Clyne and Holt [16]; (▲), Zhang et al. [37]; (▼), Liu et al. [32]; (■), Bednarek et al. [47]; (◆), Martin and Paraskevopoulos [45]; (★), Orkin and Khamaganov [18]; (☆), Gierczak et al. [31]; red dotted line, DeMore [44]; blue dashed line, JPL 06-2 [2]; blue thick line, recommendation of this work.

The results reported by Clyne and Holt [16] and Jeong et al. [33] are considerably larger than ours over the entire temperature range. The recommended rate expression was derived from the present results; those of Leu and Lee [46], Liu et al. [32], Orkin and Khamaganov [18], and Gierczak et al. [31] (above 273 K); the results of the relative rate study by DeMore [44]; the room temperature rate constants of Martin and Paraskevopoulos [45] and Bednarek et al. [47]; and the 270 K rate constant of Zhang et al. [37]. The present recommended rate expression agrees with that of JPL within 10% over the temperature range 250–500 K.

CH_2FCHF_2 (HFC-143)

From the values for sample purity and the measured rate constants for CH_2FCHF_2 (HFC-143) listed in Table 1, the influence of impurities on the rate constant was estimated to be smaller than 5%, on the assumption that the rate constant for reaction of the impurities with OH radicals is as large as 1×10^{-11} cm^3 $molecule^{-1}$ s^{-1} (the worst case conceivable). Therefore, we concluded that the effect of any impurities remaining in the purified samples was negligible.

The rate constants for reaction of HFC-143 with OH radicals and the experimental conditions for individual measurements over the temperature range 250–430 K measured by means of the various methods are summarized in Table 30. The Arrhenius plots and rate parameters obtained in this work as well as kinetic data reported by other groups are shown in Figure 23 and summarized in Table 31. The result of Barry et al. [48] obtained by the relative rate technique was recalculated on the basis of the value recommended by JPL [2] for reference reaction of OH radicals with CH_3CCl_3. The room temperature rate constant reported by Clyne and Holt [16] is 2.6 times as large as the present result.

In contrast, the present value agrees well with those of the relative rate study by Barry et al. [48] over the entire temperature range. In addition, the room temperature rate constant reported by Martin and Paraskevopoulos [45] is very close to our value. The recommended rate expression was derived from the present study, the results of Barry et al. [48], and the room temperature rate constant of Martin and Paraskevopoulos [45] and is very close to the JPL expression [2] in the middle temperature range (Figure 23), although the frequency factor and temperature dependence were 36 and 9% smaller than those of JPL.

Table 30. Experimental conditions and results for measurements of OH radicals with HFC-143

temperature, K	technique	k, 10^{-15}, cm^3 $molecule^{-1}$ s^{-1}	$\bar{t}$, s or U, m s^{-1} [a]	pressure, torr	[HFC-143], 10^{15} molecule cm^{-3}	no. of expts.
250	FP	7.69±0.38	0.34 - 0.42	20 - 40	0.90 - 9.20	6
	LP-H_2O	8.26±0.38	0.25 - 0.56	20 - 80	1.24 - 9.64	7
273	LP-H_2O	12.3±0.6	0.27 - 0.38	20 - 60	0.77 - 9.49	5
298	FP	16.4±0.9	0.19 - 0.38	20 - 40	0.62 - 9.48	8
	LP-H_2O	18.4±0.9	0.23 - 0.33	20 - 40	0.84 - 9.15	6
	DF	17.1±0.4	5.9 - 11.0	4 - 6	0.79 - 5.79	8
331	FP	28.0±1.4	0.26 - 0.46	20 - 40	0.71 - 8.97	5
375	LP-H_2O	50.2±2.0	0.25 - 0.34	20 - 40	1.10 - 7.40	6
430	FP	88.7±3.4	0.19 - 0.34	20 - 40	0.66 - 7.66	6
	LP-H_2O	90.9±4.7	0.26 - 0.37	20 - 60	0.62 - 7.52	6

[a]. $\bar{t}$, residence time for FP and LP methods; U, linear flow velocity for DF method.
The quoted errors represent 95% confidence level from linear least squares analysis.
The purity of the sample used in the measurement was 99.992%.

Table 31. Summary of the rate constants for the reaction of OH radicals with HFC-143

A [a], 10^{-12} cm^3 $molecule^{-1}$ s^{-1}	E/R [a], K	k_{298} [a], 10^{-14} cm^3 $molecule^{-1}$ s^{-1}	T range, K	technique [b]	reference
3.62 [c]	1622 [c]	1.57 [c, d]	278-323	RR	Barry et al. [48]
		1.83±0.18	298	FP-RA	Martin and Paraskevopoulos [45]
1.48 +0.56, -0.41	1000±100	4.9±0.5	293-441	DF-RF	Clyne and Holt [16]
2.46±0.90	1460±110	1.86±0.12 [d]	250-430	FP-LIF LP-LIF DF-LIF	this work
3.9	1620	1.7			JPL 06-2 [2]
2.49±1.22	1480±150	1.73±0.14			this work

[a] The error limits are those quoted by the authors. Our values are 95% confidence level and do not include systematic errors.

[b] FP, flash photolysis; LP, laser photolysis; DF, discharge flow; LIF, laser induced fluorescence; RF, resonance fluorescence; RA, resonance absorption; RR, relative method.

[c] Recalculated based on the recommendation [2] of reference reaction.

[d] Derived from the Arrhenius rate parameters.

Table 32. Experimental conditions and results for measurements of OH radicals with HFC-152a

temperature, K	technique	k, 10^{-14}, cm^3 $molecule^{-1}$ s^{-1}	$\bar{t}$, s or U, m s^{-1} [a]	pressure, torr	[HFC-152a], 10^{15} molecule cm^{-3}	no. of expts.
250	FP	1.77±0.12	0.32 - 0.37	20 - 40	0.68 - 9.29	5
	LP-H_2O	1.92±0.08	0.25 - 0.35	20 - 40	0.65 - 9.65	5
273	LP-H_2O	2.56±0.14	0.27 - 0.38	20 - 60	0.61 - 9.61	6
298	FP	3.61±0.24	0.19 - 0.38	20 - 40	0.52 - 7.09	5
	LP-H_2O	3.65±0.11	0.23 - 0.35	20 - 40	1.25 - 9.14	7
	DF	3.72±0.10	12.0 - 15.8	2 - 3	0.63 - 3.88	7
331	FP	5.29±0.20	0.26 - 0.39	20 - 40	0.58 - 9.25	5
375	LP-H_2O	9.10±0.27	0.25 - 0.34	20 - 40	1.08 - 7.49	6
430	FP	14.0±0.4	0.19 - 0.34	20 - 40	0.58 - 7.53	6
	LP-H_2O	14.5±0.4	0.26 - 0.33	20 - 60	0.65 - 7.02	7

[a] $\bar{t}$, residence time for FP and LP methods; U, linear flow velocity for DF method. The quoted errors represent 95% confidence level from linear least squares analysis. The purity of the sample used in the measurement was 99.999%.

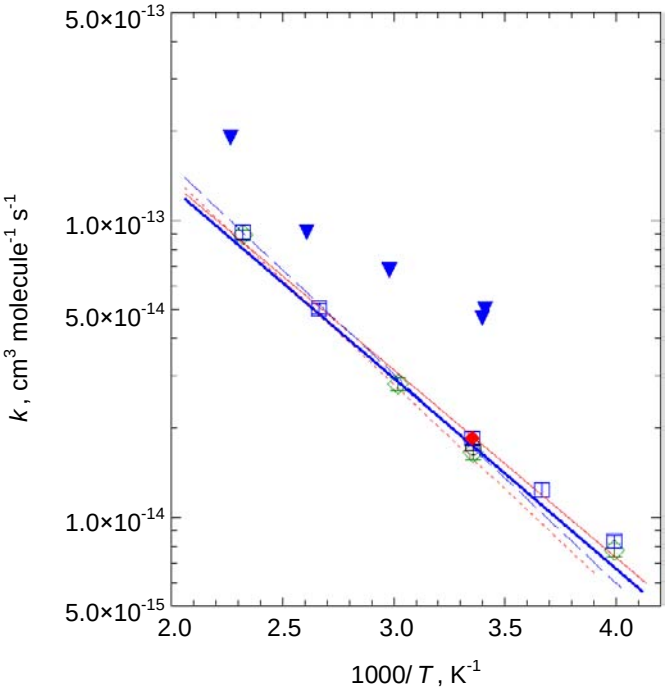

Figure 23. Arrhenius plots of the reaction rate coefficients for OH with HFC-143. The error bars represent 95% confidence level from linear least squares analysis. (◇), FP; (□), LP-H_2O; (○), DF; red solid line, nonlinear fit to the present work. (◆), Martin and Paraskevopoulos [45]; (▼), Clyne and Holt [16]; red dotted line, Barry et al. [48]; blue dashed line, JPL 06-2 [2]; blue thick line, recommendation of this work.

CH_3CHF_2 (HFC-152a)

The measured rate constants for the original and purified samples of CH_3CHF_2 (HFC-152a) are identical (Table 1). From the purity and the measured rate constants, the influence of impurities was estimated to be smaller than 0.3% for the worst case conceivable.

The rate constants for reaction of HFC-152a with OH radicals and the experimental conditions are summarized in Table 32. The Arrhenius plots and rate parameters measured in this work and values reported by other groups are shown in Figure 24 and listed in Table 33. The results of the relative rate study by Hsu and DeMore [14] were recalculated on the basis of the values recommended by JPL [2] for reference compounds CH_4 and CH_3CCl_3.

The frequency factor and temperature dependence reported by Nielsen [26] are slightly larger than ours, whereas those of Brown et al. [27] and Liu et al. [32] are slightly smaller than ours. The rate constants of Clyne and Holt [16] are larger than ours over the entire temperature range. The recommended rate expression was derived from the present results; those of Gierczak et al. [31] (above 258 K) and Kozlov et al. [49] (above 250 K); the relative rate study of Hsu and DeMore [14]; and the room temperature rate constants of Handwerk and Zellner [23], Howard and Evenson [28], and Nip et al. [43]. Our rate constants and those derived from the rate expression recommended by JPL (for $T \geq 298$ K) agree with each other within 5% over the temperature range 250–500 K.

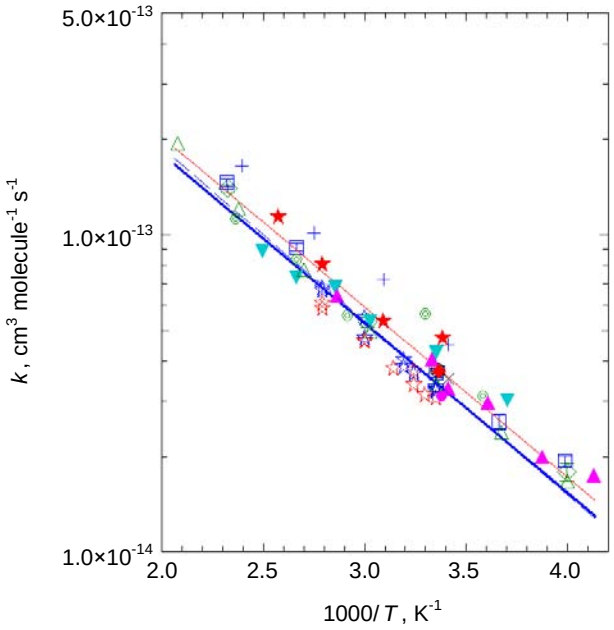

Figure 24. Arrhenius plots of the reaction rate coefficients for OH with HFC-152a. The error bars represent 95% confidence level from linear least squares analysis. (◇), FP; (□), LP-H_2O; (○), DF; red solid line, nonlinear fit to the present work. (★), Nielsen [26]; (+), Clyne and Holt [16]; (×), Handwerk and Zellner [23]; (◎), Brown et al. [27]; (●), Howard and Evenson [28]; (◆), Nip et al. [43]; (▼), Liu et al. [32]; (▲), Gierczakrt al. [31]; (△), Kozlov et al. [49]; (☆), Hsu and DeMore [14]; blue dashed line, JPL 06-2 [2] for T≥298K; blue thick line, recommendation of this work.

$CF_3CHFCHF_2$ (HFC-236ea)

The concentration of impurities in the purified sample of $CF_3CHFCHF_2$ (HFC-236ea) is approximately 1/500 that in the original sample, and the measured rate constants of the purified sample are on average about 43% smaller than those of the original sample (Table 1). If the rate constant for reaction of the impurities remaining in the purified sample is as large as 1×10^{-11} cm^3 $molecule^{-1}$ s^{-1}, their influence on the measured rate constant can be estimated to be about 6.5%. If, however, the sum total of impurities removed from the original sample is responsible for the decreases in the observed rate constants, the rate constant for the impurities is 2.4×10^{-13} cm^3 $molecule^{-1}$ s^{-1}. If the rate constant for reaction of impurities remaining in the purified sample is as large as 2.4×10^{-13} cm^3 $molecule^{-1}$ s^{-1}, their influence on the measured rate constants can be no larger than 0.2% of the observed values for the purified sample. Therefore, we concluded that the effect of any impurities remaining in the purified samples was negligible.

The rate constants and the experimental conditions for reaction of OH radicals with HFC-236ea are summarized in Table 34. The Arrhenius plots and rate parameters obtained in this work as well as kinetic data reported by other groups are shown in Figure 25 and summarized in Table 35. The results of Hsu and DeMore [14] obtained by the relative rate method were recalculated on the basis of the value recommended by JPL [2] for reference reaction of OH radicals with CH_4. As shown in Figure 25, the present results agree with those of Nelson et al. [50] and Hsu and DeMore [14]. The room temperature rate constants of Garland et al. [51] and Zhang et al. [52] are about 48 and 85% larger than ours, but the discrepancy between their values and ours is smaller at higher temperature. The recommended rate expression was derived from the present results and those of Nelson et al. [50] and Hsu and DeMore [14] and is listed in Table 35. As shown in the table, the recommended room temperature rate constant and the temperature dependence reported by JPL [2] agree with ours within about 20%, although our frequency factor is about 2 times as large as that of JPL.

Table 33. Summary of the rate constants for the reaction of OH radicals with HFC-152a

A [a], 10^{-12}cm^3 molecule^{-1} s^{-1}	E/R [a],K	k_{298} [a], 10^{-14}cm^3 molecule^{-1} s^{-1}	T range,K	technique [b]	reference
3.9	1370±260	3.93 [d]	295-388	PR-KS	Nielsen [26]
2.95 +1.03, -0.76	1200±100	5.1±0.5	293-417	DF-RF	Clyne and Holt [16]
		3.5±0.6 [e]	293	FP-RA	Handwerk and Zellner [23]
1.42	1050±250	5.6±0.9	220-423	DF-RF	Brown et al. [27]
		3.1±0.7 [f]	296	DF-LMR	Howard and Evenson [28]
		3.70±0.37 [g]	297	FP-RA	Nip et al. [43]
0.96±0.20	940±130	4.10 [d]	270-400	FP-RF	Liu et al. [32]
1.00 +0.18, -0.15	980±50	3.76±0.60	212-349	FP-LIF DF-LMR	Gierczakrt al. [31]
7.72×10^{-2} $(T/298)^{3.02}$	247	3.37 [d]	210-480	FP-RF	Kozlov et al. [49]
2.00 [c]	1241 [c]	3.12 [c, d]	298-358	RR	Hsu and DeMore [14]
2.41±0.61	1240±80	3.81±0.17 [d]	250-430	FP-LIF LP-LIF DF-LIF	this work
2.33	1260	3.4	$\geq$298		JPL 06-2 [2]
2.11±0.54	1230±80	3.38±0.12			this work

[a] The error limits are those quoted by the authors. Our values are 95% confidence level and do not include systematic errors.

[b] FP, flash photolysis; LP, laser photolysis; DF, discharge flow; PR, pulse radiolysis; LIF, laser induced fluorescence; KS, kinetic spectroscopy; LMR, laser magnetic resonance; RF, resonance fluorescence; RR, relative rate method.

[c] Recalculated based on the recommendation [2] of reference reaction.

[d] Derived from the Arrhenius rate parameters.

[e] at 293K. [f] at 296K. [g] at 297K.

Table 34. Experimental conditions and results for measurements of OH radicals with HFC-236ea

temperature,K	technique	k, 10^{-15},cm^3 $molecule^{-1}$ s^{-1}	$\bar{t}$, s [a]	pressure, torr	[HFC-236ea], 10^{15} molecule cm^{-3}	no. of expts.
250	FP	1.30±0.09	0.36 - 0.50	40 - 80	0.82 - 9.37	6
	LP-H_2O	1.42±0.10	0.34 - 0.50	60 - 100	0.90 - 9.89	6
273	FP	2.56±0.12	0.32 - 0.48	20 - 80	0.72 - 9.37	6
298	FP	4.56±0.23	0.32 - 0.41	20 - 60	0.90 - 9.42	6
	LP-H_2O	4.63±0.28	0.35 - 0.48	20 - 80	0.77 - 9.51	6
331	FP	8.71±0.48	0.30 - 0.44	20 - 40	0.86 - 9.46	6
375	FP	16.7±0.6	0.33 - 0.44	20 - 60	0.80 - 9.27	6
430	FP	31.7±0.8	0.32 - 0.47	20 - 60	0.74 - 9.47	6
	LP-H_2O	31.4±1.2	0.31 - 0.48	20 - 40	0.75 - 9.56	6
	LP-H_2O_2	31.5±0.7	0.36 - 0.46	40 - 60	0.95 - 9.21	6

[a] $\bar{t}$, residence time for FP and LP methods.

The quoted errors represent 95% confidence level from linear least squares analysis.

The purity of the sample used in the measurement was 99.997%.

Table 35. Summary of the rate constants for the reaction of OH radicals with HFC-236ea

A [a], 10^{-12}cm^3 molecule^{-1} s^{-1}	E/R [a], K	k_{298} [a], 10^{-15}cm^3 molecule^{-1} s^{-1}	T range, K	technique [b]	reference
		5.3±0.7	298	DF-LIF	Nelson et al. [50]
1.05	1434±161	8.51±0.26	260-365	FP-RF	Zhang et al. [52]
0.882 [c]	1544 [c]	4.96 [c]	298-380	RR	Hsu and DeMore [14]
0.20±0.09	1006±151	6.83 [d]	251-311	LP-LIF	Garland et al. [51]
2.51±0.22	1880±30	4.59±09 [d]	250-430	FP-LIF LP-LIF	this work
0.94	1550	5.2			JPL 06-2 [2]
2.00±0.43	1810±70	4.62±0.19			this work

[a] The error limits are those quoted by the authors. Our values are 95% confidence level and do not include systematic errors.

[b] FP, flash photolysis; LP, laser photolysis; DF, discharge flow; LIF, laser induced fluorescence; RF, resonance fluorescence; RR, relative rate method.

[c] Recalculated based on the recommendation [2] of reference reaction.

[d] Derived from the Arrhenius rate parameters.

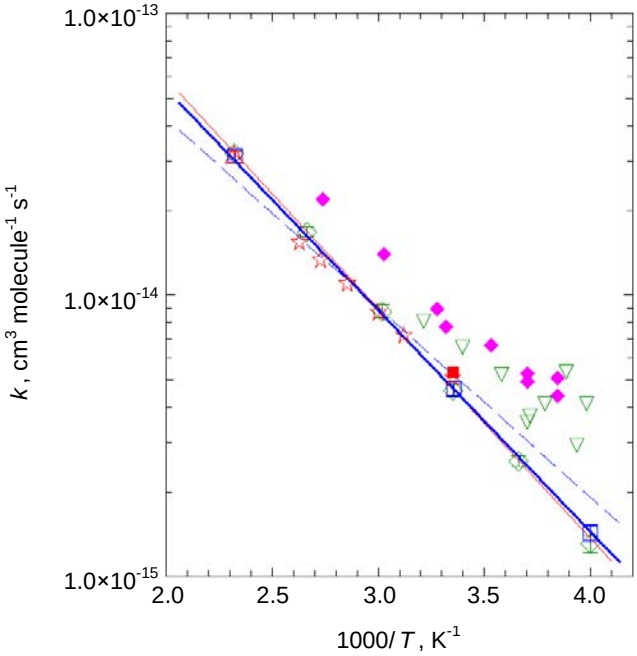

Figure 25. Arrhenius plots of the reaction rate coefficients for OH with HFC-236ea. The error bars represent 95% confidence level from linear least squares analysis. (◇), FP; (□), LP-H_2O; (△), LP-H_2O_2; red solid line, nonlinear fit to the present work. (■), Nelson et al. [50]; (▽), Garland et al. [51]; (◆), Zhang et al. [52]; (☆), Hsu and DeMore [14]; blue dashed line, JPL 06-2 [2]; blue thick line, recommendation of this work.

$CH_2FCF_2CHF_2$ (HFC-245ca)

The measured rate constants for the purified sample of $CH_2FCF_2CHF_2$ (HFC-245ca) are on average about 9% smaller than those of the original sample, and the concentration of impurities in the purified sample is approximately 1/45 that in the original sample (Table 1). The influence of impurities remaining in the purified sample on the measured rate constants is about 25% for the worst case. If, however, the sum total of impurities removed from the original sample is responsible for the decreases in the observed rate constants, the rate constant for reaction of the impurities with OH radicals is 1.0×10^{-13} cm^3 $molecule^{-1}$ s^{-1}. From the estimated rate constant for impurities contained in the original sample, their influence on the measured rate constants can be no larger than 0.2% for the

purified sample. Therefore, we concluded that the effect of any impurities remaining in the purified samples was negligible.

Table 36 summarizes our experimental conditions and results for reaction of OH radicals with HFC-245ca. The Arrhenius plots and rate parameters are shown in Figure 26 and Table 37, together with results reported by other groups.

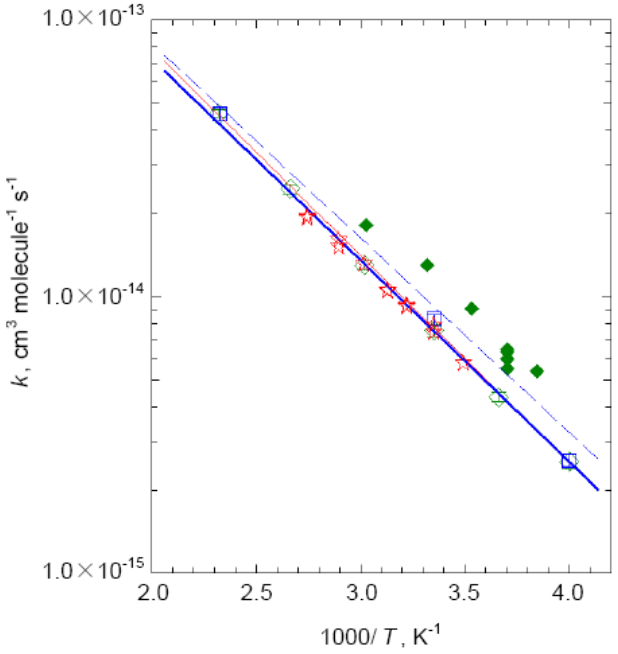

Figure 26. Arrhenius plots of the reaction rate coefficients for OH with HFC-245ca. The error bars represent 95% confidence level from linear least squares analysis. (◇), FP; (□), LP-H_2O; red solid line, nonlinear fit to the present work. (◆), Zhang et al. [52]; (☆), Hsu and DeMore [14]; blue dashed line, JPL 06-2 [2]; blue thick line, recommendation of this work.

Table 36. Experimental conditions and results for measurements of OH radicals with HFC-245ca

temperature, K	technique	k, 10^{-15}, cm^3 $molecule^{-1}$ s^{-1}	$\bar{t}$, s [a]	pressure, torr	[HFC-245ca],10^{15} molecule cm^{-3}	no. of expts.
250	FP	2.52±0.16	0.33 - 0.50	40 - 60	0.92 - 9.32	7
	LP-H_2O	2.54±0.13	0.34 - 0.51	20 - 60	0.84 - 9.39	6
273	FP	4.32±0.17	0.29 - 0.47	20 - 60	0.88 - 9.54	7
298	FP	7.50±0.37	0.26 - 0.47	20 - 60	0.72 - 9.39	7
	LP-H_2O	8.24±0.34	0.32 - 0.47	20 - 80	0.84 - 9.71	6
331	FP	12.9±0.5	0.31 - 0.47	20 - 60	0.76 - 9.42	6
375	FP	24.4±1.0	0.32 - 0.46	20 - 60	0.95 - 9.47	6
430	FP	45.7±1.4	0.31 - 0.48	20 - 60	0.83 - 9.42	6
	LP-H_2O	45.5±2.6	0.33 - 0.46	20 - 60	1.00 - 9.52	6

[a] $\bar{t}$, residence time for FP and LP methods.

The quoted errors represent 95% confidence level from linear least squares analysis.

The purity of the sample used in the measurement was 99.98%.

Table 37. Summary of the rate constants for the reaction of OH radicals with HFC-245ca

A [a], 10^{-12}cm^3 molecule^{-1} s^{-1}	E/R [a],K	k_{298} [a], 10^{-15}cm^3 molecule^{-1} s^{-1}	T range,K	technique [b]	reference
2.87	1661±170	10.9±0.3	260-365	FP-RF	Zhang et al. [52]
1.64 [c]	1611 [c]	7.37 [c, d]	286-364	RR	Hsu and DeMore [14]
2.47±0.41	1720±50	7.63±0.25 [d]	250-430	FP-LIF LP-LIF	this work
2.1	1620	9.2			JPL 06-2 [2]
2.07±0.32	1680±50	7.44±0.17			this work

[a] The error limits are those quoted by the authors. Our values are 95% confidence level and do not include systematic errors.
[b] FP, flash photolysis; LP, laser photolysis; LIF, laser induced fluorescence; RF, resonance fluorescence; RR, relative rate method.
[c] Recalculated based on the recommendation [2] of reference reaction.
[d] Derived from the Arrhenius rate parameters.

The results reported by Hsu and DeMore [14] using the relative rate method were recalculated on the basis of the value recommended by JPL [2] for reference compound CH_4. The temperature dependencies of the present results and the results of two other groups agree with one another, and the results of Zhang et al. [52] are about 30-40% larger than ours over the entire temperature range. Our results are in excellent agreement with those of Hsu and DeMore [14] over the entire temperature range. The recommended rate expression was derived from the present results and those of Hsu and DeMore [14]. The rate constant derived from the present recommended rate expression is about 22% smaller than the JPL value at 250 K, and the difference is reduced to about 12% at 500 K.

CF_3CHFCH_2F (HFC-245eb)

The concentration of impurities in the purified sample of CF_3CHFCH_2F (HFC-245eb) is approximately 1/285 that in the original sample, and the measured rate constants for the purified sample are about 0.45 times those of the original sample (Table 1). If the sum total of impurities removed from the original sample is responsible for the decreases in the observed rate constants, the rate constant for reaction of the impurities with OH radicals is 3.3×10^{-13} cm^3 $molecule^{-1}$ s^{-1}. If the rate constant for reaction of the impurities is as large as 1×10^{-11} cm^3 $molecule^{-1}$ s^{-1}, their influence on the measured rate constant can be estimated to be about 14%. If, however, the rate constant for the impurities is as large as 3.3×10^{-13} cm^3 $molecule^{-1}$ s^{-1}, their influence on the measured rate constants can be no larger than 0.4% of the observed values for the purified sample. Thus, the effect of any impurities remaining in the purified sample seems to be negligible.

The results and experimental conditions for reaction of OH radicals with HFC-245eb are summarized in Table 38. The Arrhenius plots are shown in Figure 27, and the Arrhenius rate parameters are summarized in Table 39. The only available result for HFC-245eb is the room temperature rate constant reported by Nelson et al. [50]. This value is also shown in Figure 27 and Table 39. As shown in Figure 27 and Table 39, the present results are very close to those of Nelson et al. The recommended rate expression was calculated on the basis of the present results and the room temperature rate constant of Nelson et al. [50]. The rate constant at 298 K recommended by JPL [2] is identical to that of Nelson et al. [50] and agrees with the present recommendation.

Table 38. Experimental conditions and results for measurements of OH radicals with HFC-245eb

temperature,K	technique	k, 10^{-15}, cm^3 $molecule^{-1}$ s^{-1}	$\bar{t}$, s [a]	pressure,torr	[HFC-245eb], 10^{15} molecule cm^{-3}	no. of expts.
250	FP	5.77±0.19	0.31 - 0.48	20 - 60	0.97 - 9.43	7
	LP-H_2O	6.04±0.29	0.33 - 0.50	20 - 60	0.80 - 9.19	7
273	FP	9.09±0.33	0.31 - 0.47	20 - 60	1.06 - 9.52	7
298	FP	14.5±0.6	0.24 - 0.47	20 - 60	0.77 - 9.52	8
	LP-H_2O	15.3±0.6	0.32 - 0.46	20 - 40	0.82 - 9.37	6
331	FP	24.5±1.0	0.33 - 0.49	20 - 60	0.94 - 9.44	6
375	FP	41.9±1.2	0.34 - 0.48	20 - 60	0.84 - 9.58	6
430	FP	74.9±2.7	0.32 - 0.47	20 - 60	0.94 - 9.53	6
	LP-H_2O	76.9±2.9	0.33 - 0.45	20 - 40	0.97 - 9.34	6

[a] $\bar{t}$, residence time for FP and LP methods.

The quoted errors represent 95% confidence level from linear least squares analysis.

The purity of the sample used in the measurement was 99.98%.

Table 39. Summary of the rate constants for the reaction of OH radicals with HFC-245eb

A [a], 10^{-12}cm^3 molecule^{-1} s^{-1}	E/R [a],K	k_{298} [a], 10^{-14}cm^3 molecule^{-1} s^{-1}	T range,K	technique [b]	reference
		1.48±0.17	298	DF-LIF	Nelson et al. [50]
2.55±0.48	1530±60	1.52±0.06 [c]	250-430	FP-LIF LP-LIF	this work
		1.5			JPL 06-2 [2]
2.54±0.45	1530±50	1.52±0.05			this work

[a] The error limits are those quoted by the authors. Our values are 95% confidence level and do not include systematic errors.
[b] FP, flash photolysis; LP, laser photolysis; DF, discharge flow; LIF, laser induced fluorescence.
[c] Derived from the Arrhenius rate parameters.

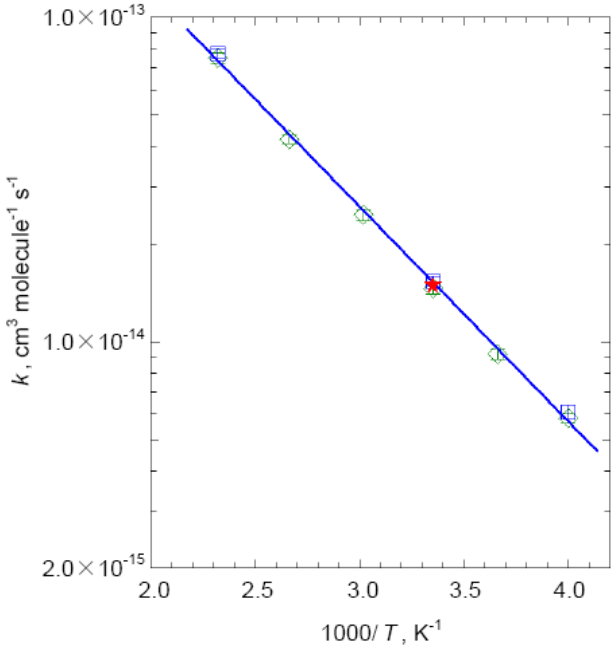

Figure 27. Arrhenius plots of the reaction rate coefficients for OH with HFC-245eb. The error bars represent 95% confidence level from linear least squares analysis. (◇), FP; (□), LP-H_2O; red solid line, nonlinear fit to the present work. (★), Nelson et al. [50]; blue thick line, recommendation of this work.

$CHF_2CH_2CF_3$ (HFC-245fa)

The concentration of impurities in the purified sample of $CHF_2CH_2CF_3$ (HFC-245fa) is approximately 1/900 that in the original sample, and the measured rate constants of the purified sample are on average about 10% smaller than those of the original sample (Table 1). From the purity and the measured rate constants, the influence of impurities was estimated to be 0.34% for the worst case.

The rate constants for reaction of HFC-245fa with OH radicals and the experimental conditions are summarized in Table 40. The Arrhenius plots and rate parameters obtained in this work as well as results reported by other groups are shown in Figure 28 and summarized in Table 41. The room temperature rate constant of Orkin et al. [53] is about 27% larger than ours. The temperature dependence of their results is about 25% smaller than ours, and the discrepancy between their value and ours becomes larger at lower temperature. They reported that the impurities in their sample were lower than the detection limit (1 ppm) of

GC-MS and GC-FID. Although they state that olefin impurities were present at less than 0.0005%, as measured by means of a UV absorption technique, the most likely reason for the discrepancy between our results and theirs is the presence of reactive impurities in their sample. The room temperature rate constant of Nelson et al. [50] is about 15% larger than ours, but the two values agree with each other within the estimated uncertainties.

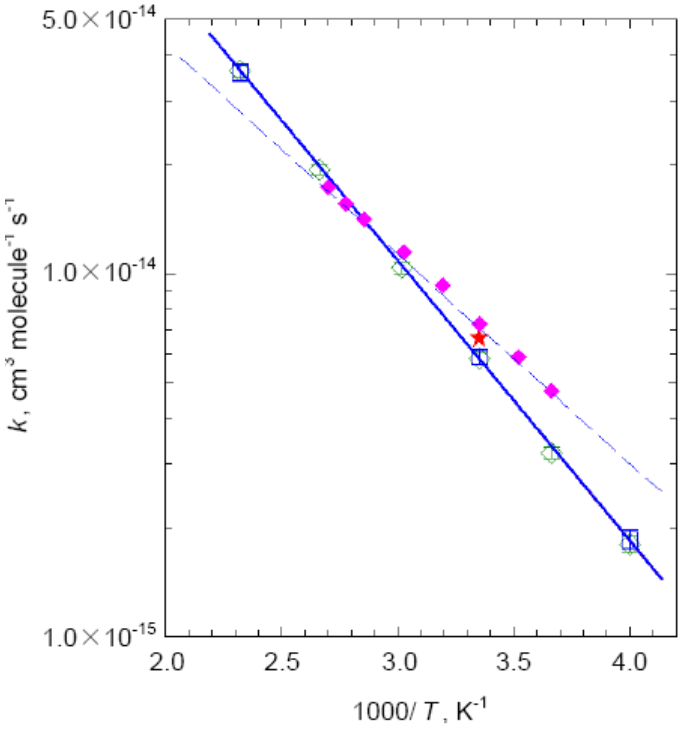

Figure 28. Arrhenius plots of the reaction rate coefficients for OH with HFC-245fa. The error bars represent 95% confidence level from linear least squares analysis. (◇), FP; (□), LP-H_2O; red solid line, nonlinear fit to the present work. (★), Nelson et al. [50]; (◆), Orkin et al. [53]; dashed line, blue JPL 06-2 [2]; blue thick line, recommendation of this work.

Table 40. Experimental conditions and results for measurements of OH radicals with HFC-245fa

temperature, K	technique	k, 10^{-15},cm^3 $molecule^{-1}$ s^{-1}	$\bar{t}$, s [a]	pressure, torr	[HFC-245fa],10^{15} molecule cm^{-3}	no. of expts.
250	FP	1.79±0.09	0.32 - 0.49	20 - 60	1.15 - 9.42	7
	LP-H_2O	1.85±0.12	0.32 - 0.50	20 - 60	0.99 - 9.56	6
273	FP	3.19±0.11	0.27 - 0.47	20 - 60	1.04 - 9.31	7
298	FP	5.79±0.20	0.26 - 0.47	20 - 60	0.77 - 9.38	7
	LP-H_2O	5.87±0.24	0.32 - 0.45	20 - 60	0.87 - 9.35	7
331	FP	10.3±0.4	0.33 - 0.46	20 - 60	0.95 - 9.55	6
375	FP	19.3±0.6	0.34 - 0.48	20 - 60	0.89 - 9.39	7
430	FP	35.9±1.2	0.30 - 0.47	20 - 60	0.84 - 9.22	6
	LP-H_2O	35.6±2.0	0.32 - 0.46	20 - 60	1.08 - 9.25	6

[a] $\bar{t}$, residence time for FP and LP methods.

The quoted errors represent 95% confidence level from linear least squares analysis.

The purity of the sample used in the measurement was 99.9998%.

Table 41. Summary of the rate constants for the reaction of OH radicals with HFC-245fa

A [a], 10^{-12}cm^3 molecule^{-1} s^{-1}	E/R [a],K	k_{298} [a], 10^{-15}cm^3 molecule^{-1} s^{-1}	T range, K	technique [b]	reference
		6.6±0.7	298	DF-LIF	Nelson et al. [50]
0.632 +0.089, -0.078	1331±43	7.28±0.5	273-370	FP-RF	Orkin et al. [53]
2.24±0.19	1780±30	5.72±0.09 [c]	250-430	FP-LIF LP-LIF	this work
0.61	1330	7.0			JPL 06-2 [2]
2.27±0.46	1780±60	5.79±0.22			this work

[a] The error limits are those quoted by the authors. Our values are 95% confidence level and do not include systematic errors.
[b] FP, flash photolysis; LP, laser photolysis; DF, discharge flow; LIF, laser induced fluorescence RF, resonance fluorescence.
[c] Derived from the Arrhenius rate parameters.

The recommended rate expression was derived from the present results and the room temperature rate constant of Nelson et al. [50]. The rate constant derived from the present recommended rate expression is about 18% smaller than the JPL value at 298 K, although our frequency factor and temperature dependence were about 3.7 times as large as and 34% larger than those of JPL.

$CF_3CH_2CH_2F$ (HFC-254fb)

The concentration of impurities in the purified sample of $CF_3CH_2CH_2F$ (HFC-254fb) is approximately 1/200 that in the original sample, and the measured rate constants of the purified sample is on average about 0.3% smaller than those of the original sample (Table 1). From the purity and the measured rate constants, the influence of impurities on the rate constants for the purified sample was estimated to be 1.2% for the worst case. Table 42 summarizes the experimental conditions and the results for reaction of OH radicals with HFC-254fb. The Arrhenius plots and rate parameters are shown in Figure 29 and Table 43.

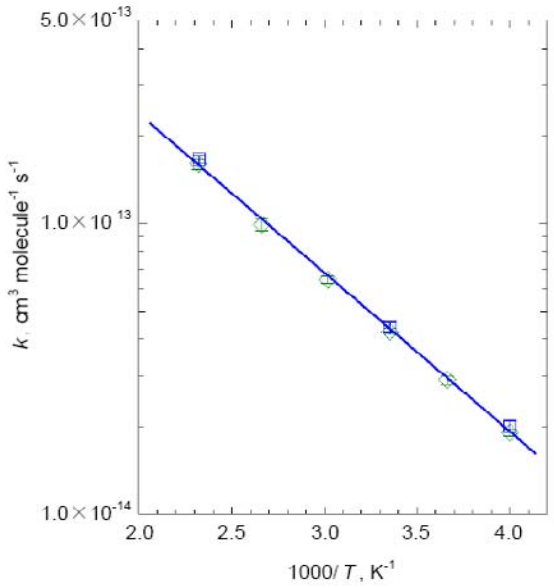

Figure 29. Arrhenius plots of the reaction rate coefficients for OH with HFC-254fb. The error bars represent 95% confidence level from linear least squares analysis. (◇), FP; (□), LP-H_2O; blue thick line, nonlinear fit to the present work.

Table 42. Experimental conditions and results for measurements of OH radicals with HFC-254fb

temperature, K	technique	k, 10^{-14}, cm^3 $molecule^{-1}$ s^{-1}	$\bar{t}$, s [a]	pressure, torr	[HFC-254fb],10^{15} molecule cm^{-3}	no. of expts.
250	FP	1.91±0.06	0.26 - 0.47	20 - 60	0.92 - 9.32	6
	LP-H_2O	2.00±0.09	0.28 - 0.41	20 - 60	0.81 - 9.38	7
273	FP	2.88±0.09	0.26 - 0.47	20 - 60	0.76 - 9.43	6
298	FP	4.23±0.11	0.26 - 0.47	20 - 60	0.72 - 9.57	7
	LP-H_2O	4.39±0.15	0.27 - 0.46	20 - 60	0.92 - 9.55	7
331	FP	6.39±0.18	0.31 - 0.44	20 - 60	0.87 - 9.89	6
375	FP	9.91±0.47	0.32 - 0.48	20 - 60	0.87 - 9.93	7
430	FP	15.9±0.6	0.35 - 0.46	20 - 60	0.95 - 9.26	6
	LP-H_2O	16.5±0.6	0.26 - 0.45	20 - 60	0.82 - 9.18	7

[a] $\bar{t}$, residence time for FP and LP methods. The quoted errors represent 95% confidence level from linear least squares analysis. The purity of the sample used in the measurement was *99.995%*.

Table 43. Summary of the rate constant for the reaction of OH radicals with HFC-254fb

A [a], 10^{-12} cm^3 $molecule^{-1}$ s^{-1}	E/R [a],K	k_{298} [a], $10^{-14}cm^3$ $molecule^{-1}$ s^{-1}	T range, K	technique [b]	reference
2.96±0.40	1260±40	4.32±0.11 [c]	250-430	FP-LIF LP-LIF	this work

[a] The error limits are 95% confidence level and do not include systematic errors. [b] FP, flash photolysis; LP, laser photolysis; LIF, laser induced fluorescence. [c] Derived from the Arrhenius rate parameters.

No data are available for the reaction of OH radicals with HFC-254fb. Therefore, the recommended rate expression is that derived from the present results.

$CH_3CF_2CH_3$ (HFC-272ca)

The concentration of impurities in the purified sample of $CH_3CF_2CH_3$ (HFC-272ca) is 1/37 that in the original sample, and the measured rate constants of the purified sample are on average about 56% smaller than those of the original sample (Table 1). From the purity and the measured rate constants of the purified sample, the influence of impurities on the measured rate constant was estimated to be about 28%, for the worst case. If, however, the sum total of impurities removed from the original sample is responsible for the decreases in the observed rate constants, the rate constant for reaction of the impurities is 1.3×10^{-12} cm^3 $molecule^{-1}$ s^{-1}, and their influence on the measured rate constants of the purified sample can be no larger than 3.7%.

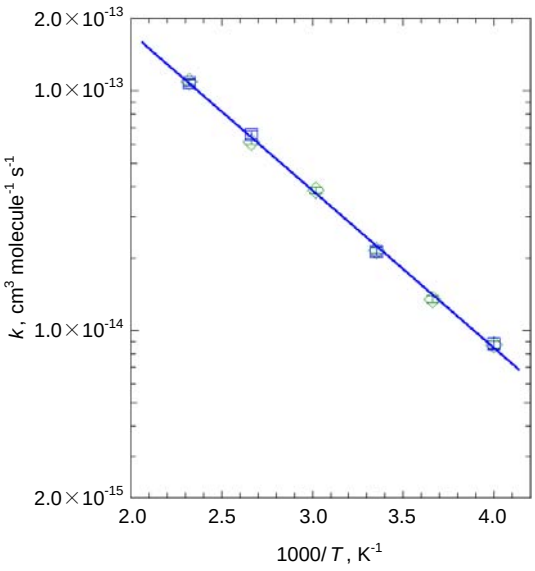

Figure 30. Arrhenius plots of the reaction rate coefficients for OH with HFC-272ca. The error bars represent 95% confidence level from linear least squares analysis. (◇), FP; (□), LP-H_2O; blue thick line, nonlinear fit to the present work.

Table 44. Experimental conditions and results for measurements of OH radicals with HFC-272ca

temperature, K	technique	k, 10^{-14},cm^3 $molecule^{-1}$ s^{-1}	$\bar{t}$, s [a]	pressure, torr	[HFC-272ca],10^{15} molecule cm^{-3}	no. of expts.
250	FP	0.869±0.032	0.31 - 0.61	20 - 60	1.28 - 9.44	6
	LP-H_2O	0.876±0.049	0.33 - 0.56	20 - 80	1.08 - 9.48	6
273	FP	1.34±0.04	0.27 - 0.48	20 - 60	1.05 - 9.65	6
298	FP	2.14±0.06	0.26 - 0.48	20 - 60	0.98 - 9.52	7
	LP-H_2O	2.13±0.10	0.29 - 0.48	20 - 60	1.08 - 9.47	7
331	FP	3.82±0.11	0.27 - 0.46	20 - 60	1.10 - 9.33	7
375	FP	6.10±0.16	0.31 - 0.45	20 - 60	1.38 - 9.43	6
	LP-H_2O	6.53±0.26	0.28 - 0.45	20 - 60	1.31 - 10.2	7
430	FP	10.9±0.3	0.30 - 0.44	20 - 60	1.25 - 9.37	6
	LP-H_2O	10.8±0.4	0.27 - 0.44	20 - 60	1.00 - 9.32	7

[a] $\bar{t}$, residence time for FP and LP methods. The quoted errors represent 95% confidence level from linear least squares analysis. The purity of the sample used in the measurement was *99.94%*.

Table 45. Summary of the rate constant for the reaction of OH radicals with HFC-272ca

A [a], $10^{-12}$$cm^3$ $molecule^{-1}$ s^{-1}	E/R [a],K	k_{298} [a], 10^{-14} cm^3 $molecule^{-1}$ s^{-1}	T range,K	technique [b]	reference
3.62±0.56	1520±50	2.23±0.07 [c]	250-430	FP-LIF LP-LIF	this work

[a] The error limits are 95% confidence level and do not include systematic errors. [b] FP, flash photolysis; LP, laser photolysis; LIF, laser induced fluorescence. [c] Derived from the Arrhenius rate parameters.

Therefore, the effect of any impurities remaining in the purified sample seems to be negligible. Table 44 summarizes the experimental conditions and the results for reaction of OH radicals with HFC-272ca. The Arrhenius plots and rate parameters are shown in Figure 30 and Table 45. No data are available for the reaction of OH radicals with HFC-272ca. Therefore, the recommended rate expression is that derived from the present results.

$CF_3CHFCHFCF_2CF_3$ (HFC-43-10mee)

The concentration of impurities in the purified sample of $CF_3CHFCHFCF_2CF_3$ (HFC-43-10mee) is 1/24 that in the original sample, and the measured rate constants of the purified sample are on average about 2% smaller than those of the original sample (Table 1). From the purity and measured rate constants of the purified sample, the influence of remaining impurities on the measured rate constant was estimated to be about 80%. If, however, the sum total of impurities removed from the original sample is responsible for the decreases in the observed rate constants, the rate constant for reaction of the impurities is 1.2×10^{-14} cm^3 $molecule^{-1}$ s^{-1}, and their influence on the measured rate constants of the purified sample can be no larger than 0.1%. Therefore, the effect of any impurities remaining in the purified sample seems to be negligible. Table 46 summarizes our experimental conditions and the results for reaction of OH radicals with HFC-43-10mee. The Arrhenius plots and rate parameters are shown in Figure 31 and Table 47 together with literature data.

The temperature dependence of Zhang et al. [54] is about 20% smaller than ours, and their room temperature rate constant is about 46% larger than ours. Similar comparisons can be made between our results and those of Schmoltner et al. [55], and the discrepancy between value of Schmoltner et al. and ours is small. At 250 K, the rate constant measured by Schmoltner et al. is about 27% larger than ours, but the two values agree with each other within the estimated uncertainties. The recommended rate expression was derived from the present results and those of Schmoltner et al. [55]. The rate constant derived from the present recommended rate expression is about 18% smaller than the JPL value at 298 K, although our frequency factor and temperature dependence were about 56 and 13% larger than those of JPL.

Table 46. Experimental conditions and results for measurements of OH radicals with HFC-43-10mee

temperature, K	technique	k, 10^{-15},cm^3 $molecule^{-1}$ s^{-1}	$\bar{t}$, s [a]	pressure, torr	[HFC-43-10mee], 10^{15} molecule cm^{-3}	no. of expts.
250	FP	0.895±0.081	0.40 - 0.53	20 - 60	0.73 - 9.34	6
	LP-H_2O	0.960±0.091	0.35 - 0.53	40 - 80	0.79 - 9.50	9
273	FP	1.42±0.08	0.38 - 0.55	20 - 60	0.62 - 9.52	7
298	FP	2.48±0.14	0.32 - 0.47	20 - 60	0.47 - 9.45	8
	LP-H_2O	2.56±0.13	0.32 - 0.64	20 - 80	0.70 - 9.40	8
331	FP	4.49±0.14	0.34 - 0.49	40 - 60	0.77 - 9.46	6
375	FP	9.10±0.41	0.34 - 0.47	20 - 60	0.63 - 9.47	7
430	FP	16.9±0.6	0.35 - 0.50	20 - 60	0.53 - 9.51	12
	LP-H_2O	16.2±1.0	0.26 - 0.51	20 - 80	0.61 - 9.36	7

[a] $\bar{t}$, residence time for FP and LP methods.

The quoted errors represent 95% confidence level from linear least squares analysis.

The purity of the sample used in the measurement was *99.98*%.

Table 47. Summary of the rate constants for the reaction of OH radicals with HFC-43-10mee

A [a], 10^{-12} cm^3 molecule^{-1} s^{-1}	E/R [a], K	k_{298} [a], 10^{-15} cm^3 molecule^{-1} s^{-1}	T range, K	technique [b]	reference
0.65±0.10	1600±50	3.01±0.36	252-375	FP-LIF LP-LIF	Schmoltner et al. [55]
0.421±0.128	1400±180	3.84 [c]	250-400	FP-RF	Zhang et al. [54]
0.942±0.282	1750±90	2.64±0.15 [c]	250-430	FP-LIF LP-LIF	this work
0.52	1500	3.4			JPL 06-2 [2]
0.811±0.250	1690±90	2.80±0.14			this work

[a] The error limits are those quoted by the authors. Our values are 95% confidence level and do not include systematic errors.

[b] FP, flash photolysis; LP, laser photolysis; LIF, laser induced fluorescence; RF, resonance fluorescence.

[c] Derived from the Arrhenius rate parameters.

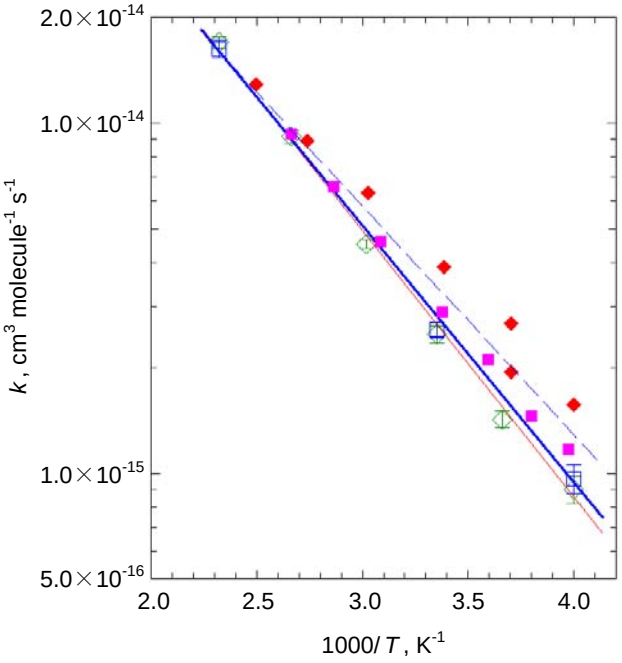

Figure 31. Arrhenius plots of the reaction rate coefficients for OH with HFC-43-10mee. The error bars represent 95% confidence level from linear least squares analysis. (◇), FP; (□), LP-H_2O; red solid line, nonlinear fit to the present work. (■), Schmoltner et al. [55]; (◆), Zhang et al. [54]; blue dashed line, JPL 06-2 [2]; blue thick line, recommendation of this work.

3.4. TROPOSPHERIC LIFETIMES OF FLUORINATED COMPOUNDS

The lifetime of a fluorinated compound (τ) with respect to removal by tropospheric OH radicals can be estimated from the following simple scaling equation [56]:

$$\tau = k_{\mathrm{MC,272K}} \big/ k_{\mathrm{272K}} \cdot \tau_{\mathrm{MC}} \qquad (3.4.1)$$

where τ_{MC} is the tropospheric lifetime of CH_3CCl_3 (MC) with respect to reaction with OH radicals in the troposphere only (6 years) [57]; $k_{MC,272K}$ is the rate constant for the reaction of OH radicals with MC at 272 K (6.14×10^{-15} cm^3

molecule^{-1} s^{-1} [2]); and k_{272K} is the rate constant for the reaction of OH radicals with the fluorinated compound at 272 K and is calculated from the Arrhenius rate parameters. Arrhenius rate parameters, rate constants at 298 and 272 K calculated from those parameters, and estimated lifetimes for the fluorinated compounds considered in this study are summarized in Table 48. In many cases, the lifetimes of the fluorinated compounds are 10 years or less and are shorter than the lifetime of HFC-134a (14.6 years) which is widely used as a refrigerant. Therefore, the global warming potentials of these fluorinated compounds, which are a function of lifetime and IR absorption intensity, seem to be smaller than the global warming potential of HFC-134a.

Table 48. Summary of Arrhenius parameter, rate constants at 298K and 272K, and lifetime

fluorinated compound	A, 10^{-12}cm^3 molecule^{-1} s^{-1}	E/R, K	k_{298}, 10^{-15}cm^3 molecule^{-1} s^{-1}	k_{272}, 10^{-15}cm^3 molecule^{-1} s^{-1}	lifetime, year
HCFC-22	1.10±0.13	1620±40	4.77±0.12	2.83±0.09	13.0
HCFC-123	1.08±0.24	1020±70	35.5±1.4	25.6±1.5	1.4
HCFC-123a	1.00±0.16	1320±50	11.9±0.4	7.78±0.32	4.7
HCFC-124	0.813±0.214	1350±90	8.90±0.39	5.79±0.36	6.4
HCFC-132b	2.44±0.63	1480±90	17.4±1.0	10.8±0.9	3.4
HCFC-133a	1.05±0.41	1240±130	16.7±1.2	11.2±1.1	3.3
HCFC-141	2.71±0.37	1070±40	75.0±2.1	53.2±2.0	0.7
HCFC-141b	1.30±0.25	1610±60	5.93±0.18	3.55±0.15	10.4
HCFC-142b	1.78±0.45	1870±80	3.42±0.17	1.88±0.12	19.6
HCFC-243db	1.70±0.47	1050±80	50.1±2.5	35.8±2.2	1.0
HCFC-253fb	3.27±0.69	1160±70	66.3±2.9	45.7±2.6	0.8
HFC-32	2.28±0.43	1590±60	10.9±0.3	6.53±0.27	5.7
HFC-125	0.616±0.182	1710±90	2.00±0.09	1.16±0.07	29.7
HFC-134a	1.36±0.28	1710±70	4.39±0.18	2.54±0.14	14.6
HFC-143	2.49±1.22	1480±150	17.3±1.4	10.8±1.1	3.4
HFC-152a	2.11±0.54	1230±80	33.8±1.2	22.8±1.2	1.6
HFC-236ea	2.00±0.43	1810±70	4.62±0.19	2.59±0.14	14.3

fluorinated compound	A, 10^{-12}cm^3 molecule^{-1} s^{-1}	E/R, K	k_{298}, 10^{-15}cm^3 molecule^{-1} s^{-1}	k_{272}, 10^{-15}cm^3 molecule^{-1} s^{-1}	lifetime, year
HFC-245ca	2.07±0.32	1680±50	7.44±0.17	4.34±0.14	8.5
HFC-245eb	2.54±0.45	1530±50	15.2±0.5	9.29±0.37	4.0
HFC-245fa	2.27±0.46	1780±60	5.79±0.22	3.27±0.15	11.3
HFC-254fb	2.96±0.40	1260±40	43.2±1.1	28.9±0.9	1.3
HFC-272ca	3.62±0.56	1520±50	22.3±0.7	13.7±0.5	2.7
HFC-43-10mee	0.811±0.250	1690±90	2.80±0.14	1.63±0.10	22.7

The error limits are 95% confidence level derived from non-linear least squares fit to the data and not include systematic errors.

Chapter 4

ESTIMATION OF RATE CONSTANTS BY THE NEURAL NETWORK METHOD

4.1. EMPIRICAL METHODS FOR ESTIMATION OF RATE CONSTANTS OF REACTIONS WITH OH RADICALS

Atkinson and a co-worker have developed a method of predicting rate constants for reactions with OH radicals based on structure–activity-relationship (SAR) [4, 5, 6]. The SAR method can be applied to a wide range of reactions, such as H-atom abstraction from C–H and O–H bonds, OH radical addition to double and triple bonds, OH radical addition to aromatic rings, and interactions of OH radicals with N-, S-, and P-containing functional groups.

In the case of H-atom abstraction from a C–H bond, the reaction rate, k_{total}, is calculated from Equation 4.1.1:

$$k_{\text{total}} = \sum\left[k_{\text{prim}} \cdot F(\text{X})\right] + \sum\left[k_{\text{sec}} \cdot F(\text{X}) \cdot F(\text{Y})\right] + \sum\left[k_{\text{tert}} \cdot F(\text{X}) \cdot F(\text{Y}) \cdot F(\text{Z})\right] \quad (4.1.1)$$

where k_{prim}, k_{sec}, and k_{tert} are the rate constants for H-atom abstraction from $–CH_3$, $–CH_2–$, and >CH– groups, respectively; and F(X), F(Y), and F(Z) are substituent factors for substituent groups X, Y, and Z. The substituent factors for $–CH_3$ (= 1.00, by definition), $–CH_2–$, >CH–, >C<, –F, –Cl, –Br, $–CH_2Cl$, $–CHCl_2$, and so on have been optimized on the basis of available data and are given by Atkinson and a co-worker [4, 5, 6]. This method can be used to calculate reaction rates for a wide variety of organic compounds with sufficient accuracy. In fact, for calculated room temperature rate constants for H-atom abstraction from C–H and O–H bonds, values for only 36 out of a total of 290 compounds disagree with the corresponding experimental values by more than a factor of 2 [6]. Examples of

compounds for which the experimental and calculated 298 K rate constants disagree by more than a factor of 2 include CHF_3, CH_3CF_3, $CHFBrCF_3$, $CHClBrCF_3$, $CHFClCF_2Cl$, and $CHF_2CF_2CF_2CHF_2$ [6]. With the exception of CH_3CF_3, these compounds have structures in which three substituent groups are attached to the target C–H. The reason for the low accuracy of the estimates for these compounds may be that the magnitude of the substituent effects of two or three halogen atoms differ from the effect of a single substituent.

DeMore [7] has proposed another method for estimating rate constants. This method is similar to the SAR method in principle but somewhat different in detail. In this method, the total rate constant is obtained by summation of the reactivities of each C–H bond contained in the molecule, and the logarithm (base 10) of the rate constant for each C–H bond is given by Equation 4.1.2:

$$\log k = \log k(\mathrm{CH_4}) + G_1 + \cdots + G_3 \tag{4.1.2}$$

where G_1, ···, G_3 are the contributions of the various substituent groups, such as –F, –Cl, –Br, $–CF_3$, and so on, that are connected to each carbon atom; and $k(CH_4)$ is rate constant of CH_4 with OH radicals per H-atom. The synergistic effects of multiple substituents are considered by using substituent factors such as G(2F), G(2Cl), G(F, Cl), and so on. When three substituent groups are present, a third-group multiplier is introduced to account for the contribution of the third group. This method has been used to calculate the rate constants for 32 compounds, including HFCs, HCFCs, hydrochlorocarbons, and brominated compounds. As a result, calculated rate constants agree to experimental rate constants within a factor of 1.35 [7].

In our previous study, we examined the contribution of synergistic effects to the estimation of rate constants for reactions of 5 hydrocarbons, 22 hydrofluorocarbons, 4 alcohols, and 3 hydrofluoroalcohols with OH radicals [8] (in this study, however, we discuss only the hydrocarbons and hydrofluorocarbons). For H-atom abstraction from a C–H bond, the reaction rate, k_{total}, is obtained from Equation 4.1.3:

$$\begin{aligned} k_{\mathrm{total}} = & \sum \left[k_{(\mathrm{CH})} \cdot F(\mathrm{X})_1 \cdot F(\mathrm{Y})_1 \cdot F(\mathrm{Z})_1 \cdot MP_3 \right] \\ & + \sum \left[k_{(\mathrm{CH})} \cdot F(\mathrm{X})_1 \cdot F(\mathrm{Y})_2 \cdot MP_2 \right] + \sum \left[k_{(\mathrm{CH})} \cdot F(\mathrm{X})_3 \right] \end{aligned} \tag{4.1.3}$$

where $k_{(CH)}$ is the rate constant per C–H, and $F(X)$, $F(Y)$, and $F(Z)$ are substituent factors for substituent groups X, Y, and Z. The subscript "1" for $F(X)$ indicates that only one substituent group X is attached to the target C–H, and the subscripts "2" and "3" indicate that two or three identical atoms (or groups) are attached to the C–H. The multipliers MP_2 and MP_3 represent the synergistic effects of having two or three different substituent groups attached to the C–H. When a F atom or fluorine-containing substituent groups, such as $–CF_3$, $–CH_nF_{(3–n)}$ (n = 1, 2), $–CF_2–$, and –CHF–, are attached to the C–H, the number of substituent groupsis considered for evaluation of the multiplier. In contrast, when a H atom or a $–CH_3$, $–CH_2–$, or –CH< group is attached to the C–H, the number of these groups is not considered for evaluation of the multiplier. Ratios between calculated and experimental rate constants, k_{cal}/k_{exp}, determined by this method for 27 hydrocarbons and hydrofluorocarbons have been found to range from 0.50 to 1.42 [8].

The substituent factors for a F atom and fluorine-containing substituent groups $F(F)_1$, $F(CF_3)_1$, $F(CHF_2)_1$, $F(CH_2F)_1$, $F(CF_2)_1$, and $F(CHF)_1$ are 0.0888, 0.00577, 0.00771, 0.0426, 0.00688, and 0.0121, respectively. These substituent factors are smaller than $F(H)_1$ (= 0.15) and $F(CH_3)_1$ (= 1.0, by definition), which indicates that the reactivity of a C–H bond is decreased when a H atom or a $–CH_3$ group is replaced by a F atom or fluorine-containing groups. To investigate the synergistic effect of substituent factor $F(X)$, we compared $F(X)_2/F(X)_1^2$ ratios for various substituent groups [8]. The ratios for $F(F)_2/F(F)_1^2$, $F(CF_3)_2/F(CF_3)_1^2$, and $F(CHF_2)_2/F(CHF_2)_1^2$ are 1.33, 12.5, and 47.1, respectively. The multipliers for the synergistic effects between different substituent groups, MP_2 (= 10.0) and MP_3 (= 78.1), are larger than unity, and MP_3 is larger than MP_2. These facts indicate that the degree to which the C–H reactivity is decreased by the addition of one X group (X = F, $–CF_3$, or $–CHF_2$) is reduced when two X groups are attached together to the carbon. In addition, when two or three different substituent groups are attached to C–H, the degree of the decrease in the C–H reactivity due to each individual substituent group becomes smaller. Therefore, we concluded that consideration of synergistic effects is indispensable for the development of a method for empirical estimation of reactivity with OH radicals.

The SAR method, as well as DeMore's method and our previous method, basically consider only the effects of nearest-neighbor atomic groups. The SAR method reportedly does not accurately predict values for partially fluorinated ethers [58] if the old parameters reported by Atkinson [4, 5] are used for the calculations. However, when additional substituent groups such as $–OCF_3$ [6] are introduced, agreement between calculated and measured rate constants improves. The rate constants of $CH_3OCF_2CHF_2$, $CHF_2OCH_2CF_2CHF_2$, $CHF_2OCH_2CF_2CF_3$,

and $CF_3CH_2OCF_2CHF_2$ are predicted within a factor of 2 [59] when additional substituent groups are used in the calculations. When additional substituent factors such as $–OCF_3$ are introduced, the result is that the effects of next to the nearest-neighbor groups are considered in the calculations. However, the SAR method cannot always accurately reproduce the experimental rate constants [60] for partially halogenated ethers. The estimated rate constants by SAR method for $CH_2FCF_2CHF_2$ (HFC-245ca), $CF_3CH_2CH_2F$ (HFC-254fb), and $CH_3CF_2CH_3$ (HFC-272ca) are 1.89×10^{-15}, 1.48×10^{-13}, and 4.90×10^{-15}, respectively; and the corresponding ratios between the calculated and experimental rate constants, k_{cal}/k_{exp}, are 0.25, 3.5, and 0.22, respectively. For comparison, the rate constants estimated by our previous method [8] are 8.13×10^{-15}, 5.95×10^{-14}, and 2.55×10^{-15}; and the k_{cal}/k_{exp} values are 1.1, 1.4, and 0.12 for $CH_2FCF_2CHF_2$, $CF_3CH_2CH_2F$, and $CH_3CF_2CH_3$, respectively.

In many cases, the SAR method and analogous methods give sufficiently accurate estimated rate constants. And agreement between predicted and experimental rate constants is improved by introducing new substituent groups. However, if this method is applied to a wide variety of compounds, the number of substituent groups will become huge. In some cases, no substituent factor is available [61]. In addition, our previous method and DeMore's method seem to be unable to reproduce synergistic effects accurately because the contribution of a particular group may depend on what other groups are connected to the carbon under consideration. Therefore, the development of new prediction methods that sufficiently consider synergistic effects and neighbor effects is important.

Urata et al. [9] have studied a method for estimating bond dissociation enthalpies (BDEs) for the C–H bonds of HFCs and partially fluorinated ethers (HFEs) using the three-layer feed-forward neural network technique. Using the estimated BDEs and a modified version of Heicklen's empirical relationship, they then calculated rate constants of reaction with OH radicals [10]. They reported that calculated rate constants for 15 of 43 compounds (23 HFCs and 20 HFEs) disagreed with the experimental rate constants by more than a factor of 2. This error level is somewhat large compared with that of the empirical estimation methods described above. To estimate the BDEs, Urata et al. used a number of structures, such as H–C···H, H–C···F, and so on, as the input parameters of the neural network. The neural network method may turn out to be a powerful tool for estimating rate constants; and estimation of rate constants for reactions with OH radicals using input parameters similar to those used by Urata et al. [9] may be possible. However, there have been no reports regarding direct estimation of rate constants using the neural network method.

4.2. TRENDS IN REACTIVITY OF FLUORINATED COMPOUNDS WITH OH RADICALS

From the results of the present study and available literature data, we can describe some trends in the reactivity of fluorinated compounds with OH radicals.

First, the fact that the room temperature rate constants of $CF_3CH_2CH_2F$ (HFC-254fb, $k_{298} = 4.32 \times 10^{-14}$) and $CF_3CF_2CH_2CH_2F$ (HFC-356mcf, $k_{298} = 4.2 \times 10^{-14}$ [2]) are similar indicates that the contributions of terminal $–CF_3$ and $–CF_2CF_3$ groups have almost the same magnitude. Similar behavior has been reported for the rate constants of the following sets of compounds: CHF_2CF_3 (HFC-125, $k_{298} = 2.00 \times 10^{-15}$) and $CHF_2CF_2CF_2CF_2CF_2CF_3$ (HFC-52-13p, $k_{298} = 1.98 \times 10^{-15}$ [11]); $CF_3CH_2CH_2CF_3$ (HFC-356mff, $k_{298} = 7.6 \times 10^{-15}$ [2]) and $CF_3CF_2CH_2CH_2CF_2CF_3$ (HFC-55-10mcff, $k_{298} = 8.3 \times 10^{-15}$ [2]); CH_3OCF_3 ($k_{298} = 1.2 \times 10^{-14}$ [2]), $CH_3OCF_2CF_3$ ($k_{298} = 1.1 \times 10^{-14}$ [2]), and $CH_3OCF_2CF_2CF_3$ ($k_{298} = 1.1 \times 10^{-14}$ [2]); $CHF_2OCH_2CF_3$ ($k_{298} = 1.2 \times 10^{-14}$ [2]) and $CHF_2OCH_2CF_2CF_3$ ($k_{298} = 1.0 \times 10^{-14}$ [2]); and CF_3CH_2OH ($k_{298} = 9.8 \times 10^{-14}$ [2]) and $CF_3CF_2CH_2OH$ ($k_{298} = 1.1 \times 10^{-13}$ [2]). In these cases, the rate constants differ by 20% or less. However, note that the rate constant of $CF_3CF_2CHCl_2$ (HFC-255ca, $k_{298} = 2.5 \times 10^{-14}$ [2]) is 30% smaller than that of CF_3CHCl_2 (HCFC-123, $k_{298} = 3.55 \times 10^{-14}$).

Second, the room temperature rate constant of CF_3CHFCH_2F (HFC-245eb, $k_{298} = 1.52 \times 10^{-14}$) is 0.88 times that of CHF_2CH_2F (HFC-143, $k_{298} = 1.73 \times 10^{-14}$). Similarly, the rate constants of $CF_3CHFCHF_2$ (HFC-236ea, $k_{298} = 4.62 \times 10^{-15}$) and CF_3CHFCF_3 (HFC-227ea, $k_{298} = 1.34 \times 10^{-15}$) are 0.76 and 0.67 times those of CHF_2CHF_2 (HFC-134, $k_{298} = 6.1 \times 10^{-15}$ [2]) and CHF_2CF_3 (HFC-125, $k_{298} = 2.00 \times 10^{-15}$), respectively. These results indicate that substitution of $–CF_3$ for –F in a $–CHF_2$ group reduces the rate constant by 10–30%.

Third, the room temperature rate constant of $CHF_2CH_2CF_3$ (HFC-245fa, $k_{298} = 5.79 \times 10^{-15}$) is 0.33 times that of CHF_2CH_2F (HFC-143, $k_{298} = 1.73 \times 10^{-14}$). Similarly, the rate constants of $CF_3CH_2CF_3$ (HFC-236fa, $k_{298} = 3.3 \times 10^{-16}$ [2]), $CF_3CH_2CH_2F$ (HFC-254fb, $k_{298} = 4.32 \times 10^{-14}$), and $CF_3CH_2CH_3$ (HFC-263fb, $k_{298} = 4.2 \times 10^{-14}$ [2]) are 0.075, 0.45, and 0.19 times those of CH_2FCF_3 (HFC-134a, $k_{298} = 4.39 \times 10^{-15}$), CH_2FCH_2F (HFC-152, $k_{298} = 9.7 \times 10^{-14}$ [2]), and CH_3CH_2F (HFC-161, $k_{298} = 2.2 \times 10^{-13}$ [2]), respectively. Furthermore, the rate constant of $CF_3CF_2CH_2CH_2CF_2CF_3$ (HFC-55-10mcff, $k_{298} = 8.3 \times 10^{-15}$ [2]) is 0.20 times that of $CF_3CF_2CH_2CH_2F$ (HFC-356mcf, $k_{298} = 4.2 \times 10^{-14}$ [2]). These results indicate that substitution of $–CF_3$ or $–CF_2CF_3$ for the –F of a $–CH_2F$ group reduces the rate constant by at least 50%.

Table 49. Rate constants of RfCF2Rf' at 298K estimated from the summation of RfCF3 and CF3Rf'

$R_fCF_2R_f$'		k_{obs} [a]	reference	k_{cal} [a]	k_{cal} / k_{obs}	R_fCF_3 or CF_3R_f'		
							k_{obs} [a]	reference
$CH_3CF_2CH_3$	HFC-272ca	2.23×10^{-14}	this work	2.6×10^{-15}	0.12	CH_3CF_3	1.3×10^{-15}	JPL 06-2 [2]
$CH_2FCF_2CHF_2$	HFC-245ca	7.44×10^{-15}	this work	6.39×10^{-15}	0.86	CH_2FCF_3	4.39×10^{-15}	this work
						CF_3CHF_2	2.00×10^{-15}	this work
$CF_3CH_2CF_2CH_3$	HFC-365mfc	6.9×10^{-15}	JPL 06-2 [2]	1.63×10^{-15}	0.24	$CF_3CH_2CF_3$	3.3×10^{-16}	JPL 06-2 [2]
						CF_3CH_3	1.3×10^{-15}	JPL 06-2 [2]
$CHF_2CF_2CF_2CHF_2$	HFC-338pcc	4.4×10^{-15}	JPL 06-2 [2]	4.00×10^{-15}	0.91	CHF_2CF_3	2.00×10^{-15}	this work
$CF_3CH_2CF_2CH_2CF_3$	HFC-458mfcf	2.6×10^{-15}	JPL 06-2 [2]	6.6×10^{-16}	0.25	$CF_3CH_2CF_3$	3.3×10^{-16}	JPL 06-2 [2]
$CH_3OCF_2CHF_2$		2.24×10^{-14}	Tokuhashi et al. [59]	1.4×10^{-14}	0.63	CH_3OCF_3	1.2×10^{-14}	JPL 06-2 [2]
						CF_3CHF_2	2.00×10^{-15}	this work
$CHF_2OCH_2CF_2CHF_2$		1.62×10^{-14}	Tokuhashi et al. [59]	1.4×10^{-14}	0.86	$CHF_2OCH_2CF_3$	1.2×10^{-14}	JPL 06-2 [2]
						CF_3CHF_2	2.00×10^{-15}	this work
CH_3OCF_2CHFCl		3.76×10^{-14}	Tokuhashi et al. [60]	2.09×10^{-14}	0.56	CH_3OCF_3	1.2×10^{-14}	JPL 06-2 [2]
						CF_3CHFCl	8.90×10^{-15}	this work
CHF_2OCF_2CHFCl		1.19×10^{-14}	Tokuhashi et al. [60]	9.39×10^{-15}	0.79	CHF_2OCF_3	4.9×10^{-16}	JPL 06-2 [2]
						CF_3CHFCl	8.90×10^{-15}	this work

a Units are cm3 molecule-1 s-1.

In our previous study, we found that the substituent factor for $–CF_3$ is almost equivalent to that of $–CF_2–$ ($F(CF_3)_1$ and $F(CF_2)_1$ are 0.00577 and 0.00688, respectively) [8], whereas the substituent factor obtained by means of the SAR method for $–CF_3$ is about 3.9 times that of $–CF_2–$ ($F(CF_3)$ and $F(CF_2)$ obtained by the SAR method are 0.071 and 0.018, respectively) [6]. Our previous results suggest that the reactivity of $R_fCF_2R_f'$ can be obtained from the summation of the reactivities of R_fCF_3 and CF_3R_f'. Here R_f and R_f' are reactive site containing hydrogen atom. Previously, we examined summing the reactivities [59, 60] for halogenated ethers. The results obtained in our previous study [59, 60] were recalculated on the basis of the present recommended rate constants and other new data and are summarized in Table 49. As shown in the table, the k_{cal}/k_{obs} values are always less than unity; that is, the summation of the reactivities of R_fCF_3 and CF_3R_f' always gives an underestimated value. In particular, for $CH_3CF_2CH_3$ (HFC-272ca), $CF_3CH_2CF_2CH_3$ (HFC-365mfc), and $CF_3CH_2CF_2CH_2CF_3$ (HFC-458mfcf), the k_{cal}/k_{obs} values are less than 0.25 and are at least 50% smaller than those of other compounds. These facts suggest that an R_f or R_f' group is activated by an R_f' or R_f group connected to the opposite site of the $–CF_2–$ group and that this effect may be particularly dominant if the reactivity of R_f or R_f' is lower. The fact that the calculated rate constant for $CHF_2CF_2CF_2CHF_2$ (HFC-338pcc) is only 9% smaller than the observed value suggests that the $–CHF_2$ group is about 10% activated by the $–CHF_2$ group connected to the opposite end of the molecule. Therefore, for the development of empirical methods for estimating reactivity, the effects of next-neighboring groups must be considered.

4.3. ESTIMATION OF RATE CONSTANTS FOR REACTION WITH OH RADICALS BY THE NEURAL NETWORK METHOD

The artificial neural network method has been successfully used in many fields. In particular, the three-layer feed-forward neural network method is widely used to predict physical and chemical properties. Back propagation is usually used to optimize the parameters between the neurons in each layer. However, there is a problem with back propagation when there are two or more reaction sites, and the reactivities of the individual sites are not known. For example, CH_2FCHF_2 (HFC-143) has two reactive sites ($CH_2F–$ and $–CHF_2$). In many cases, the reactivities of individual sites are not known, and the reactivities of these sites may differ from one another. Therefore, the development of the optimum method for such a situation was one of the main objectives of this work.

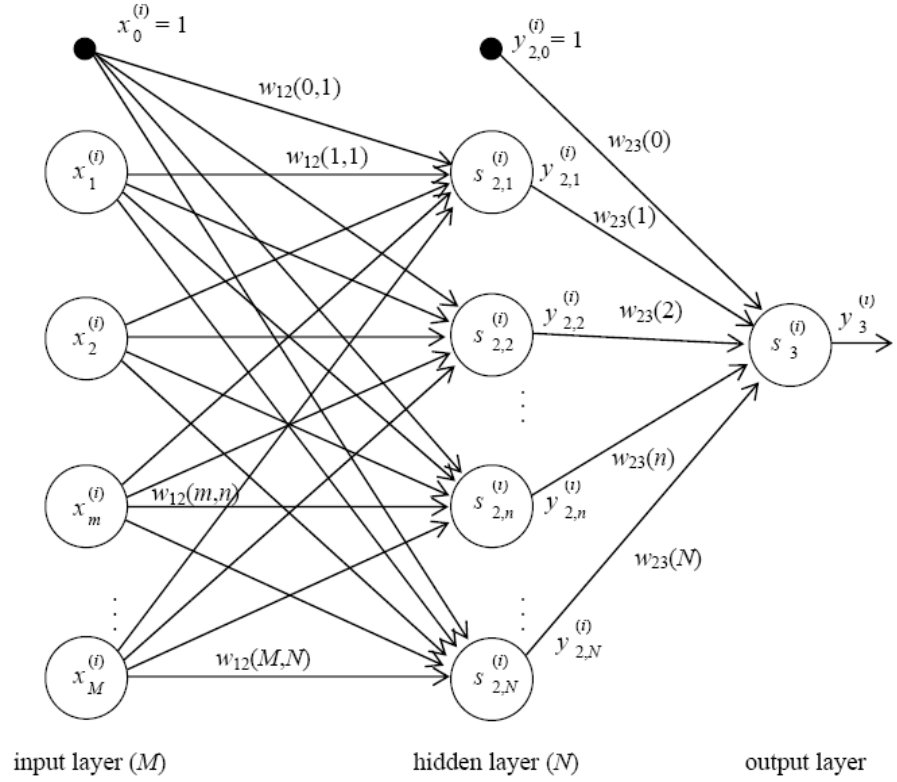

Figure 32. Schematic illustration of the neural network.

We used the three-layer feed-forward neural network method to estimate the rate constants for H-atom abstraction by OH radicals from fluorinated compounds at 298 K. Figure 32 is a schematic of the neural network used in this study. The neural network system consists of an input layer, a hidden layer, and an output layer; and the numbers of units (called neurons) in these layers are *M*, *N*, and 1, respectively.

The output of the neural network, namely, the estimated rate constant for the *i*-th reactive site, can be calculated by means of conventional procedures. The value of the *n*-th neuron in the hidden layer, $s_{2,n}^{(i)}$, is obtained from Equation 4.3.1; and the output of the neuron, $y_{2,n}^{(i)}$, is obtained with the sigmoid function defined in Equation 4.3.2 from the value of hidden layer:

$$s_{2,n}^{(i)} = \sum_{m=0}^{M} w_{12}(m,n) \cdot x_m^{(i)} \tag{4.3.1}$$

$$y_{2,n}^{(i)} = \mathrm{sigmoid}\left(s_{2,n}^{(i)}\right) = \frac{1}{1+\exp\left(-\alpha \cdot s_{2,n}^{(i)}\right)} \tag{4.3.2}$$

In these equations, superscript (*i*) represents the *i*-th reactive site in a compound, $w_{12}(m,n)$ represents a parameter (called the weight) to represent the connection between unit *m* in the input layer and unit *n* in the hidden layer, α is an adjustable parameter for the sigmoid function, and $x_m^{(i)}$ is an input parameter scaled by Equation 4.3.3 from 0.1 to 0.9 ($x_0^{(i)}$ is called the bias and is always 1):

$$x_m^{(i)} = \frac{0.8 \cdot c_m^{(i)} + 0.1 \cdot c_{m,\max} - 0.9 \cdot c_{m,\min}}{c_{m,\max} - c_{m,\min}} \tag{4.3.3}$$

where $c_m^{(i)}$ is the number of structural connections (such as H–C···H) for the *i*-th reactive site, and $c_{m,\max}$ and $c_{m,\min}$ are the maximum and minimum values of unit *m* in the input layer (summarized in Table 50). The values in Table 50 were selected as the maximum and minimum values that are the structural possibilities. The value of the output layer, $s_3^{(i)}$, is obtained with Equation 4.3.4 from the output values of the hidden layer, $y_{2,n}^{(i)}$; and the normalized output of the neural network for reaction site *i*, $y_3^{(i)}$, is obtained from Equation 4.3.5:

$$s_3^{(i)} = \sum_{n=1}^{N} w_{23}(n) \cdot y_{2,n}^{(i)} \tag{4.3.4}$$

$$y_3^{(i)} = \mathrm{sigmoid}\left(s_3^{(i)}\right) = \frac{1}{1+\exp\left(-\alpha \cdot s_3^{(i)}\right)} \tag{4.3.5}$$

where $w_{23}(n)$ represents the weight between unit *n* in the hidden layer and the output layer. The output of the neural network, namely, the natural logarithm of the estimated rate constant for reaction site *i*, $r^{(i)}$, is calculated with Equation 4.3.6:

$$r^{(i)} = \frac{\left(r_{\max} - r_{\min}\right) \cdot y_3^{(i)} - \left(0.1 \cdot r_{\max} - 0.9 \cdot r_{\min}\right)}{0.8} \tag{4.3.6}$$

where $r_{\max}$ and $r_{\min}$ are the maximum and minimum values of the natural logarithm of the reaction rate constant ($r_{\max} = -23 = \ln(1.03 \times 10^{-10})$ and $r_{\min} = -40 = \ln(4.25 \times 10^{-18})$). The estimated rate constant can be obtained from the sum total of the reactivities of the individual reaction sites, as shown in Equation 4.3.7:

$$k_{\text{est}} = \sum_{i=1}^{I} \left[n^{(i)} \cdot \exp\left(r^{(i)}\right) \right] \tag{4.3.7}$$

where k_{est} represents the estimated rate constant, and $n^{(i)}$ represents the number of C–H bonds at reaction site *i*.

Table 50. Minimum and maximum numbers of each descriptor ($c_{m,\min}$ and $c_{m,\max}$) and logarithm of reaction rate constant ($r_{\min}$ and $r_{\max}$)

descriptor	*m*	minimum ($c_{m,\min}$ or $r_{\min}$)	maximum ($c_{m,\max}$ or $r_{\max}$)
H-C···H	1	0	3
H-C···F	2	0	3
H-C···Cl	3	0	3
H-C···Br	4	0	3
H-C-C···H	5	0	9
H-C-C···F	6	0	9
H-C-C···Cl	7	0	9
H-C-C···Br	8	0	9
H-C-C-C···H	9	0	27
H-C-C-C···F	10	0	27
H-C-C-C···Cl	11	0	27
H-C-C-C···Br	12	0	27
rate constant		$-40 = \ln(4.25\times10^{-18})$	$-23 = \ln(1.03\times10^{-10})$

An algorithm for optimizing the weights by back propagation has not been developed for the situation in which a compound has multiple reactive sites for which the reactivities are unknown. In this study, we developed a method for optimizing the weights in such a situation by back propagation. It is described

below. The error (e) between the observed rate constant and the estimated rate constant is defined by Equations 4.3.8, 4.3.9, and 4.3.10:

$$b_{\text{obs}} = \frac{0.8 \cdot \ln\left(k_{\text{obs}}\right) + 0.1 \cdot r_{\max} - 0.9 \cdot r_{\min}}{r_{\max} - r_{\min}} \tag{4.3.8}$$

$$b_{\text{est}} = \frac{0.8 \cdot \ln\left(k_{\text{est}}\right) + 0.1 \cdot r_{\max} - 0.9 \cdot r_{\min}}{r_{\max} - r_{\min}} \tag{4.3.9}$$

$$e = \left(b_{\text{est}} - b_{\text{obs}}\right)^2 \tag{4.3.10}$$

where b_{obs} and b_{est} are normalized natural logarithm of observed and estimated rate constants of the compound, respectively. k_{obs} is the observed rate constant (called the training value). The effect on e of a small change in weight w, that is, the differential coefficient of e with respect to w, can be calculated as follows.

First, the value of the output layer $s_3^{(i)}$ and the resultant value $y_3^{(i)}$ are affected by a change in the weight between the hidden layer and the output layer, $w_{23}(n)$, as shown in Figure 32. Thus the differential coefficient of error e (expressed in Equation 4.3.10) with respect to weight $w_{23}(n)$ is calculated with Equation 4.3.11:

$$\frac{\partial e}{\partial w_{23}(n)} = \frac{\partial e}{\partial s_3^{(i)}} \frac{\partial s_3^{(i)}}{\partial w_{23}(n)} \tag{4.3.11}$$

Here $\partial e / \partial s_3^{(i)}$ is given by the following equation:

$$\frac{\partial e}{\partial s_3^{(i)}} = \frac{\partial e}{\partial b_{\text{est}}} \frac{\partial b_{\text{est}}}{\partial k_{\text{est}}} \frac{\partial k_{\text{est}}}{\partial r^{(i)}} \frac{\partial r^{(i)}}{y_3^{(i)}} \frac{\partial y_3^{(i)}}{\partial s_3^{(i)}} \tag{4.3.12}$$

Substitution of the differential coefficients from Equations 4.3.10, 4.3.9, 4.3.7, 4.3.6, and 4.3.5 into Equation 4.3.12 gives Equation 4.3.13:

$$\frac{\partial e}{\partial s_3^{(i)}} = 2\left(b_{\text{est}} - b_{\text{obs}}\right) \cdot \frac{n^{(i)} \cdot \exp\left(r^{(i)}\right)}{\sum_{i=1}^{I}\left[n^{(i)} \cdot \exp\left(r^{(i)}\right)\right]} \cdot \text{sigmoid}'\left(s_3^{(i)}\right) \tag{4.3.13}$$

The differential equation for the sigmoid function is obtained from Equation 4.3.14:

$$\text{sigmoid}'\left(s_3^{(i)}\right) = \alpha \cdot y_3^{(i)}\left(1 - y_3^{(i)}\right) \tag{4.3.14}$$

The differential coefficient of Equation 4.3.4 with respect to $w_{23}(n)$ is

$$\frac{\partial s_3^{(i)}}{\partial w_{23}(n)} = y_{2,n}^{(i)} \tag{4.3.15}$$

Thus by the substitution of Equations 4.3.13 and 4.3.15 into Equation 4.3.11, we obtain Equation 4.3.16:

$$\frac{\partial e}{\partial w_{23}(n)} = 2\left(b_{\text{est}} - b_{\text{obs}}\right) \cdot \frac{n^{(i)} \cdot \exp\left(r^{(i)}\right)}{\sum_{i=1}^{I}\left[n^{(i)} \cdot \exp\left(r^{(i)}\right)\right]} \cdot \text{sigmoid}'\left(s_3^{(i)}\right) \cdot y_{2,n}^{(i)} \tag{4.3.16}$$

Second, the value of the hidden layer $s_{2,n}^{(i)}$ and the resultant value $y_{2,n}^{(i)}$ are affected by a change in the weight between the input layer and the hidden layer, $w_{12}(m,n)$. Thus the differential coefficient of error e with respect to weight $w_{12}(m,n)$ is calculated with Equation 4.3.17:

$$\frac{\partial e}{\partial w_{12}(m,n)} = \frac{\partial e}{\partial s_3^{(i)}} \frac{\partial s_3^{(i)}}{\partial s_{2,n}^{(i)}} \frac{\partial s_{2,n}^{(i)}}{\partial w_{12}(m,n)} \tag{4.3.17}$$

Here $\partial s_3^{(i)} \big/ \partial s_{2,n}^{(i)}$ is given by the following equation:

$$\frac{\partial s_3^{(i)}}{\partial s_{2,n}^{(i)}} = \frac{\partial s_3^{(i)}}{\partial y_{2,n}^{(i)}} \frac{\partial y_{2,n}^{(i)}}{\partial s_{2,n}^{(i)}} \tag{4.3.18}$$

Substitution of the differential coefficients from Equations 4.3.4 and 4.3.2 into 4.3.18 gives Equation 4.3.19:

$$\frac{\partial s_3^{(i)}}{\partial s_{2,n}^{(i)}} = w_{23}(n) \cdot \text{sigmoid}'\left(s_{2,n}^{(i)}\right) \tag{4.3.19}$$

The differential coefficient of Equation 4.3.1 with respect to $w_{12}(m,n)$ is

$$\frac{\partial s_{2,n}^{(i)}}{\partial w_{12}(m,n)} = x_m^{(i)} \tag{4.3.20}$$

Thus, by substitution of Equations 4.3.13, 4.3.19, and 4.3.20 into Equation 4.3.17, we obtain Equation 4.3.21:

$$\frac{\partial e}{\partial w_{12}(m,n)} = \frac{\partial e}{\partial s_3^{(i)}} \cdot w_{23}(n) \cdot \text{sigmoid}'\left(s_{2,n}^{(i)}\right) \cdot x_m^{(i)} \tag{4.3.21}$$

The corrected weight between the hidden layer and the output layer, $\hat{w}_{23}(n)$, can be obtained from Equation 4.3.22, using $\partial e/\partial w_{23}(n)$, which is defined by Equation 4.3.16:

$$\hat{w}_{23}(n) = w_{23}(n) - \varepsilon \frac{\partial e}{\partial w_{23}(n)} \tag{4.3.22}$$

where $w_{23}(n)$ and $\hat{w}_{23}(n)$ represent the weights before and after correction, and ε is a positive constant (usually, ε << 1). Similarly, the weight between the input layer and the hidden layer, $w_{12}(m,n)$, can be corrected with $\partial e/\partial w_{12}(m,n)$, which is defined by Equation 4.3.21. The correction of the weight is repeated until the average of the deviation, E, defined by Equation 4.3.23 becomes smaller than a threshold value, E_{th}:

$$E = \frac{1}{L}\sum_{l=1}^{L}\left|\ln\left(k_{\text{est}}\right) - \ln\left(k_{\text{obs}}\right)\right| \tag{4.3.23}$$

where L represents the number of compounds.

The neural network method developed in this study was used to calculate rate constants for 94 compounds, including 12 hydrocarbons, 32 hydrofluorocarbons, 18 hydrochlorofluorocarbons, 16 hydrochlorocarbons, and 16 brominated compounds. As discussed in sections 4.1 and 4.2, consideration of the effects of atoms connected to the second neighboring carbon is indispensable for estimation of rate constants, whereas the contribution of atoms connected to the third neighboring carbon is small. Therefore, to estimate the rate constants by using the neural network method, we must consider the number of hydrogen, fluorine, chlorine, and bromine atoms connected to the carbon under consideration, as well as the first and second neighboring carbons; and the numbers of these structural connections are used as the input parameters of the neural network. Consequently, 12 kinds of descriptors, such as H–C···X, H–C–C···X, and H–C–C–C···X (X = H, F, Cl, Br), were selected as the input parameters. These descriptors are summarized in Table 50. The sigmoid function defined by Equations 4.3.2 and 4.3.5 gives an S-shaped output when plotted against an input value, and the center of the S-shape is shifted to the right or left by weight $w_{12}(0,n)$ or $w_{23}(0)$, respectively. Thus, the synergistic effects discussed in section 4.1 may also be accounted for by the sigmoid function in the hidden and output layers.

Table 51 summarizes some examples of input data for the neural network. The meaning of the input data is as follows:

1. CH_4 has 1 carbon and 4 equivalent C–H bonds. Thus, CH_4 has 1 reactive site, and the number of C–H bonds is 4. Because another 3 H atoms are connected to the carbon, there are 3 H–C···H structures for each C–H bond.
2. Because the 2 CH_3 groups of CH_3CH_3 are equivalent, this molecule has 1 reactive site. CH_3CH_3 has 6 equivalent C–H bonds. Another 2 H atoms are connected to the same carbon with the C–H bond under consideration, and 3 H atoms are connected to the neighboring carbon. Thus, there are 2 H–C···H and 3 H–C–C···H structures for each C–H bond.
3. $CH_3CH_2CH_3$ has 3 reaction sites: 2 $–CH_3$ and $–CH_2–$. However, because the 2 $–CH_3$ groups connected to the central $–CH_2–$ group are equivalent, we consider only 2 reaction sites: $–CH_3$ and $–CH_2–$. About the first site ($–CH_3$, site 1), there are 6 equivalent C–H bonds. Another 2 H atoms are connected to the same carbon, and 2 and 3 H atoms are connected to the first and second neighboring carbons, respectively. Consequently, for site 1, each C–H bond has 2 H–C···H, 2 H–C–C···H, and 3 H–C–C–C···H structures. The second site (–

CH_2–, site 2) has 2 C–H bonds, and another 1 H atom is connected to the same carbon. Three H atoms are connected to the neighboring carbons on both sides. Because 6 H atoms are equivalent with respect to the central –CH_2–, each central C–H bond has 1 H–C···H and 6 H–C–C···H structures.

4. $CH_2FCF_2CHF_2$ has 2 reaction sites: –CH_2F and –CHF_2. The first site (–CH_2F, site 1) has 2 C–H bonds. Another 1 H atom and 1 F atom are connected to the same carbon with the C–H bond under consideration; 2 F atoms are connected to the first neighboring carbon; and 1 H atom and 2 F atoms are connected to the second neighboring carbon. Consequently, reaction site 1 has 1 H–C···H, 1 H–C···F, 2 H–C–C···F, 1 H–C–C–C···H, and 2 H–C–C–C···F structures. Similarly, site 2 has 1 C–H bond and 2 H–C·F, 2 H–C–C···F, 2 H–C–C–C···H, and 1 H–C–C–C···F structures.

Input data for additional compounds are shown in Table 51.

We examined the predictive ability of the neural network by using a leave-one-out test method. One compound was removed, and the remaining compounds were used to optimize the weights (this optimization process is called training). After training, the rate constant for the compound removed during training was estimated using the weights obtained in this process. This procedure was sequentially applied to all compounds.

In the back propagation method developed in this study, the average error for optimized weights depends slightly on the initial value of weights. At first, 30 sets of randomly generated initial values for the weights were used in the training. From the results of the training, few sets of initial value were then selected and used in the following study.

In the beginning, we examined the dependence of the number of neurons in the hidden layer by using the leave-one-out method. The results are shown in Figure 33. Here, the lowest values of the average error obtained with various threshold values (E_{th}) are plotted as a function of the number of neurons in the hidden layer. The average error is reduced by 20% when the number of neurons in the hidden layer is increased from 2 to 3. The average error does not change drastically when the number of neurons is larger than 3. When the numbers of neurons in the hidden layer are 2, 3, 4, 5, and 6, the total numbers of weights are 29, 43, 57, 71, and 85, respectively.

Table 51. Examples of input data $c_m^{(i)}$ of the neural network

	CH_4	CH_3CH_3	$CH_3CH_2CH_3$		CH_2F_2	$CH_2FCF_2CHF_2$		$CHClF_2$	$CF_3CH_2CH_2Cl$	
	Methane	ethane	propane		HFC-32	HFC-245ca		HCFC-22	HCFC-253fb	
	site 1	site 1	site 1	site 2	site 1	site 1	site 2	site 1	site 1	site 2
number of C-H	4	6	6	2	2	2	1	1	2	2
H-C···H	3	2	2	1	1	1			1	1
H-C···F					2	1	2	2		
H-C···Cl								1		1
H-C···Br										
H-C-C···H		3	2	6					2	2
H-C-C···F						2	2		3	
H-C-C···Cl									1	
H-C-C···Br										
H-C-C-C···H			3			1	2			
H-C-C-C···F						2	1			3
H-C-C-C···Cl										
H-C-C-C···Br										

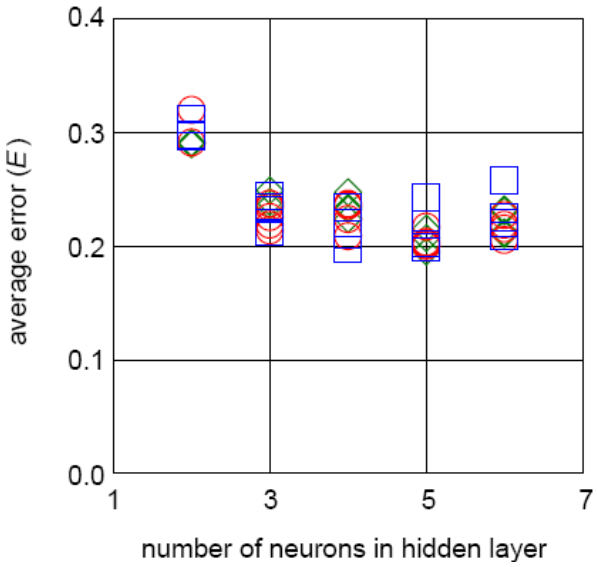

Figure 33. Relation of minimum average error and number of neurons in hidden layer. (◇), α = 0.5; (○), α = 1.0; (□), α = 2.0.

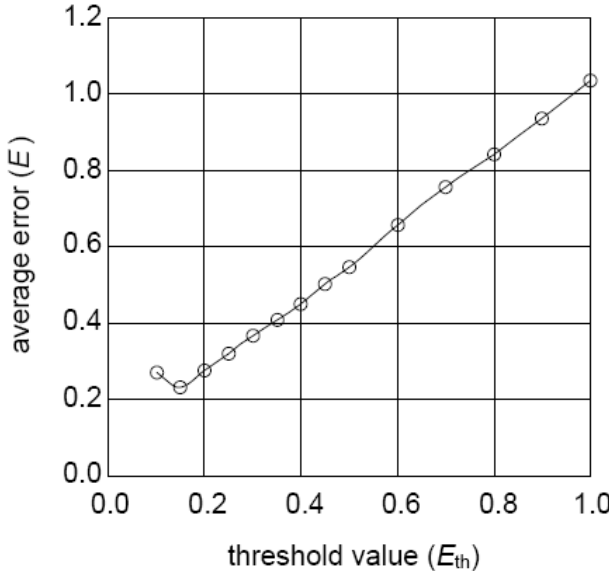

Figure 34. Relation between the threshold value and average error. Number of hidden layer = 3, α = 1.0.

The total number of weights exceeds the number of compounds when the number of neurons in the hidden layer is larger than 7. As is apparent in Figure 33, an adjustable parameter for the sigmoid function α does not significantly affect the average error. However, the dependence of the initial values on the average error becomes slightly large when α = 2.0. On the other hand, many repetition cycles are required to obtain optimized weights when α = 0.5. From these results, we determined the number of neurons in the hidden layer and the α value to be 3 and 1.0, respectively.

Figure 34 shows an example of the average error E as a function of the threshold value E_{th} obtained by using the leave-one-out method. The average error decreases as the threshold value decreases, and reaches a minimum at E_{th} = 0.15. Overtraining, in which the average error becomes large if the threshold is smaller than a certain value, is observed in this figure. In some cases, when a different set of initial values is used in the leave-one-out test, the average error reaches a minimum at E_{th} = 0.15, and overtraining is not observed. Therefore, we determined that an adequate value of the optimal threshold value for training is 0.15 when the number of units in the hidden layer and the α value are 3 and 1.0, respectively.

The results obtained for the estimated rate constants for reactions of 94 compounds with OH radicals obtained by the leave-one-out method are plotted in Figure 35 and listed in Table 52. The scatter and k_{est}/k_{obs} ratios obtained using another set of initial values are about the same as those shown in this figure. For the results shown in this figure and table, the range of k_{est}/k_{obs} ratios is 0.57–1.79, excluding the value for CHF_3 (HFC-23). The estimated rate constant for CHF_3 obtained by the leave-one-out test is about 3.2 times as large as the observed one. Note that for the leave-one-out test, the estimated rate constant for CHF_3 was calculated from weights that were optimized with the other 93 compounds. Therefore, k_{est} obtained by the leave-one-out test means an "estimated value" in the meaning of the truth. The reactivity of CHF_3 is unique because the presence of three F atoms considerably reduces the molecule's reactivity. For that reason, the accuracy of the CHF_3 rate constant calculated by empirical estimation methods is generally poor. For example, the rate constant for CHF_3 calculated by the SAR method is about 5.8 times as large as the observed one. As is apparent in Figure 35, we did not observe any scatter that depended on whether the compounds were hydrocarbons, HFCs, HCFCs, hydrochlorocarbons, or brominated compounds (with the exception of CHF_3). That is, we found that the rate constants for reactions with OH radicals can be estimated with the same accuracy for compounds of these types.

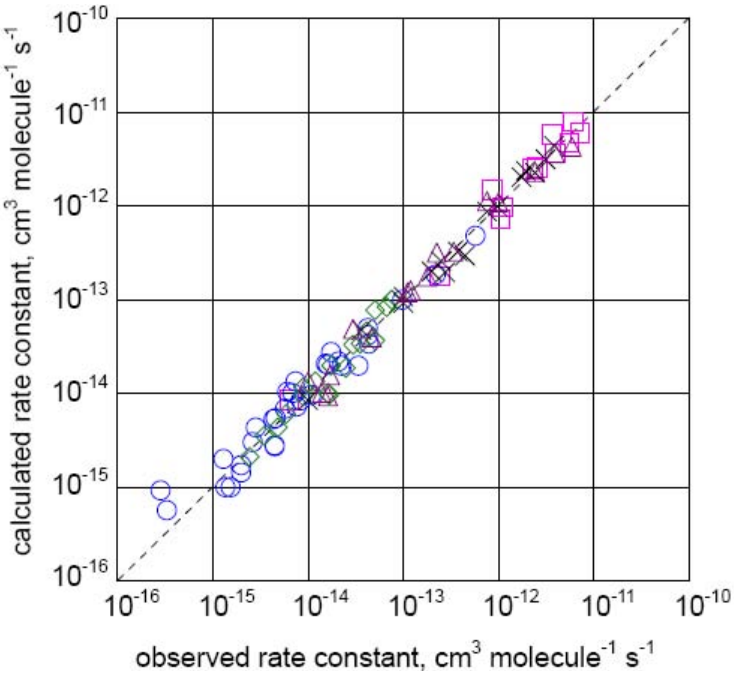

Figure 35. Plot of estimated OH rate constants by the neural network. Number of hidden layer = 3, α = 1.0, threshold value E_{th} = 0.15. (□), hydrocarbon; (○), HFC; (◇), HCFC; (×), hydrochlorocarbons; (△), brominated compound.

Figure 36 and Table 52 summarize the results of the correlated rate constants for reactions with OH radicals. In this case, the weights were optimized by a training procedure in which all 94 compounds were used. The optimized weights are listed in Table 53. The calculated rate constants well reproduce the observed values (Figure 36). The range of the correlated rate constant k_{cor}, to the observed rate constant k_{obs}, k_{cor}/k_{obs} ratios for all 94 compounds was 0.54–1.48, and this range is less than a factor of 2. The fact that the rate constant for CHF_3 is also well reproduced by this calculation suggests that synergistic effects are accounted for by this neural network method. In addition, there was no scatter between the types of compounds. Therefore, we concluded that accurate rate constants for reactions with OH radicals can be calculated by means of the neural network technique developed in this study.

We have developed and examined a method for estimating rate constants for reactions of hydrocarbons and related halogenated compounds with OH radicals. The method does not deal with compounds of other types, such as ethers,

alcohols, or unsaturated compounds. However, the method might easily be applied to such compounds if new descriptors, such as H–C–O–C···H for ethers, were added. Urata et al. [9] have introduced such descriptors for the estimation of bond dissociation enthalpies of C–H bonds by means of the neural network technique.

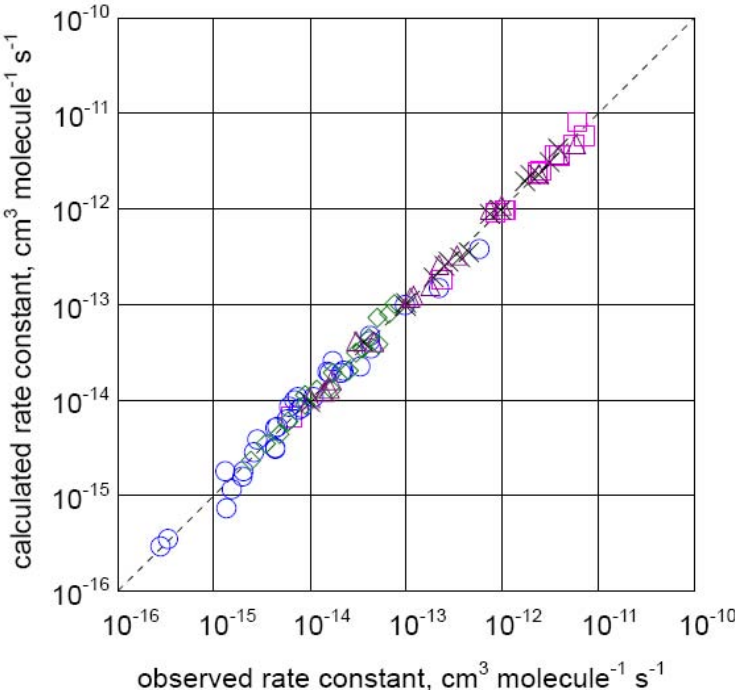

Figure 36. Plot of correlated OH rate constants by the neural network. Number of hidden layer = 3, α = 1.0, threshold value E_{th} = 0.15. (□), hydrocarbon; (○), HFC; (◇), HCFC; (×), hydrochlorocarbons; (△), brominated compound.

Our method can be used to calculate the reactivities of individual sites in compounds that have two or more reactive sites. Therefore, examining the reactivities of individual sites is of interest. Table 54 summarizes calculated reactivities for various HFCs.

Table 52. Results of the correlation and estimation (in 10-15 cm3 molecule-1 s-1) by using the neural network

no.	compound		reference	k_{obs}	correlation		estimation	
					k_{cor}	k_{cor} / k_{obs}	k_{est}	k_{est} / k_{obs}
1	CH_4		JPL 06-2 [2]	6.3×10^{-15}	6.65×10^{-15}	1.06	8.43×10^{-15}	1.34
2	CH_3CH_3		JPL 06-2 [2]	2.4×10^{-13}	1.83×10^{-13}	0.76	1.72×10^{-13}	0.72
3	$CH_3CH_2CH_3$		JPL 06-2 [2]	1.1×10^{-12}	9.74×10^{-13}	0.89	9.51×10^{-13}	0.86
4	$CH_3CH_2CH_2CH_3$		Atkinson [3]	2.54×10^{-12}	2.51×10^{-12}	0.99	2.51×10^{-12}	0.99
5	$CH_3CH_2CH_2CH_2CH_3$		Atkinson [3]	3.94×10^{-12}	3.60×10^{-12}	0.91	3.57×10^{-12}	0.91
6	$CH_3CH_2CH_2CH_2CH_2CH_3$		Atkinson [4]	5.58×10^{-12}	4.74×10^{-12}	0.85	4.68×10^{-12}	0.84
7	$CH_3(CH_2)_5CH_3$		Atkinson [4]	7.2×10^{-12}	5.86×10^{-12}	0.81	5.88×10^{-12}	0.82
8	$(CH_3)_3CH$		Atkinson [3]	2.33×10^{-12}	2.42×10^{-12}	1.04	2.48×10^{-12}	1.07
9	$(CH_3)_4C$		Atkinson [3]	8.49×10^{-13}	9.17×10^{-13}	1.08	1.47×10^{-12}	1.74
10	$(CH_3)_2CHCH(CH_3)_2$		Atkinson [3]	5.99×10^{-12}	8.24×10^{-12}	1.38	7.92×10^{-12}	1.32
11	$(CH_3)_3CCH_2CH(CH_3)_2$		Atkinson [3]	3.59×10^{-12}	3.63×10^{-12}	1.01	5.80×10^{-12}	1.62
12	$(CH_3)_3CC(CH_3)_3$		Atkinson [3]	1.06×10^{-12}	9.84×10^{-13}	0.93	7.17×10^{-13}	0.68
13	CHF_3	HFC-23	JPL 06-2 [2]	2.8×10^{-16}	2.89×10^{-16}	1.03	9.07×10^{-16}	3.24
14	CH_2F_2	HFC-32	this work	1.09×10^{-14}	1.08×10^{-14}	0.99	9.61×10^{-15}	0.88
15	CH_3F	HFC-41	JPL 06-2 [2]	2.1×10^{-14}	1.91×10^{-14}	0.91	2.19×10^{-14}	1.04
16	CHF_2CF_3	HFC-125	this work	2.00×10^{-15}	1.80×10^{-15}	0.90	1.71×10^{-15}	0.86
17	CHF_2CHF_2	HFC-134	JPL 06-2 [2]	6.1×10^{-15}	8.48×10^{-15}	1.39	1.01×10^{-14}	1.66
18	CH_2FCF_3	HFC-134a	this work	4.39×10^{-15}	5.07×10^{-15}	1.15	5.28×10^{-15}	1.20
19	CH_2FCHF_2	HFC-143	this work	1.73×10^{-14}	2.56×10^{-14}	1.48	2.70×10^{-14}	1.56
20	CH_3CF_3	HFC-143a	JPL 06-2 [2]	1.3×10^{-15}	1.77×10^{-15}	1.36	1.97×10^{-15}	1.51

Table 52. (Continued)

no.	compound		reference	k_{obs}	correlation		estimation	
					k_{cor}	k_{cor} / k_{obs}	k_{est}	k_{est} / k_{obs}
21	CH_2FCH_2F	HFC-152	JPL 06-2 [2]	9.7×10^{-14}	9.89×10^{-14}	1.02	9.92×10^{-14}	1.02
22	CH_3CHF_2	HFC-152a	this work	3.38×10^{-14}	2.25×10^{-14}	0.67	1.94×10^{-14}	0.57
23	CH_3CH_2F	HFC-161	JPL 06-2 [2]	2.2×10^{-13}	1.50×10^{-13}	0.68	1.81×10^{-13}	0.82
24	CF_3CHFCF_3	HFC-227ea	Tokuhashi et al. [62]	1.34×10^{-15}	7.28×10^{-16}	0.54	9.84×10^{-16}	0.73
25	$CF_3CF_2CH_2F$	HFC-236cb	JPL 06-2 [2]	4.4×10^{-15}	3.05×10^{-15}	0.69	2.74×10^{-15}	0.62
26	$CF_3CHFCHF_2$	HFC-236ea	this work	4.62×10^{-15}	5.17×10^{-15}	1.12	5.43×10^{-15}	1.17
27	$CF_3CH_2CF_3$	HFC-236fa	JPL 06-2 [2]	3.3×10^{-16}	3.52×10^{-16}	1.07	5.62×10^{-16}	1.70
28	$CH_2FCF_2CHF_2$	HFC-245ca	this work	7.44×10^{-15}	1.06×10^{-14}	1.43	1.33×10^{-14}	1.79
29	$CH_3CF_2CF_3$	HFC-245cb	Orkin et al. [63]	1.52×10^{-15}	1.15×10^{-15}	0.76	9.82×10^{-16}	0.65
30	$CHF_2CHFCHF_2$	HFC-245ea	JPL 06-2 [2]	1.6×10^{-14}	1.91×10^{-14}	1.19	1.98×10^{-14}	1.24
31	CF_3CHFCH_2F	HFC-245eb	this work	1.52×10^{-14}	1.96×10^{-14}	1.29	2.05×10^{-14}	1.35
32	$CHF_2CH_2CF_3$	HFC-245fa	this work	5.79×10^{-15}	6.31×10^{-15}	1.09	6.80×10^{-15}	1.17
33	$CF_3CH_2CH_2F$	HFC-254fb	this work	4.32×10^{-14}	3.47×10^{-14}	0.80	3.33×10^{-14}	0.77
34	$CF_3CH_2CH_3$	HFC-263fb	JPL 06-2 [2]	4.2×10^{-14}	4.12×10^{-14}	0.98	4.12×10^{-14}	0.98
35	$CH_3CF_2CH_3$	HFC-272ca	this work	2.23×10^{-14}	2.00×10^{-14}	0.90	1.96×10^{-14}	0.88
36	CH_3CHFCH_3	HFC-281ea	JPL 06-2 [2]	5.8×10^{-13}	3.87×10^{-13}	0.67	4.78×10^{-13}	0.82
37	$CHF_2CF_2CF_2CHF_2$	HFC-338pcc	JPL 06-2 [2]	4.4×10^{-15}	3.12×10^{-15}	0.71	2.71×10^{-15}	0.62
38	$CF_3CF_2CH_2CH_2F$	HFC-356mcf	JPL 06-2 [2]	4.2×10^{-14}	4.77×10^{-14}	1.14	4.97×10^{-14}	1.18
39	$CF_3CH_2CH_2CF_3$	HFC-356mff	JPL 06-2 [2]	7.6×10^{-15}	7.89×10^{-15}	1.04	7.15×10^{-15}	0.94
40	$CF_3CH_2CF_2CH_3$	HFC-365mfc	JPL 06-2 [2]	6.9×10^{-15}	9.84×10^{-15}	1.43	9.99×10^{-15}	1.45

Table 52. (Continued)

no.	compound		reference	k_{obs}	correlation		estimation	
					k_{cor}	k_{cor} / k_{obs}	k_{est}	k_{est} / k_{obs}
41	$CF_3CHFCHFCF_2CF_3$	HFC-43-10mee	this work	2.80×10^{-15}	3.81×10^{-15}	1.36	4.28×10^{-15}	1.53
42	$CF_3CH_2CF_2CH_2CF_3$	HFC-458mfcf	JPL 06-2 [2]	2.6×10^{-15}	2.82×10^{-15}	1.09	3.00×10^{-15}	1.15
43	$CHF_2CF_2CF_2CF_2CF_2CF_3$	HFC-52-13p	Chen et al. [11]	1.98×10^{-15}	1.56×10^{-15}	0.79	1.41×10^{-15}	0.71
44	$CF_3CF_2CH_2CH_2CF_2CF_3$	HFC-55-10mcff	JPL 06-2 [2]	8.3×10^{-15}	8.33×10^{-15}	1.00	8.40×10^{-15}	1.01
45	$CHFCl_2$	HCFC-21	JPL 06-2 [2]	3.0×10^{-14}	3.17×10^{-14}	1.06	3.23×10^{-14}	1.08
46	CHF_2Cl	HCFC-22	this work	4.77×10^{-15}	4.43×10^{-15}	0.93	4.32×10^{-15}	0.91
47	CH_2FCl	HCFC-31	JPL 06-2 [2]	4.1×10^{-14}	4.52×10^{-14}	1.10	4.57×10^{-14}	1.11
48	$CHCl_2CF_2Cl$	HCFC-122	JPL 06-2 [2]	5.1×10^{-14}	3.81×10^{-14}	0.75	3.63×10^{-14}	0.71
49	$CHFClCFCl_2$	HCFC-122a	JPL 06-2 [2]	1.6×10^{-14}	1.35×10^{-14}	0.84	9.93×10^{-15}	0.62
50	$CHCl_2CF_3$	HCFC-123	this work	3.55×10^{-14}	3.49×10^{-14}	0.98	3.34×10^{-14}	0.94
51	$CHFClCF_2Cl$	HCFC-123a	this work	1.19×10^{-14}	1.29×10^{-14}	1.08	1.33×10^{-14}	1.12
52	$CHFClCF_3$	HCFC-124	this work	8.90×10^{-15}	1.13×10^{-14}	1.27	1.14×10^{-14}	1.28
53	CH_2ClCF_2Cl	HCFC-132b	this work	1.74×10^{-14}	1.92×10^{-14}	1.10	1.95×10^{-14}	1.12
54	CH_2ClCF_3	HCFC-133a	this work	1.67×10^{-14}	1.28×10^{-14}	0.76	9.60×10^{-15}	0.57
55	$CH_2ClCHFCl$	HCFC-141	this work	7.50×10^{-14}	1.01×10^{-13}	1.35	9.99×10^{-14}	1.33
56	CH_3CFCl_2	HCFC-141b	this work	5.93×10^{-15}	5.95×10^{-15}	1.00	5.98×10^{-15}	1.01
57	CH_3CF_2Cl	HCFC-142b	this work	3.42×10^{-15}	3.45×10^{-15}	1.01	3.44×10^{-15}	1.01
58	$CF_3CF_2CHCl_2$	HCFC-225ca	JPL 06-2 [2]	2.5×10^{-14}	2.03×10^{-14}	0.81	1.84×10^{-14}	0.74
59	CF_2ClCF_2CHFCl	HCFC-225cb	JPL 06-2 [2]	8.9×10^{-15}	9.03×10^{-15}	1.01	9.15×10^{-15}	1.03
60	$CH_3CF_2CFCl_2$	HCFC-243cc	JPL 06-2 [2]	2.4×10^{-15}	2.29×10^{-15}	0.95	2.08×10^{-15}	0.87

Table 52. (Continued)

no.	compound		reference	k_{obs}	correlation		estimation	
					k_{cor}	k_{cor} / k_{obs}	k_{est}	k_{est} / k_{obs}
61	$CF_3CHClCH_2Cl$	HCFC-243db	this work	5.01×10^{-14}	7.25×10^{-14}	1.45	7.68×10^{-14}	1.53
62	$CF_3CH_2CH_2Cl$	HCFC-253fb	this work	6.63×10^{-14}	7.97×10^{-14}	1.20	8.33×10^{-14}	1.26
63	$CHCl_3$		JPL 06-2 [2]	1.0×10^{-13}	9.56×10^{-14}	0.96	9.25×10^{-14}	0.93
64	CH_2Cl_2		JPL 06-2 [2]	1.0×10^{-13}	1.04×10^{-13}	1.04	1.07×10^{-13}	1.07
65	CH_3Cl		JPL 06-2 [2]	3.6×10^{-14}	4.01×10^{-14}	1.11	4.71×10^{-14}	1.31
66	$CH_2ClCHCl_2$		Atkinson [3]	1.96×10^{-13}	1.93×10^{-13}	0.99	1.97×10^{-13}	1.00
67	CH_3CCl_3		JPL 06-2 [2]	1.0×10^{-14}	9.37×10^{-15}	0.94	8.36×10^{-15}	0.84
68	CH_2ClCH_2Cl		Atkinson [3]	2.48×10^{-13}	2.55×10^{-13}	1.03	2.54×10^{-13}	1.03
69	CH_3CHCl_2		*1	2.75×10^{-13}	2.81×10^{-13}	1.02	1.94×10^{-13}	0.70
70	CH_2ClCH_3		JPL 06-2 [2]	3.7×10^{-13}	3.13×10^{-13}	0.84	3.19×10^{-13}	0.86
71	$CH_2ClCH_2CH_3$		*2	9.7×10^{-13}	9.88×10^{-13}	1.02	9.86×10^{-13}	1.02
72	$CH_3CHClCH_3$		*3	7.55×10^{-13}	8.88×10^{-13}	1.18	8.54×10^{-13}	1.13
73	$CH_2ClCH_2CH_2CH_3$		*4	1.75×10^{-12}	1.98×10^{-12}	1.13	2.01×10^{-12}	1.15
74	$CH_3CHClCH_2CH_3$		Loison et al. [64]	2.45×10^{-12}	2.26×10^{-12}	0.92	2.21×10^{-12}	0.90
75	$CH_2ClCH(CH_3)_2$		Loison et al. [64]	1.95×10^{-12}	2.26×10^{-12}	1.16	2.33×10^{-12}	1.20
76	$CH_3CCl(CH_3)_2$		Loison et al. [64]	4.5×10^{-13}	3.57×10^{-13}	0.79	2.94×10^{-13}	0.65
77	$CH_2ClCH_2CH_2CH_2CH_3$		Markert and Nielsen [65]	3.1×10^{-12}	3.12×10^{-12}	1.01	3.12×10^{-12}	1.01
78	$CH_2ClCH_2CH_2CH_2CH_2CH_3$		Markert and Nielsen [65]	3.8×10^{-12}	4.27×10^{-12}	1.12	4.32×10^{-12}	1.14
79	$CHBr_3$		JPL 06-2 [2]	1.8×10^{-13}	1.58×10^{-13}	0.88	1.76×10^{-13}	0.98
80	CH_2Br_2		JPL 06-2 [2]	1.2×10^{-13}	1.26×10^{-13}	1.05	1.24×10^{-13}	1.04

Table 52. (Continued)

no.	compound	reference	k_{obs}	correlation		estimation	
				k_{cor}	k_{cor} / k_{obs}	k_{est}	k_{est} / k_{obs}
81	CH_3Br	JPL 06-2 [2]	3.0×10^{-14}	4.12×10^{-14}	1.37	4.86×10^{-14}	1.62
82	CH_2BrCH_2Br	Atkinson [3]	2.22×10^{-13}	2.58×10^{-13}	1.16	3.13×10^{-13}	1.41
83	CH_2BrCH_3	JPL 06-2 [2]	3.4×10^{-13}	3.29×10^{-13}	0.97	3.26×10^{-13}	0.96
84	$CH_2BrCH_2CH_3$	JPL 06-2 [2]	1.0×10^{-12}	1.08×10^{-12}	1.08	1.09×10^{-12}	1.09
85	$CH_3CHBrCH_3$	JPL 06-2 [2]	7.5×10^{-13}	9.76×10^{-13}	1.30	1.10×10^{-12}	1.46
86	$CH_2BrCH_2CH_2CH_3$	Donaghy et al. [66]	2.45×10^{-12}	2.33×10^{-12}	0.95	2.29×10^{-12}	0.93
87	$CH_2BrCH_2CH_2CH_2CH_3$	Donaghy et al. [66]	3.96×10^{-12}	3.70×10^{-12}	0.93	3.62×10^{-12}	0.91
88	$CH_2BrCH_2CH_2CH_2CH_2CH_3$	Donaghy et al. [66]	5.85×10^{-12}	4.76×10^{-12}	0.81	4.21×10^{-12}	0.72
89	CHF_2Br	JPL 06-2 [2]	1.0×10^{-14}	1.06×10^{-14}	1.06	1.33×10^{-14}	1.33
90	$CHFBrCF_3$	JPL 06-2 [2]	1.7×10^{-14}	1.60×10^{-14}	0.94	1.55×10^{-14}	0.91
91	CH_2BrCF_3	JPL 06-2 [2]	1.6×10^{-14}	1.32×10^{-14}	0.82	9.22×10^{-15}	0.58
92	CH_2ClBr	JPL 06-2 [2]	1.1×10^{-13}	1.17×10^{-13}	1.06	1.18×10^{-13}	1.07
93	$CHClBrCF_3$	JPL 06-2 [2]	4.7×10^{-14}	4.04×10^{-14}	0.86	3.88×10^{-14}	0.82
94	$CHFClCF_2Br$	JPL 06-2 [2]	1.4×10^{-14}	1.23×10^{-14}	0.88	9.88×10^{-15}	0.71

The “correlation” means the correlated values using all 94 compounds, while the “estimation” means estimated values by using leave-one-test.

*1 Mean value of Howard and Evenson [28], and Jiang et al. [67].

*2 Mean value of Donaghy et al. [66], and Markert and Nielsen [65].

*3 Mean value of Donaghy et al. [66], and Markert and Nielsen [68].

*4 Mean value of Markert and Nielsen [65], and Loison et al. [64].

Table 53. Optimized weight of the neural network

descriptor	*m*	weight	neuron in hidden layer			
			n = 0	*n* = 1	*n* = 2	*n* = 3
bias	0	$w_{12}(m, n)$	-	1.93967	0.89432	3.19107
H-C···H	1		-	-1.00289	-0.63407	1.96945
H-C···F	2		-	0.45035	-1.74703	-3.83019
H-C···Cl	3		-	0.79062	-1.81163	-0.50057
H-C···Br	4		-	0.70079	-1.66614	0.94426
H-C-C···H	5		-	0.42130	0.14961	0.00158
H-C-C···F	6		-	-2.11605	1.01820	0.52180
H-C-C···Cl	7		-	0.36172	-3.05015	0.11227
H-C-C···Br	8		-	-1.03767	-0.95017	0.94931
H-C-C-C···H	9		-	-0.72791	5.49639	-0.25684
H-C-C-C···F	10		-	-2.01862	-1.45414	0.25319
H-C-C-C···Cl	11		-	-0.93948	0.38032	0.73783
H-C-C-C···Br	12		-	1.77521	1.24102	0.74445
-	-	$w_{23}(n)$	-8.45751	6.24413	1.98783	2.64250

Unfortunately, there are no observed data for comparison. Note that in the present estimation method, the reactivity of individual sites is not limited in the optimization process, although the total reactivity of compounds is well reproduced by the calculation. Thus, at first, some sets of randomly generated initial values for the weights were used in the training. The results of the training indicate that the dependence of the calculated reactivities of individual sites on the initial values of the weights is slightly larger than the dependence of the total reactivity. However, the trends for substituent effects (described below) are not affected by the initial value.

Table 54. Calculated reactivity (in 10-15 cm3 molecule-1 s-1) of individual reaction site

compound [a]		$k_{cor,C-H}$ [b]	ratio [c]	k_{cor} / k_{obs}
C*H_2FCHF_2	HFC-143	8.47×10^{-15}	0.98	1.48
CH_2FC*HF_2		8.68×10^{-15}		
C*$H_3$$CHF_2$	HFC-152a	2.37×10^{-15}	0.15	0.67
CH_3C*HF_2		1.54×10^{-14}		
C*$H_3$$CH_2$F	HFC-161	9.06×10^{-15}	0.15	0.68
CH_3C*H_2F		6.12×10^{-14}		
CF_3C*HFCHF_2	HFC-236ea	2.76×10^{-15}	1.14	1.12
CF_3CHFC*HF_2		2.42×10^{-15}		
C*H_2F$CF_2$$CHF_2$	HFC-245ca	3.24×10^{-15}	0.79	1.43
CH_2FCF_2C*HF_2		4.12×10^{-15}		
C*HF_2CHFCHF_2	HFC-245ea	4.69×10^{-15}	0.48	1.19
CHF_2C*HFCHF_2		9.70×10^{-15}		
CF_3C*HFCH_2F	HFC-245eb	9.70×10^{-15}	1.96	1.29
CF_3CHFC*H_2F		4.96×10^{-15}		
C*$HF_2$$CH_2$$CF_3$	HFC-245fa	4.88×10^{-15}	6.84	1.09
CHF_2C*$H_2$$CF_3$		7.13×10^{-16}		
CF_3C*$H_2$$CH_2$F	HFC-254fb	3.05×10^{-15}	0.21	0.80
$CF_3$$CH_2$C*$H_2$F		1.43×10^{-14}		
$CF_3$$CH_2$C*$H_3$	HFC-263fb	5.43×10^{-15}	0.43	0.98
CF_3C*$H_2$$CH_3$		1.25×10^{-14}		
C*H_3CHFCH_3	HFC-281ea	1.41×10^{-14}	0.05	0.67
CH_3C*HFCH_3		3.02×10^{-13}		
CF_3CF_2C*$H_2$$CH_2$F	HFC-356mcf	1.97×10^{-15}	0.09	1.14
$CF_3CF_2CH_2$C*H_2F		2.19×10^{-14}		
CF_3C*$H_2$$CF_2$$CH_3$	HFC-365mfc	7.84×10^{-16}	0.28	1.43
$CF_3$$CH_2$$CF_2$C*$H_3$		2.76×10^{-15}		
CF_3C*HFCHFCF_2CF_3	HFC-43-10mee	2.78×10^{-15}	2.70	1.36
CF_3CHFC*HFCF_2CF_3		1.03×10^{-15}		

a asterisk represents reaction site of C-H bond considered.
b correlated rate constant per C-H bond.
c ratio of kcor,C-H of upper row against lower low.

In Table 54, some general trends for the reactivities of individual sites are observed. For CH_3CHF_2 (HFC-152a), CH_3CH_2F (HFC-161), $CF_3CH_2CH_3$ (HFC-263fb), and CH_3CHFCH_3 (HFC-281ea), which have a CH_3CHX– (X = H or F)

structure, the ratio of the reactivity of $–CH_3$ relative to that of –CHX– is always less than unity; that is, the reactivity of $–CH_3$ is always lower than that of –CHX–. For CH_3CHFCH_3 in particular, the reactivity of $–CH_3$ is about 5% of the reactivity of –CHX–, whereas the reactivity of $–CH_3$ in this compound is larger than that in the other compounds. In addition, for $CF_3CH_2CH_2F$ (HFC-254fb) and $CF_3CF_2CH_2CH_2F$ (HFC-356mcf), which have a $C_nF_{2n+1}CH_2CH_2F$ (n = 1 or 2) structure, the reactivity of $–CH_2–$ is about 9–21% of that of $–CH_2F$.

For $CF_3CHFCHF_2$ (HFC-236ea), the reactivity of –CHF– is about the same as that of $–CHF_2$. This similarity reflects the trend observed upon substitution of $–CF_3$ for –F in a $–CHF_2$ group (section 4.2). The respective reactivities of $–CHF_2$ and –CHF– are also about the same magnitude in CH_2FCHF_2 (HFC-143) and CF_3CHFCH_2F (HFC-245eb), which have a CH_2FCHFX (X = F or CF_3) structure. The $–CH_2F$ group of CH_2FCHF_2 is obviously more reactive than that of CF_3CHFCH_2F. Therefore, the cause of the reduction in reactivity upon substitution of $–CF_3$ for –F in the $–CHF_2$ group of CH_2FCHF_2 is attributed to the decrease in reactivity of the $–CH_2F$ group caused by the presence of three F atoms connected to the second neighboring carbon. On the other hand, the reactivity of the $–CHF_2$ group of CH_2FCHF_2 (HFC-143) is about 2 times that of the $–CHF_2$ group of $CHF_2CH_2CF_3$ (HFC-245fa), and the reactivity of the $–CH_2F$ group of CH_2FCHF_2 is about one order of magnitude higher than that of the $–CH_2–$group of $CHF_2CH_2CF_3$. Therefore, the reactivity of the $–CH_2X$ group (X = F or CF_3) decreases considerably when the –F of the $–CH_2F$ group of CH_2FCHF_2 is replaced by $–CF_3$. Similar behavior has been found upon substitution of $–CF_3$ for –F in the $–CH_2F$ group of CH_3CH_2F and $CF_3CH_2CH_3$.

In section 4.2, we mentioned that the difference between the reactivities of compounds of the type $R_fC_nF_{2n+1}$ (n = 1–3) is small. On the other hand, for $CF_3CHFCHFCF_2CF_3$ (HFC-43-10mee), which has terminal $–CF_3$ and $–CF_2CF_3$ groups, the reactivity of –CHF– connected to $–CF_3$ is at least twice as large as the reactivity of –CHF– connected to $–CF_2CF_3$. In these calculations, we considered only the effects of atoms connected to a second neighboring carbon. Thus, the cause of the reduced reactivity of –CHF– connected to $–CF_2CF_3$ seems to be deactivation by both $–CF_3$ and $–CF_2CF_3$, whereas –CHF– connected to $–CF_3$ is affected only by $–CF_3$ and $–CF_2–$. In other words, the difference between the input data for both sites for the neural network is as follows: –CHF– connected to $–CF_3$ has 4 H–C–C···F and 2 H–C–C–C···F structures, whereas –CHF– connected to $–CF_2CF_3$ has 3 H–C–C···F and 6 H–C–C–C···F structures. This fact suggests that the F atom connected to the second neighboring carbon considerably reduces the reactivity of the C–H bond.

The reactivities of the $CH_2F–$ and $–CHF_2$ groups of $CH_2FCF_2CHF_2$ (HFC-245ca) are at least 50% less than those of CH_2FCHF_2 (HFC-143). Thus insertion of $–CF_2–$ for CH_2FCHF_2 considerably reduces the reactivity of $CH_2F–$ and $–CHF_2$. The reactivity of the $–CHF_2$ group of $CHF_2CHFCHF_2$ (HFC-245ea) is about 1.7 times that of $CF_3CHFCHF_2$ (HFC-236ea), about 0.3 times that of CH_3CHF_2 (HFC-152a), and about the same as the reactivities of $CH_2FCF_2CHF_2$ (HFC-245ca) and $CHF_2CH_2CF_3$ (HFC-245fa). Thus, the substituent effects of $CH_nF_{2-n}CH_{2-n}F_{1+n}$ (n = 0–2) connected to $–CHF_2$ are about the same, whereas $–CHFCF_3$ reduces the reactivity and $–CH_3$ increases the reactivity of a $–CHF_2$ group. The reactivities of the $–CH_2–$ groups of $CHF_2CH_2CF_3$ (HFC-245fa) and $CF_3CH_2CF_2CH_3$ (HFC-365mfc) are about the same, whereas the reactivities of the $–CH_2–$ groups is at least 50% less reactive than that of $CF_3CH_2CH_3$ (HFC-263fb), $CF_3CH_2CH_2F$ (HFC-254fb), and $CF_3CF_2CH_2CH_2F$ (HFC-356mcf). Thus, these results indicate that $–CF_3$, $–CHF_2$, and $–CF_2–$ deactivate $–CH_2–$ than $–CH_2F$ and $–CH_3$. This trend corresponds to the magnitude of substituent factors of the SAR method [4, 5, 6], DeMore's method [7], and our previous method [8]. The results mentioned here are based on calculations by neural network only and were not confirmed by comparison with experimental data. Therefore, not only total reactivity but also branching ratios must be measured if we are to understand the reactivity of fluorinated compounds in detail.

Chapter 5

CONCLUSION

Rate constants for reactions of OH radicals with 11 hydrochlorofluorocarbons and 12 hydrofluorocarbons were measured over the temperature range 250–430 K. Kinetic data were measured by means of flash photolysis, laser photolysis, and discharge flow methods, combined with laser-induced fluorescence to monitor the OH radical concentration. The samples used in the measurements were purified by gas chromatography. The purification method was effective for the kinetic measurements, and the remaining impurities were found to have no sizeable effect on the measured rate constants for the purified samples. The recommended rate expressions were determined from the present results and available literature data. In many cases, the recommended Arrhenius frequency factor (A) and the temperature dependence (E/R) of JPL are smaller than ours, because JPL focused on the temperature range below 300 K, whereas we focused on the 250–500 K range. The recommended rate constants at 298 K by JPL and ours agree with each other within uncertainty in almost all cases. The discrepancy between our recommended rate constants and those of JPL seems to be due in some cases to the fact that the value recommended by JPL is based on data of low reliability, because the available experimental data for some compounds are very limited.

The neural network technique was used to predict rate constants for reactions with OH radicals at 298 K obtained in this study as well as available literature data. An algorithm for the back-propagation method used to optimize the weights between neurons was developed for compounds with multiple reactive sites for which the individual reactivities are not known. The neural network method was used to calculate rate constants for 94 compounds, including 12 hydrocarbons, 32 hydrofluorocarbons, 18 hydrochlorofluorocarbons, 16 hydrochlorocarbons, and 16 brominated compounds. To examine the predictive ability of the neural network,

the leave-one-out test method was used, and the results indicate that rate constants for 93 compounds, excluding CHF_3, could be estimated within a factor of 2. Rate constants for all 94 compounds were successfully correlated to observed rate constants within a factor of 2 when the calculation was carried out using optimized weights determined using all the compounds.

REFERENCES

[1] Houghton, J. T., Ding Y., Griggs, D. J., Noguer, M., van der Linden, P. J., Dai, X., Maskell, K., Johnson, C. A. (2001). Climate Change 2001: The Scientific Basis. Contribution of Working Group I to the Third Assessment Report of the Intergovernmental Panel on Climate Change (IPCC). Geneva, Switzerland: Cambridge University Press.

[2] Sander, S. P., Friedl, R. R., Golden, D. M., Kurylo, M. J., Moortgat, G. K., Keller-Rudek, H., Wine, P. H., Ravishankara, A. R., Kolb, C. E., Molina, M. J., Finlayson-Pitts, B. J., Huie, R. E., and Orkin, V. L. (2006). *Chemical Kinetics and Photochemical Data for Use in Atmospheric Studies; Evaluation No. 15*. JPL Publication 06-2; Jet Propulsion Laboratory, California Institute of Technology, Pasadena, CA.

[3] Atkinson, R. (1994). Gas-phase tropospheric chemistry of organic compounds. *J. Phys. Chem. Ref. Data Monograph 2*, 1-216.

[4] Atkinson, R. (1986). Kinetics and mechanisms of the gas-phase reactions of the hydroxyl radical with organic compounds under atmospheric conditions. *Chem. Rev.*, 86, 69-201.

[5] Atkinson, R. (1987). A structure-activity relationship for the estimation of rate constants for the gas-phase reactions of OH radicals with organic compounds. *Int. J. Chem. Kinet.*, *19*, 799-828.

[6] Kwok, E. S. C., and Atkinson, R. (1995). Estimation of hydroxyl radical reaction rate constants for gas-phase organic compounds using a structure-reactivity relationship: An update. *Atmos. Env.*, *29*, 1685-1695.

[7] DeMore, W.B. (1996). Experimental and estimated rate constants for the reactions of hydroxyl radicals with several halocarbons. *J. Phys. Chem.*, *100*, 5813-5820.

[8] Tokuhashi, K., Nagai, H., Takahashi, A., Kaise, M., Kondo, S., Sekiya, A., Takahashi, M., Gotoh, Y., Suga, A. (1993). Measurement of the OH reaction rate constants for CF_3CH_2OH, $CF_3CF_2CH_2OH$, and $CF_3CH(OH)CF_3$. *J. Phys. Chem. A, 103*, 2664-2672.

[9] Urata, S., Takada, A., Uchimaru, T., Chandra, A. K., and Sekiya, A. (2002). Artificial neural network study for the estimation of the C-H bond dissociation enthalpies. *J. Fluorine Chem., 116*, 163-171.

[10] Urata, S., Takada, A., Uchimaru, T., and Chandra, A. K. (2003). Rate constants estimation for the reaction of hydrofluorocarbons and hydrofluoroethers with OH radicals. *Chem. Phys. Lett., 368*, 215-223.

[11] Chen, L., Tokuhashi, K., Kutsuna, S., and Sekiya, A. (2004). Rate Constants for the gas-phase reaction of $CF_3CF_2CF_2CF_2CF_2CHF_2$ with OH radicals at 250–430 K. *Int. J. Chem. Kinet., 36*, 26-33.

[12] Burrows, J. P., Wallington, T. J., and Wayne, R. P. (1983). Kinetics of the Gas-phase Reactions of OH with NO_2 and with NO. *J. Chem. Soc. Faraday Trans. 2, 79*, 111-122.

[13] Kaufman, F. J. (1961). Reactions of oxygen atoms. *Prog. React. Kinet., 1*, 1-39.

[14] Hsu, K.-J., and DeMore, W. B. (1995). Rate constants and temperature dependences for the reactions of hydroxyl radical with several halogenated methanes, ethanes, and propanes by relative rate measurements. *J. Phys. Chem., 99*, 1235-1244.

[15] Cavalli, F., Glasius, M., Hjorth, J., Rindone, B., and Jensen, N. R. (1998). Atmospheric lifetimes; infrared spectra and degradation products of a series of hydrofluoroethers. *Atmos. Environ., 32*, 3767-3773.

[16] Clyne, M. A. A., and Holt, P. M. (1979). Reaction kinetics involving ground X^2II and excited $A^2\Sigma^+$ hydroxyl radicals; Part 2-Rate constants for reactions of OH X^2II with halogenomethanes and halogenoethanes. *J. Chem. Soc. Faraday Trans. 2, 75*, 582-591.

[17] Howard, C.J., and Evenson, K. M. (1976). Rate constants for the reactions of OH with CH_4 and fluorine, chlorine, and bromine substituted methanes at 296K. *J. Chem. Phys., 64*, 197-202.

[18] Orkin, V. L., and Khamaganov, V. G. (1993). Determination of rate constants for reactions of some hydrohaloalkanes with OH radicals and their atmospheric lifetimes. *J. Atmos. Chem., 16*, 157-167.

[19] Atkinson, R., Hansen, D. A., and Pitts, J. N., Jr. (1975). Rate constants for the reaction of OH radicals with CHF_2Cl, CF_2Cl_2, $CFCl_3$, and H_2 over the temperature range 297-434K. *J. Chem. Phys., 63*, 1703-1706.

[20] Watson, R. T., Machado, G., Conaway, B., Wagner, S., and Davis, D. D. (1977). A temperature dependent kinetics study of the reaction of OH with CH_2ClF, $CHCl_2F$, $CHClF_2$, CH_3CCl_3, CH_3CF_2Cl, and $CF_2ClCFCl_2$. *J. Phys. Chem., 81*, 256-262.

[21] Chang, J. S., and Kaufman, F. (1977). Kinetics of the reactions of hydroxyl radicals with some halocarbons: $CHFCl_2$, CHF_2Cl, CH_3CCl_3, C_2HCl_3, and C_2Cl_4. *J. Chem. Phys., 66*, 4989-4994.

[22] Jeong, K-M., and Kaufman, F. (1982). Kinetics of the reaction of hydroxyl radical with methane and with nine Cl- and F-substituted methanes: 1. Experimental results, comparisons and applications. *J. Phys. Chem., 86*, 1808-1815.

[23] Handwerk, V. and Zellner, R. (1978). Kinetics of the reactions of OH radicals with some halocarbons ($CHClF_2$, CH_2ClF, CH_2ClCF_3, CH_3CClF_2, CH_3CHF_2) in the temperature range 260-370 K. *Ber. Bunsenges. Phys. Chem., 82*, 1161-1166.

[24] Fang, T. D., Taylor, P. H., and Dellinger, B. (1996). Absolute rate measurements of the reaction of OH radicals with HCFC-21 ($CHFCl_2$) and HCFC-22 (CHF_2Cl) over an extended temperature range. *J. Phys. Chem., 100*, 4048-4054.

[25] Paraskevopoulos, G., Singleton, D. L., and Irwin, R. S. (1981). Rates of OH radical reactions. 8. Reactions with CH_2FCl, CHF_2Cl, $CHFCl_2$, CH_3CF_2Cl, CH_3Cl, and C_2H_5Cl at 297 K. *J. Phys. Chem., 85*, 561-564.

[26] Nielsen, O. J. (1991). Rate constants for the gas-phase reactions of OH radicals with CH_3CHF_2 and $CHCl_2CF_3$ over the temperature range 295-388 K. *Chem. Phys. Lett., 187*, 286 – 290.

[27] Brown, A. C., Canosa-Mas, C. E., Parr, A. D., and Wayne, R. P. (1990). Laboratory studies of some halogenated ethanes and ethers: measurements of rates of reaction with OH and OF infrared absorption cross-sections. *Atmos. Environ., 24*, 2499–2511.

[28] Howard, C. J., and Evenson, K. M. (1976). Rate constants for the reactions of OH with ethane and some halogen substituted ethanes at 269K. *J. Chem. Phys., 64*, 4303-4306.

[29] Watson, R. T., Ravishankara, A. R., Machado, G., Wagner, S., and Davis, D. D. (1979). A kinetics study of the temperature dependence of the reactions of $OH(^2\Pi)$ with CF_3CHCl_2, CF_3CHClF, and CF_2ClCH_2Cl. *Int. J. Chem. Kinet., 11*, 187-197.

[30] Yamada, T., Fang, T. D., Taylor, P. H., and Berry, R. J. (2000). Kinetics and thermochemistry of the OH radical reaction with CF_3CCl_2H and CF_3CFClH. *J. Phys. Chem. A, 104*, 5013-5022.

[31] Gierczak, T., Talukdar, R., Vaghjiani, G. L., Lovejoy, E. R., and Ravishankara, A.R. (1991). Atmospheric fate of hydrofluoroethanes and hydrofluorochloroethanes: 1. Rate coefficients for reactions with OH. *J. Geophys. Res.*, *96*, 5001 – 5011.

[32] Liu, R., Huie, R. E., and Kurylo, M. J. (1990). Rate constants for the reactions of the OH radical with some hydrochlorofluorocarbons over the temperature range 270-400 K. *J. Phys. Chem.*, *94*, 3247-3249.

[33] Jeong, K.-M., Hsu, K.-J., Jeffries, J. B., and Kaufman, F. (1984). Kinetics of the reactions of OH with C_2H_6, CH_3CCl_3, $CH_2ClCHCl_2$, $CH_2ClCClF_2$, and CH_2FCF_3. *J. Phys. Chem.*, *88*, 1222-1226.

[34] Fang, T. D., Taylor, P. H., and Berry, R. J. (1999). Kinetics of the reaction of OH radicals with CH_2ClCF_2Cl and CH_2ClCF_3 over an extended temperature range. *J. Phys. Chem. A*, *103*. 2700-2704.

[35] Talukdar, R., Mellouki, A., Gierczak, T., Burkholder, J. B., McKeen, S. A., and Ravishankara, A. R. (1991). Atmospheric fate of CF_2H_2, CH_3CF_3, CHF_2CF_3, and CH_3CFCl_2; Rate coefficients for reactions with OH and UV absorption cross sections of CH_3CFCl_2. *J. Phys. Chem.*, *95*, 5815-5821.

[36] [Huder, K., and DeMore, W.B. (1993). Rate constant for the reaction of OH with CH_3CCl_2F(HCFC-141b) determined by relative rate measurements with CH_4 and CH_3CCl_3. *Geophys. Res. Lett.*, *20*, 1575-1577.

[37] Zhang, Z., Huie, R. E., and Kurylo, M. J. (1992). Rate constants for the reactions of OH with CH_3CFCl_2 (HCFC-141b), CH_3CF_2Cl (HCFC-142b), and CH_2FCF_3 (HFC-134a). *J. Phys. Chem.*, *96*, 1533-1535.

[38] Lancar, I., LeBras, G., and Poulet, G. (1993). Oxidation of CH_3CCl_3 and CH_3CFCl_2 in the atmosphere: kinetic study of OH reactions. *J. Chim. Phys.*, *90*, 1897-1908.

[39] Mors, V., Hoffmann, A., Malms, W., and Zellner, R. (1996). Time resolved studies of intermediate products in the oxidation of HCFC 141b ($CFCl_2CH_3$) and HCFC 142b (CF_2ClCH_3). *Ber. Bunsenges. Phys. Chem.*, *100*, 540-552.

[40] Fang, T. D., Taylor, P. H., Dellinger, B., Ehlers, C. J., and Berry, R. J. (1977). Kinetics of the OH + CH_3CF_2Cl reaction over an extended temperature range. *J. Phys. Chem. A*, *101*, 5758-5764.

[41] Bera, R. K., and Hanrahan, R. J. (1988). Investigation of gas phase reactions of OH radicals with fluoromethane using Ar-sensitized pulse radiolysis. *Radiation Physics and Chemistry*, *32*, 579-584.

[42] Szilagyi, I., Dobe S., and Berces, T. (2000). Rate constant for the reaction of the OH-radical with CH_2F_2. *Reaction Kinetics and Catalysis Letters*, *70*, 319-324.

[43] Nip, W. S., Singleton, D. L., Overend, R., and Paraskevopoulos, G.. (1979). Rates of OH radical reactions 5; Reactions with CH_3F, CH_2F_2, CHF_3, CH_3CH_2F, and CH_3CHF_2 at 297 K. *J. Phys. Chem.*, *83*, 2440-2443.

[44] DeMore, W.B. (1993). Rate constants for the reactions of OH with HFC-134a (CF_3CH_2F) and HFC-134 (CHF_2CHF_2). *Geophys. Res. Lett.*, *20*, 1359-1362.

[45] Martin, J-P., and Paraskevopoulos, G. (1983). A kinetic study of the reactions of OH radicals with fluoroethanes; Estimates of C-H bond strengths in fluoroalkanes. *Can. J. Chem.*, *61*, 861-865.

[46] Leu, G-H., and Lee, Y-P. (1994). Temperature dependence of the rate coefficient of the reaction OH + CF_3CH_2F over the range 255-424 K. *J. Chin. Chem. Soc.* (*Taipei*), *41*, 645-649.

[47] Bednarek, G., Breil, M., Hoffmann, A., Kohlmann, J. P., Mors, V., and Zellner, R. (1996). Rate and mechanism of the atmospheric degradation of 1,1,1,2-tetrafluoroethane (HFC-134a). *Ber. Bunsenges. Phys. Chem.*, *100*, 528-539.

[48] Barry, J., Sidebottom, H., Treacy, J., and Franklin, J. (1995). Kinetics and mechanism for the atmospheric oxidation of 1,1,2-trifluoroethane (HFC-143). *Int. J. Chem. Kinet.*, *27*, 27-36.

[49] Kozlov, S. N., Orkin V. L., and Kurylo, M. J. (2003). An investigation of the reactivity of OH with fluoroethanes: CH_3CH_2F (HFC-161), CH_2FCH_2F (HFC-152), and CH_3CHF_2 (HFC-152a). *J. Phys. Chem. A*, *107*, 2239-2246.

[50] Nelson, D. D., Jr., Zahniser, M. S., Kolb, C. E., and Magid, H. (1995). OH reaction kinetics and atmospheric lifetime estimates for several hydrofluorocarbons. *J. Phys. Chem.*, *99*, 16301-16306.

[51] Garland, N. L., Medhurst, L. J., and Nelson, H. H. (1993). Potential chlorofluorocarbon replacements; OH reaction rate constants between 250 and 315 K and infrared absorption spectra. *J. Geophys. Res.*, *98*, 23107-23111.

[52] Zhang, Z., Padmaja, S., Saini, R. D., Huie, R. E., and Kurylo, M.J. (1994). Reactions of hydroxyl radicals with several hydrofluorocarbons; The temperature dependencies of the rate constants for $CHF_2CF_2CH_2F$ (HFC-245ca), $CF_3CHFCHF_2$ (HFC-236ea), CF_3CHFCF_3 (HFC-227ea), and $CF_3CH_2CH_2CF_3$ (HFC-356ffa). *J. Phys. Chem.*, *98*, 4312-4315.

[53] Orkin, V. L., Huie, R. E., and Kurylo, M. J. (1996). Atmospheric lifetimes of HFC-143a and HFC-245fa: Flash photolysis resonance fluorescence measurements of the OH reaction rate constants. *J. Phys. Chem.*, *100*, 8907-8912.

[54] Zhang, Z., Saini, R. D., Kurylo, M. J., and Huie, R. E. (1992). Rate constants for the reactions of the hydroxyl radical with $CHF_2CF_2CF_2CHF_2$ and $CF_3CHFCHFCF_2CF_3$. *Chem. Phys. Lett.*, *200*, 230-234.

[55] Schmoltner, A. M., Talukdar, R. K., Warren, R. F., Mellouki, A., Goldfarb, L., Gierczak, T., McKeen, S. A. and Ravishankara, A. R. (1993). Rate coefficients for reactions of several hydrofluorocarbons with OH and $O(^1D)$ and their atmospheric lifetimes. *J. Phys. Chem.*, *97*, 8976-8982.

[56] Spivakovsky, C. M., Logan, J. A., Montzka, S. A., Balkanski, Y. J., Foreman-Fowler, M., Jones, D. B. A., Horowitz, L. W., Fusco, A. C., Brenninkmeijer, C. A. M., Prather, M. J., Wofsy, S. C., and McElroy, M. B. (2000). Three-dimensional climatological distribution of tropospheric OH: Update and evaluation. *J. Geophys. Res.*, *105*, 8931-8980.

[57] Prinn, R. G., Huang, J., Weiss, R. F., Cunnold, D. M., Fraser, P. J., Simmonds, P. G., McCulloch, A., Harth, C., Salameh, P., O'Doherty, S., Wang, R. H. J., Porter, L., and Miller, B. R. (2001). Evidence for substantial variations of atmospheric hydroxyl radicals in the past two decades. *Science*, *292*, 1882-1888.

[58] Zhang, Z., Saini, R. D., Kurylo, M. J., and Huie, R. E. (1992). Rate constants for the reactions of the hydroxyl radical with several partially fluorinated ethers. *J. Phys. Chem.*, *96*, 9301-9304.

[59] Tokuhashi, K., Takahashi, A., Kaise, M., Kondo, S., Sekiya, A., Yamashita, S., and Ito, H. (2000). Rate constants for the reactions of OH radicals with $CH_3OCF_2CHF_2$, $CHF_2OCH_2CF_2CHF_2$, $CHF_2OCH_2CF_2CF_3$, and $CF_3CH_2OCF_2CHF_2$ over the temperature range 250-430 K. *J. Phys. Chem. A*, *104*, 1165-1170.

[60] Tokuhashi, K., Takahashi, A., Kaise, M., and Kondo, S. (1999). Rate constants for the reactions of OH radicals with CH_3OCF_2CHFCl, CHF_2OCF_2CHFCl, $CHF_2OCHClCF_3$, and $CH_3CH_2OCF_2CHF_2$. *J. Geophys. Res.*, *104*, 18681-18688.

[61] Tokuhashi, K., Takahashi, A., Kaise, M., Kondo, S., Sekiya, A., Yamashita, S., and Ito, H. (1999). Rate Constants for the Reactions of OH Radicals with $CH_3OCF_2CF_3$, $CH_3OCF_2CF_2CF_3$, and $CH_3OCF(CF_3)_2$. *Int J. Chem. Kinet.*, *31*, 846-853.

[62] Tokuhashi, K., Chen, L., Kutsuna, S., Uchimaru, T., Sugie, M., and Sekiya, A. (2004). Environmental assessment of CFC alternatives: Rate constants for the reactions of OH radicals with fluorinated compounds. *J. Fluorine Chem.*, *125*, 1801-1807.

[63] Orkin, V. L., Huie, R. E., and Kurylo, M. J. (1997). Rate constants for the reactions of OH with HFC-245cb ($CH_3CF_2CF_3$) and some fluoroalkenes (CH_2CHCF_3, CH_2CFCF_3, CF_2CFCF_3, and CF_2CF_2). *J. Phys. Chem.* A, *101*, 9118-9124.

[64] Loison, J.C., Ley, L., and Lesclaux, R. (1998). Kinetic study of OH radical reactions with chlorobutane isomers at 298 K. *Chem. Phys. Lett.*, *296*, 350 – 356.

[65] Markert, F., and Nielsen, O. J. (1992). Rate constants for the reaction of OH radicals with 1-chloroalkanes at 295 K. *Chem. Phys. Lett.*, *194*, 171-174.

[66] Donaghy, T., Shanahan, I., Hande, M., and Fitzpatrick, S. (1993). Rate constants and atmospheric lifetimes for the reactions of OH radicals and Cl atoms with haloalkanes. *Int. J. Chem. Kinet.*, *25*, 273-284.

[67] Jiang, Z., Taylor, P. H., Dellinger, B. (1992). Laser photolysis/laser-induced fluorescence studies of the reaction of OH with 1,1-dichloroethane over an extended temperature range. *J. Phys. Chem.*, *9*6, 8964-8966.

[68] Markert, F., and Nielsen, O. J. (1992). The reactions of OH radicals with chloralkanes in the temperature range 295-360 K. *Chem. Phys. Lett.*, *194*, 123-127.

INDEX

D

E

F

G

H

I

J

K

L

M

N

O

P

Q

R

S

T

U

V

W

Y